

Keywords: *DWPF*

SRAT

reductant

Retention: *Permanent*

Glycolic - Formic Acid Flowsheet Final Report for Downselection Decision

D.P. Lambert
B.R. Pickenheim
M.E. Stone
J.D. Newell
D.R. Best

March 9, 2011

Savannah River National Laboratory
Savannah River Nuclear Solutions, LLC
Aiken, SC 29808

Prepared for the U.S. Department of Energy under
contract number DE-AC09-08SR22470.



DISCLAIMER

This work was prepared under an agreement with and funded by the U.S. Government. Neither the U.S. Government or its employees, nor any of its contractors, subcontractors or their employees, makes any express or implied:

1. warranty or assumes any legal liability for the accuracy, completeness, or for the use or results of such use of any information, product, or process disclosed; or
2. representation that such use or results of such use would not infringe privately owned rights; or
3. endorsement or recommendation of any specifically identified commercial product, process, or service.

Any views and opinions of authors expressed in this work do not necessarily state or reflect those of the United States Government, or its contractors, or subcontractors.

Printed in the United States of America

**Prepared for
U.S. Department of Energy**

REVIEWS AND APPROVALS

AUTHORS:

D.P. Lambert, ERPS/Process Technology Programs

Date

B.R. Pickenheim, ERPS/Process Technology Programs

Date

M.E. Stone, ERPS/Process Technology Programs

Date

J.D. Newell, ERPS/Process Technology Programs

Date

TECHNICAL REVIEW:

D.C. Koopman, ERPS/Process Technology Programs

Date

APPROVAL:

C.C. Herman, Manager

ERPS/Process Technology Programs

Date

S.L. Marra, Manager

Environmental & Chemical Process Technology Research Programs

Date

J.E. Occhipinti, Manager

Waste Solidification Engineering

Date

EXECUTIVE SUMMARY

Flowsheet testing was performed to develop the nitric-glycolic-formic acid flowsheet (referred to as the glycolic-formic flowsheet throughout the rest of the report) as an alternative to the nitric/formic flowsheet currently being processed at the DWPF. This new flowsheet has shown that mercury can be removed in the Sludge Receipt and Adjustment Tank (SRAT) with minimal hydrogen generation. All processing objectives were also met, including greatly reducing the Slurry Mix Evaporator (SME) product yield stress as compared to the baseline nitric/formic flowsheet. Forty-six runs were performed in total, including the baseline run and the melter feed preparation runs. Significant results are summarized below:

Constraint	Limit	Baseline Flowsheet GF1	Glycolic-formic Flowsheet GF3
SRAT hydrogen, lb/hr	<0.65	1.62	0.03
SME hydrogen, lb/hr	<0.23	0.0072	0.0017
SRAT carbon dioxide, lb/hr	NA	375	200
SRAT nitrous oxide, lb/hr	NA	0.75	1.93
SRAT product Hg, wt %	0.8	0.66	0.56
SRAT product nitrite, mg/kg	<1000	<100	<100
SRAT product down yield stress, Pa	1.5 to 5	33.1	1.6
SRAT product down consistency, cP	5 to 12	22.8	7.1
SME product down yield stress, Pa	2.5 to 15	223	7.2
SME product down consistency, cP	10 to 40	289	24.1
Glass REDOX $\text{Fe}^{+2}/\Sigma\text{Fe}$	0.1-0.33	0.00	0.22 ^a
SME product total solids, wt %	>45	46.28	44.66
Minimal foaming	NA	No	Yes

The baseline nitric/formic flowsheet run, using the SB6 simulant produced by Harrell was extremely difficult to process successfully under existing DWPF acceptance criteria with this simulant at the HM levels of noble metals. While nitrite was destroyed and mercury was removed to near the DWPF limit, the rheology of the SRAT and SME products were well above design basis and hydrogen generation far exceeded the DWPF SRAT limit. In addition, mixing during the SME cycle was very poor. In this sense, the nitric/glycolic/formic acid flowsheet represents a significant upgrade over the current flowsheet. Mercury was successfully removed with almost no hydrogen generation and the SRAT and SME products yield stresses were within process limits or previously processed ranges.

The glycolic-formic flowsheet has a very wide processing window. Testing was completed from 100% to 200% of acid stoichiometry and using a glycolic-formic mixture from 40% to 100% glycolic acid. The testing met all processing requirements throughout these processing windows. This should allow processing at an acid stoichiometry of 100% and a glycolic-formic mixture of 80% glycolic acid with minimal hydrogen generation. It should also allow processing endpoints

^a REDOX of GF14. REDOX of GF14.

in the SRAT and SME at significantly higher total solids content and may be effective at acid stoichiometries below 100%, although no testing was performed below 100% acid stoichiometry.

There are several issues related to the development of the glycolic-formic flowsheet. First, the measurement of anions using the new glycolate anion procedure likely needs to be optimized to improve the accuracy of the anions important to DWPF processing and REDOX prediction. Second, the existing REDOX equation with an added term for glycolate did not accurately predict the glass REDOX for the glycolic-formic flowsheet. Improvement of the anion measurement or modification of the REDOX methodology or equation may be necessary to improve the REDOX prediction. Last, the glycolic-formic flowsheet dissolves a number of metals, including iron. This leads to a thinner slurries but also dissolves up a portion of the iron, which is currently used for criticality control.

It is recommended that DWPF continue to support development of the glycolic-formic flowsheet. This flowsheet meets or outperforms the baseline flowsheet in off-gas generation, mercury removal, product rheology and general ease of processing. Additional testing is in progress to demonstrate the effectiveness of the nitric-glycolic-formic flowsheet in processing a wide sludge processing window using the matrix sludge simulants.

TABLE OF CONTENTS

LIST OF TABLES	viii
LIST OF FIGURES	x
LIST OF ABBREVIATIONS	xi
1.0 Introduction	1
1.1 Evaluation of Alternative Reductants	1
1.2 Development of Glycolic-Formic Flowsheet.....	1
1.3 Preparation of Melter Feed for Testing of Baseline, Glycolic-Formic and Sugar Flowsheets	2
2.0 Experimental Procedure	3
2.1 CPC Simulation Details	3
2.2 CPC Run Details.....	6
2.3 Process Data Collection	8
2.4 Analytical Methods.....	8
2.4.1 Issues with analytical method	9
3.0 Results and Discussion	10
3.1 Small-scale Laboratory Results (SRNL)	10
3.1.1 SRAT Offgas.....	10
3.1.2 SRAT Chemistry	12
3.1.2.1 SRAT Product Data.....	13
3.1.2.2 SRAT Dissolution of Metals as a function of acid stoichiometry.....	16
3.1.2.3 SRAT Dissolution of Metals as a Function of Glycolic-Formic Acid Ratio	18
3.1.2.4 SRAT Degradation Products	21
3.1.3 SRAT Hydrogen Suppression	21
3.1.4 SRAT Carbon and Nitrogen Balance	25
3.1.4.1 SRAT Cycle Carbon Balance.....	26
3.1.4.2 SRAT Cycle Nitrogen Balance	27
3.1.5 SRAT and SME Rheology	27
3.1.6 SRAT Acid Stoichiometry	31
3.1.7 SRAT/SME REDOX	31
3.1.8 SRAT Gd Solubility.....	37
3.1.9 SRAT Mercury Reduction	39
3.1.10 SRAT pH profile	43
3.1.11 SRAT Foaming Issues.....	44

3.1.12 SRAT Condensate Data	45
3.1.13 SME Offgas.....	46
3.1.14 Ruthenium Testing	47
3.2 Melter Feed Preparation.....	48
3.2.1 Flowsheet Calculations of Acid Requirement.....	48
3.2.2 Run Details.....	50
3.2.3 Product Results.....	50
3.3 Recommended Flowsheet	53
3.4 Physical Properties.....	54
3.5 Degradation Issues	54
3.6 Analytical Issues	55
3.7 Unresolved Technical Issues	55
4.0 Conclusions	56
5.0 Recommendations	58
6.0 References	59
Appendix A	61

LIST OF TABLES

Table 1-1. Acid Properties.....	1
Table 1-2. Mercury and noble metal concentrations	2
Table 2-1. CPC Simulation Process Assumptions.....	7
Table 2-2. Final Ion Chromatography Method for Glycolate and Other Anions	9
Table 3-1. SRAT Product Anions, Solids, Density, and pH Data	13
Table 3-2. Anion Balance Data	14
Table 3-3. SRAT Product Elemental Data, wt % calcined solids basis	15
Table 3-4. SME Product Elemental Data, wt % calcined solids basis	16
Table 3-5. Acid Stoichiometry Study: SRAT Product Supernate % of Element Dissolved	18
Table 3-6. Glycolic Ratio: SRAT Product Supernate % of Element Dissolved at 125% Koopman Stoichiometry	19
Table 3-7. Hydrogen Generation.....	22
Table 3-8. SRAT Carbon and Nitrogen Species in Offgas, g.....	26
Table 3-9. Carbon and Nitrogen Species in Sludge, g.....	26
Table 3-10. SRAT Carbon and Nitrogen added as Acids, g.....	26
Table 3-11. Carbon and Nitrogen Overall Balance	27
Table 3-12. SRAT Product Rheology Summary	29
Table 3-13. SME Product Rheology Summary	30
Table 3-14. Melter Feed Rheology Summary	31
Table 3-15. Acid Stoichiometry, Hydrogen Generation and Rheology	31
Table 3-16. SRAT product anions, mg/kg.....	33
Table 3-17. SME product data for REDOX calculations	33
Table 3-18. Glass REDOX	34
Table 3-19. Comparison of SRAT and SME Product Hg results	40
Table 3-20. Mercury Balance	43
Table 3-21. Comparison of Composite Condensate Data, ICP-AES, mg/L.....	46
Table 3-22. Comparison of Composite Condensate Data, IC (mg/L), Density (g/mL), pH.....	46

Table 3-23. Comparison of SME Offgas Generation Data	47
Table 3-24. SRAT Cycle Additions and Dewater Targets, grams	48
Table 3-25. Sludge Composition for Melter Feed Preparation	49
Table 3-26. SRAT Processing Assumptions for Melter Feed Preparation.....	50
Table 3-27. SME Processing Assumptions for Melter Feed Preparation.....	50
Table 3-28. SRAT Product ICP-AES results, wt % calcined solids basis.....	51
Table 3-29. SRAT Product Anion results, mg/kg	52
Table 3-30. SRAT Product Solids Results, wt % Total Solids Basis and pH	52
Table 3-31. SRAT Product Rheology results	52
Table 3-32. SRAT Product REDOX, Inputs and Outputs	53
Table 3-33. Glycolic Acid Determination Using Density Measurement	54

LIST OF FIGURES

Figure 2-1. Schematic of SRAT Equipment Set-Up	4
Figure 3-1. SRAT cycle N ₂ O generation.....	11
Figure 3-2. SRAT cycle CO ₂ generation.....	11
Figure 3-3. GF6 GC Data	12
Figure 3-4. Iron solubility as a function of acid stoichiometry	17
Figure 3-5. Metal solubility as a function of % glycolic acid in blend	19
Figure 3-6. Iron and Gadolinium Solubility in SB6-29.....	20
Figure 3-7. Iron and Gadolinium Solubility in GF13.....	21
Figure 3-8. Max Hydrogen Generation Relative to mol% Formic in Formic/Glycolic blend.....	23
Figure 3-9. Baseline SRAT cycle hydrogen generation (GF1 vs. GF3).....	23
Figure 3-10. Baseline SME Cycle Hydrogen Generation (GF1 vs. GF3).....	24
Figure 3-11. GF2 (no Hg) hydrogen generation.....	25
Figure 3-12. pH trends for baseline SRAT/SME runs with mercury and noble metals	28
Figure 3-13. SRAT Product flow curve comparison for GF1 and GF3	29
Figure 3-14. SRAT Product Rheology	30
Figure 3-15. Measured REDOX dependence on acid stoichiometry	35
Figure 3-16. Hydrogen Generation Dependence on REDOX	36
Figure 3-17. SRAT Product REDOX comparison	37
Figure 3-18. SB6-29 Fe and Gd Solubility during SRAT Cycle.....	38
Figure 3-19. GF13 Fe and Gd Solubility during SRAT Cycle.....	38
Figure 3-20. Mercury concentration with time in baseline SRAT cycles	39
Figure 3-21. Mercury concentration with time for 100% stoichiometry run	40
Figure 3-22. Mercury collection in SRAT condenser drain tube	41
Figure 3-23. Mercury collection in SRAT condenser drain tube	42
Figure 3-24. pH trends for baseline SRAT runs with mercury and noble metals	43
Figure 3-25. pH trends for baseline SRAT runs without mercury and noble metals	44
Figure 3-26. Carbon Dioxide Generation in GF1 and GF3 SME cycles, lb/hr DWPF Scale.....	47

LIST OF ABBREVIATIONS

AD	Analytical Development
ARP	Actinide Removal Process
CPC	Chemical Process Cell
GC	Gas Chromatograph
FAVC	Formic Acid Vent Condenser
IC	Ion Chromatography
ICP-AES	Inductively Coupled Plasma-Atomic Emission Spectroscopy
MCU	Modular Caustic Side Solvent Extraction Unit
MWWT	Mercury Water Wash Tank
PSAL	Process Science Analytical Laboratory
REDOX	Reduction/Oxidation
SME	Slurry Mix Evaporator
SMECT	Slurry Mix Evaporator Condensate Tank
SRAT	Sludge Receipt and Adjustment Tank
SRNL	Savannah River National Laboratory
SRR	Savannah River Remediation
SVOA	Semi-Volatile Organics Analysis
TIC	Total Inorganic Carbon Analysis
TOC	Total Organic Carbon Analysis
TT&QAP	Task Technical and Quality Assurance Plan
TTR	Technical Task Request
VOA	Volatile/semi-volatile Organics Analysis
VSL	Vitreous State Laboratory

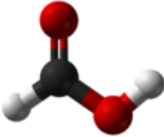
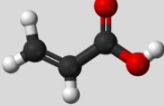
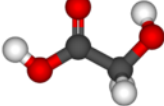
1.0 Introduction

Savannah River Remediation (SRR) is evaluating changes to its current Defense Waste Processing Facility (DWPF) flowsheet to improve processing cycle times that will enable the facility to support higher canister production while maximizing waste loading after installation of the bubblers into the melter. Due to the significant maintenance required for the DWPF Gas Chromatographs (GC) and the potential for production of flammable quantities of hydrogen, reducing the amount of formic acid used in the Chemical Process Cell (CPC) is one of the options being considered. Earlier work at Savannah River National Laboratory has shown that replacing formic acid in the existing nitric/formic acid flowsheet with an 80:20 molar blend of glycolic and formic acids has the potential to remove mercury in the SRAT without any significant catalytic hydrogen generation.

1.1 Evaluation of Alternative Reductants

At the request of SRR, a study was completed evaluating 19 reductants to replace formic acid in CPC Processing¹. In the DWPF CPC, formic acid is both an acid and a reductant. Six reductants that are not acids were evaluated in addition to thirteen reducing acids. The two best alternatives from this testing, glycolic and acrylic, are listed in Table 1-1. All. The primary drawback to acrylic acid, the only acid tested with a carbon double bond, is the potential for polymerization in the storage tank, requiring controls to be in place to allow safe storage. Since this initial study, all testing has been completed with glycolic acid, which is also both an acid and a reductant. Note that for every mole of glycolic acid added, two moles of carbon are added as glycolic acid is a two carbon organic acid. Glycolic mixed with formic acid was recommended to ensure mercury would be reduced even if glycolic acid was not effective in reducing mercury.²

Table 1-1. Acid Properties

Reductant	Formula	Acid pKa	Solubility 25 °C g/100 ml	Molarity	Typical Acid Concentration	Carbon Oxidation State	Structure
Formic Acid	CH ₂ O ₂	3.751	Miscible	23.6	90 wt %	2	
Acrylic Acid	C ₃ H ₄ O ₂	4.35	Miscible	17.5	100 wt %	0	
Glycolic Acid	C ₂ H ₄ O ₃	3.831	80	11.83	71 wt%	1	

1.2 Development of Glycolic-Formic Flowsheet

The objective of the testing detailed in this document is to summarize the data collected in developing the glycolic-formic acid flowsheet as requested by DWPF.^{3,4,5} This work was performed under the guidance of Task Technical and Quality Assurance Plans (TT&QAP).^{6,7,8}

The sludge simulant required to complete this testing was procured from an off-site vendor. This simulant is being used to support all of the alternative flowsheet testing for the downselect process. The details regarding the simulant preparation and analysis have been documented separately.⁹ The simulant was based on Sludge Batch 6 with HM basis noble metal concentrations (Table 1-2).

Table 1-2. Mercury and noble metal concentrations

Element	Concentration, wt % (solids basis)
Hg	3.263
Ag	0.014
Pd	0.079
Rh	0.038
Ru	0.217

A total of twenty-two CPC simulations including SRAT and some SME cycles were performed. The first four tests were a baseline nitric-formic flowsheet, a baseline nitric-glycolic-formic flowsheet, a run without mercury and a run with Actinide Removal Process (ARP) and Modular Caustic Side Solvent Extraction (MCU) streams added. The second set of four simulations included tests at varying acid stoichiometries to define the acid processing window and one test without any formic acid (nitric/glycolic acid only) to determine the effectiveness of glycolic acid as a reductant. No SME cycle was performed on the glycolic acid only flowsheet simulation¹⁰. Four tests were completed to produce products with a REDOX of 0-0.3 to demonstrate REDOX control for this flowsheet. Four tests were completed at glycolic-formic acid blends of 40-70% glycolic acid to determine the iron solubility at varying glycolic acid blends. Lastly, two runs were completed without mercury and noble metals to determine the conditions for producing melter feed with the baseline and glycolic-formic flowsheets as described in Section 1.3. A more complete summary of the runs is included in Table 2-1.

Total boiling time in the SRAT cycles were calculated to remove mercury to 0.60 wt% in the total solids at a stripping rate of 750 lb steam/lb Hg at the scaled maximum DWPF design rate of 5000 lb/hr steam. Process samples were taken during the runs to monitor mercury concentration with time. Off-gas data were collected to monitor hydrogen as well as CO₂ and N₂O generation.

The amount of acid used in each simulation was calculated using the Koopman minimum acid equation.¹¹ A stoichiometric factor of 125% was used for the baseline runs and factors varying from 100% to 200% were used for the acid window testing. The Hsu equivalents for these runs are 135% stoichiometry for the baseline and 108% to 215% for the acid window runs. REDOX was targeted at $0.2 \text{ Fe}^{+2}/\Sigma\text{Fe}$ using a modified REDOX equation with a term for glycolate ion included.

1.3 Preparation of Melter Feed for Testing of Baseline, Glycolic-Formic and Sugar Flowsheets

A total of twenty-four shortened SRAT cycles were performed to produce sufficient melter feed to test the baseline, glycolic-formic and sugar flowsheets in the VSL DM10 melter. Approximately 100 kg (25 gallons) of SRAT product was produced for each flowsheet. No noble metals or mercury were added to the sludge in these experiments. The same simulant was used for each of these runs.

2.0 Experimental Procedure

The experimental apparatus used in these experiments is typical for DWPF SRAT/SME testing. The first twenty-two experiments were performed in 4-L kettles, while the twenty-four melter feed runs were performed in 22-L kettles. In experiments with noble metals and mercury, test equipment included a gas chromatograph to measure offgas composition, an ammonia scrubber, and a pH meter. In experiments without noble metals and mercury, the use of this equipment was omitted. The one exception to this is that a pH meter was used in the first sugar flowsheet melter feed preparation run. In all runs except the sugar flowsheet runs, the SRNL acid calculation spreadsheet used the Koopman Equation to determine acid addition quantities and dewater targets. In the sugar flowsheet runs, the run parameters were defined by the Vitreous State Laboratory (VSL)¹².

2.1 CPC Simulation Details

The first twenty-two glycolic-formic flowsheet tests were performed at the ACTL using the four-liter kettle setup. The last twenty-four melter feed preparation runs were performed at the ACTL using the 22-liter kettle setup. The SRAT rigs were assembled following the guidelines of SRNL-PSE-2006-00074¹³. The intent of the equipment is to functionally replicate the DWPF processing vessels. Each glass kettle is used to replicate both the SRAT and SME, and it is connected to the SRAT Condenser, the Mercury Water Wash Tank (MWWT), and the Formic Acid Vent Condenser (FAVC). The Slurry Mix Evaporator Condensate Tank (SMECT) is represented by a sampling bottle that is used to remove condensate through the MWWT. For the purposes of this paper, the condensers and wash tank are referred to as the offgas components. A sketch of the experimental setup is given as Figure 2-1.

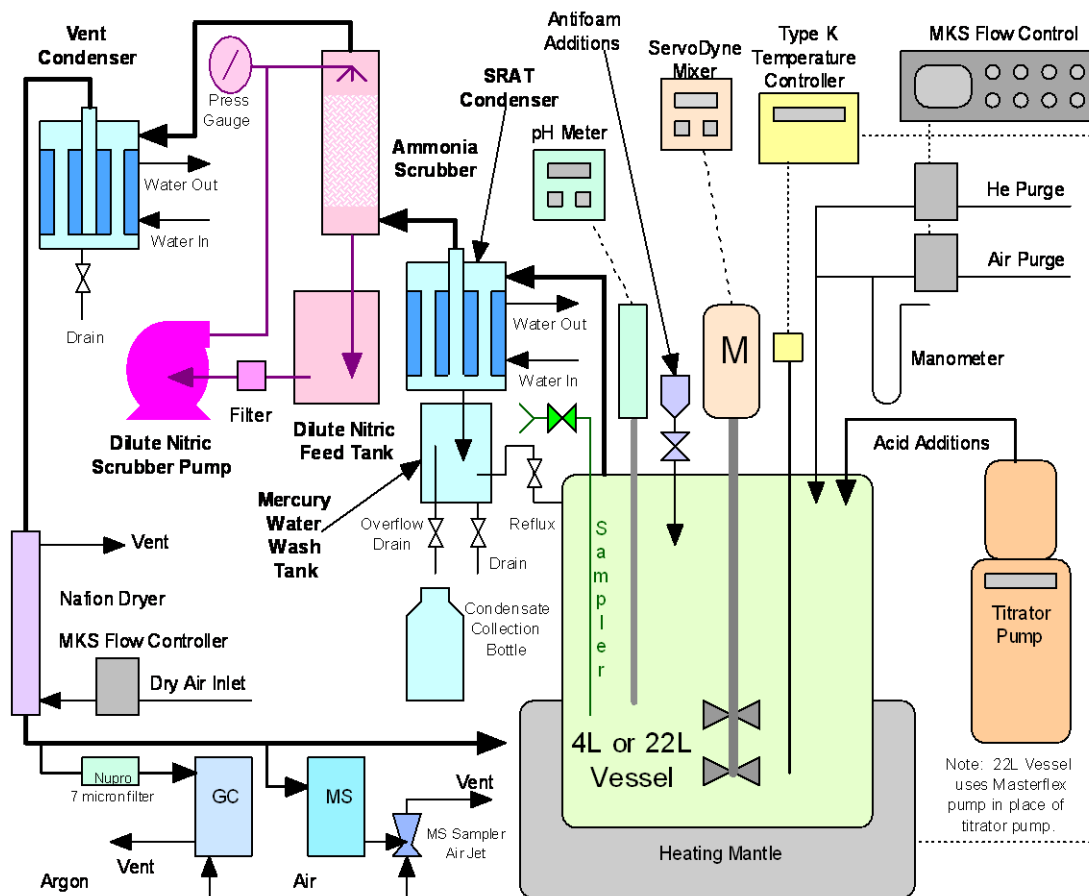


Figure 2-1. Schematic of SRAT Equipment Set-Up

The runs were performed using the guidance of Procedure ITS-0094¹⁴ (“Laboratory Scale Chemical Process Cell Simulations”) of Manual L29. In runs with noble metals and mercury, offgas hydrogen, oxygen, nitrogen, nitrous oxide, and carbon dioxide concentrations were measured during the experiments using in-line instrumentation. Nitrous dioxide was not measured but was calculated based on oxygen depletion. Helium was introduced at a concentration of 0.5% of the total air purge as an inert tracer gas so that total amounts of generated gas and peak generation rates could be calculated. This approach eliminates the impact of fugitive gas losses through small leaks on the calculated outlet gas flowrates. During the runs, the kettle was monitored to observe reactions that were occurring to include foaming, air entrainment, rheology changes, loss of heat transfer capabilities, and offgas carryover. Observations were recorded on data sheets and pasted into laboratory notebooks.^{15, 16}

Quality control measures were in place to qualify the data in this report. Helium and air purges were controlled using mass flow controllers calibrated by the SRNL calibration shop using NIST traceable standards and methods. Thermocouples were calibrated using a dry block calibrator. The GCs were calibrated with standard calibration gases. The pH probes were calibrated with pH 4 and pH 10 buffers and rechecked at the conclusion of each run using pH 4, 7 and 10 buffer solutions.

The automated data acquisition system developed for the 4-L SRAT rigs was used to collect data electronically. Data included SRAT temperature, bath temperatures for the cooling water to the SRAT condenser and Formic Acid Vent Condenser (FAVC), slurry pH, SRAT mixer speed and torque, and air and helium purge flows (He is used as an internal standard and is set to 0.5% of the nominal SRAT air purge flow). Cumulative acid addition volume data were collected from the automated dispensers using an algorithm that matches the indicated total on the dispenser. Raw GC data were acquired on separate computers dedicated to each instrument.

Dual column Agilent 3000A micro GC's were used on both runs. The GC's were baked out before and between runs. Column-A can collect data related to He, H₂, O₂, N₂, NO, and CO, while column-B can collect data related to CO₂, N₂O, and water. Calibrations were performed using a standard calibration gas containing 0.499 vol% He, 1.000 vol% H₂, 20.00 vol% O₂, 51.0 vol% N₂, 25.0 vol% CO₂ and 2.50 vol% N₂O. Instrument calibration was verified prior to starting the SRAT cycle. Room air was used to give a two point calibration for N₂. Calibration status was rechecked following the SRAT cycle.

Concentrated nitric acid (50-wt%), formic acid (90-wt%) and glycolic acid (70 wt%)-formic acid blends were used to acidify the sludge and perform neutralization and reduction reactions during processing. The amounts of acid to add for each run were determined using the Koopman acid equation.¹⁷ The split of the acid was determined using a modified version of the REDOX equation currently being used in DWPF processing.¹⁸ The first principles electron equivalents expression had a new term added for glycolate ion (see below). The REDOX target ($\text{Fe}^{2+}/\Sigma\text{Fe}$) was 0.2 for the majority of the runs. To account for the reactions and anion destructions that occur during processing, assumptions about nitrite destruction, nitrite to nitrate conversion, formate destruction, and glycolate destruction were made for each run.

To prevent foaming during SRAT processing, 200 ppm IIT 747 antifoam was added before acid addition, 100 ppm was added after nitric acid addition was complete and 500 ppm was added at the completion of formic acid addition. SRAT processing included 12-hours at boiling (dewater time plus reflux time). The SME processing did not include the addition of canister dewaterers. The frit addition was split into two equal portions. The frit was added with water and formic acid at DWPF prototypical conditions. Concentration was performed after each frit addition and then heat was removed to allow for the next frit addition. A final concentration was performed at the end of the run to meet the 50 weight percent total solids target. The SRAT condenser was maintained at 25° C during the run, while the vent condenser was maintained at 4° C.

In runs with noble metals and mercury, a standard 4-L SRAT/SME apparatus with an ammonia scrubber was used for these simulations. The scrubber solution consisted of 749 g of de-ionized water and 1 g of 50 wt% nitric acid. The solution was recirculated through the column by a MasterFlex pump at 300 mL/min through a spray nozzle at the top of the packed section. Glass rings were used as packing and did not significantly add to the back pressure on the SRAT vessel as has been seen in earlier tests with different packing.

Standard SRAT acid calculations were performed with a few modifications. The Koopman minimum acid equation was used with a 125% stoichiometric factor for the first set of all tests. The acid mix was partitioned between nitric and the formic/glycolic blend by utilizing the latest REDOX equation¹⁹ with a term added for glycolate. A coefficient of 6 was used on the glycolate term based on electron equivalence. The REDOX target for these runs was 0.2.

$$\text{REDOX} = 0.2358 + 0.1999 * ((2 * C_{\text{formate}} + 4 * C_{\text{oxalate}} + 4 * C_{\text{Carbon}} + 6 * C_{\text{glycolate}} - 5 * (C_{\text{Nitrate}} + C_{\text{Nitrite}}) - 5 * C_{\text{Mn}})) * (45/\text{TS})$$

Where C = species concentration, g-mole/kg melter feed, TS = total solids in melter feed in wt %, and REDOX is a molar ratio of $\text{Fe}^{2+}/\Sigma\text{Fe}$

Process assumptions were made to predict SME product anion concentrations. In addition to the standard assumptions needed for formate loss and nitrite to nitrate conversion, a factor was added to the acid calculation for glycolate loss. Process assumptions for the stoichiometric window testing were adjusted based on results from the first set of simulations.

2.2 CPC Run Details

The first twenty-two glycolic-formic flowsheet tests were performed at the ACTL using the four-liter kettle setup. The first four simulations (GF1-4) were developed to compare the existing nitric/formic flowsheet to the glycolic/formic flowsheet. The second set of four runs (GF5-8) was designed to determine the processing window of the glycolic-formic flowsheet by adjusting acid stoichiometry from 100% to 200% and testing the flowsheet without formic acid (GF8). The third set of four runs (GF9-12) was designed to determine how the form of the catalyst Ru impacted hydrogen generation. These runs are not pertinent to the flowsheet study so will not be discussed further in this report. The fourth set of four runs (GF13-16) was designed to demonstrate that glass produced from the formic-glycolic flowsheet did not have a steep, titration like change that would make REDOX control difficult. The fifth set of runs (GF17-20) was designed to determine what impact the glycolic/formic ratio would have on processing and especially hydrogen generation. The last two runs were designed to develop the processing parameters for melter feed preparation for VSL melt rate testing, before producing large batches of melter feed for the nitric/formic flowsheet (GF21) and the glycolic/formic flowsheet (GF22). The last twenty-four melter feed preparation runs, three sets of eight runs, were performed at the ACTL using the 22-liter kettle setup to produce approximately 100 kg of SRAT product for VSL testing of the nitric/formic flowsheet (GF23A-H), the glycolic/formic flowsheet (GF24A-H) and the sugar flowsheet (GF25A-H). Table 2-1 identifies each run and its corresponding assumptions.

Table 2-1. CPC Simulation Process Assumptions

Run	Objective	Cycles	Date	Acid Stoichiometry	Glycolic % moles	Formic % moles
GF1	Formic Baseline	SRAT/SME	17-May-10	125%	0	100
GF2	Glycolic Baseline No Hg	SRAT/SME	17-May-10	125%	80	20
GF3	Glycolic Baseline	SRAT/SME	19-May-10	125%	80	20
GF4	ARP	SRAT/SME	19-May-10	125%	80	20
GF5	150% Acid Stoichiometry	SRAT/SME	7-Jun-10	150%	80	20
GF6	100% Acid Stoichiometry	SRAT/SME	7-Jun-10	100%	80	20
GF7	200% Acid Stoichiometry	SRAT/SME	9-Jun-10	200%	80	20
GF8	125% Acid Stoichiometry	SRAT/SME	9-Jun-10	125%	100	0
GF9	Old Ru	SRAT	14-Jul-10	125%	0	100
GF10	New Ru	SRAT	14-Jul-10	125%	0	100
GF11	Old Ru	SRAT	21-Jul-10	198%	0	100
GF12	New Ru	SRAT	21-Jul-10	198%	0	100
GF13	REDOX Target 0	SRAT	25-Aug-10	100%	80	20
GF14	REDOX Target 0.2	SRAT	25-Aug-10	100%	80	20
GF15	REDOX Target 0.1	SRAT	16-Sep-10	100%	80	20
GF16	REDOX Target 0.3	SRAT	16-Sep-10	100%	80	20
GF17	40:60 Glycolic/Formic	SRAT	28-Sep-10	125%	40	60
GF18	50:50 Glycolic/Formic	SRAT	28-Sep-10	125%	50	50
GF19	70:30 Glycolic/Formic	SRAT	30-Sep-10	125%	70	30
GF20	60:40 Glycolic/Formic	SRAT	30-Sep-10	125%	60	40
GF21	Formic Baseline	SRAT	2-Nov-10	110%	0	100
GF22	80:20 Glycolic/Formic	SRAT	2-Nov-10	110%	80	20
GF23	Baseline Feed for VSL	SRAT	30 Nov to 6 Dec-10	110%	0	100
GF24	GF Feed for VSL	SRAT	8-14 Dec-10	110%	80	20
GF25	Sugar Feed for VSL	SRAT	8-14 Dec-10	73%	0	100

DWPF design basis processing conditions were scaled down and used for most processing parameters including: SRAT/SME air purges, acid addition rates, and boil-up rate. SRAT product total dried solids were targeted at 25 wt% for the baseline run. Final SME total dried solids were targeted at 45% at 36% waste loading.

The SRAT product solids targets were adjusted for the glycolic/formic flowsheet runs because of the mass of the glycolate ion. Because its molar mass is about 2/3 greater than formic, adding glycolic acid contributes an appreciable amount to SRAT product soluble (and thus total) solids. The glycolic/formic flowsheet SRAT product total dried solids targets were adjusted to higher total solids (same insoluble solids mass) in the SRAT product slurries. No adjustments were made to the SME cycle solids targets.

The melter feed preparation runs (GF21, 22, 23, 24 and 25) used abbreviated processing to allow completion of processing within a twelve-hour shift. To maximize throughput, the nitric and glycolic-formic were fed at the same molar flowrate as formic (a 2x increase in volumetric

flowrate for these more dilute acids). In addition, the boil-up rate was set at 100% power to maximize the boil-up rate. Since nitrite was destroyed prior to the concentration endpoint being reached and mercury stripping wasn't needed, the processing was complete when the concentration target was reached (calculated to be 45 wt% solids after the frit was added by VSL). No issues were noted that were associated with the higher acid feed rates. It is recommended that DWPF eventually modify the acid feed pumps to deliver the higher flow rates if the glycolic-formic flowsheet is implemented.

A flowsheet that could meet all the processing constraints would have to be a very robust flowsheet. The following constraints must be met by the DWPF CPC flowsheet:

- SRAT hydrogen <0.65 lb/hr
- SME hydrogen <0.223 lb/hr
- Reduce mercury to elemental form
- Steam strip mercury below 0.6 wt% in the SRAT product dried solids
- SRAT product less than 1000 mg nitrite/kg product slurry
- SRAT product rheology design basis 1.5 to 5 Pa yield stress and 5 to 12 cP consistency
- SME product rheology 2.5 to 15 Pa yield stress and 10 to 40 cP consistency
- Glass REDOX of 0.09-0.33 $F^{2+}/\Sigma Fe^{+2}/\Sigma Fe$
- Minimize water in SME product (45 wt% typical)
- Minimal foaming

Data are presented in Section 3 showing how the glycolic-formic flowsheet met or exceeded the processing constraints in the list above with the possible exception of REDOX.

2.3 Process Data Collection

In the 4-L experiments, an automated data acquisition system was used to collect run data every minute on a computer. In all experiments, the process data was manually recorded approximately every twenty minutes including SRAT slurry temperature, slurry pH, cooling water temperatures for the SRAT condenser and Formic Acid Vent Condenser (FAVC), SRAT mixer speed, air and helium purge rates, and raw gas chromatographs.

Agilent 3000 Series GC's were used on all simulations to measure the offgas composition. The GCs were baked out and calibrated with standard calibration gas between runs. Calibration was verified following the completion of the SME cycles.

2.4 Analytical Methods

Process samples were analyzed by various methods. Slurry and supernate elemental compositions were measured by inductively coupled plasma-atomic emission spectroscopy (ICP-AES) at the Process Science Analytical Laboratory (PSAL). Soluble anion concentrations were measured by Ion Chromatography (IC). Mercury concentration was measured by ICP-AES. Ammonium ion concentration on selected samples was measured by cation chromatography by SRNL Analytical Development (AD). Slurry and supernate densities were measured using an Anton-Parr instrument at PSAL. Reduction-Oxidation (REDOX) of glasses made from SME product slurries was measured by PSAL. Dewater and condensate samples were submitted to AD for volatile/semi-volatile organics analysis (VOA/SVOA).

A successful gradient method using the AG-11HC and AS-11HC, 2mm microbore columns was developed to run samples for the Alternative Reductant Demonstrations. The method provides good peak resolution for all nine anions. The method that will be used to analyze fluoride,

glycolate, formate, chloride, nitrite, nitrate, sulfate, oxalate and phosphate on SRAT/SME samples is as follows (Table 2-2):

Table 2-2. Final Ion Chromatography Method for Glycolate and Other Anions

Instrument	DX500
Columns	2mm AG-11HC, 2mm AS-11HC
Suppressor	ASRS-300, 2mm
Carbonate Removal Device	CRD-20, 2mm
Injection Loop	25 microliter
Calibration Standards	Three point calibration (0.1, 0.5, 1 ppm fluoride, 1, 5, 10 ppm for all other anions)
Gradient Run, Concentration (NaOH)	Time
1.8mM → 30mM Ramp	0-40 minutes
30mM → 1.8mM Ramp	40-50 minutes
Detection Limit	Lowest calibration standard

2.4.1 Issues with analytical method

Organic anions at low concentrations (1 ppm, 5 ppm, 10 ppm) degrade over a short period of time. Due to the potential degradation, it is our recommendation to keep all organic anion standards (manufacturer and calibration) refrigerated and in the dark. New calibration standards should be made every time the instrument is calibrated.

The run time is significantly long due to the request for phosphate. The stability of phosphate when analyzing SRAT and SME samples is extremely sensitive due to the high transition metals (i.e. iron) that build up in the columns. Phosphate has a tendency to bind with the transition metals creating erroneous readings. Also, the transition metals can create peak tailing. This often creates poor accuracy of calibration check standards at the end of sample runs. Phosphate is never above detection limit of the IC for typical SRAT/SME samples and is reported as a less than value. A recommendation is to obtain phosphorus by ICP-AES and remove phosphate from the list of requested anions. This could decrease run time significantly.

Another solution to significantly decrease run time is for DWPF to purchase a new ICS-5000 system that could run multiple methods simultaneously on one sample injection. For example, one method could be set up to elute the first three anions (fluoride, formate and glycolate) slowly off the column to obtain results and another method run to quickly elute these three anions off the column (no peak separation obtained) and then get good separation for the other six anions in 10-20 minutes. The same solution could be obtained on DWPF's two ICS-3000 systems.

The potential of fluoride interfering with glycolate can be a problem. Over time, baseline peak separation can diminish and a large fluoride peak in the calibration standards can create error in the glycolate analyses, if fluoride is not present. Fluoride in SRAT/SME samples is always below detection. A recommendation is to eliminate this peak to decrease the potential analytical error with glycolate.

3.0 Results and Discussion

Primary SRAT/SME simulation analytical data from the glycolic-formic acid flowsheet testing will be presented in the following sections and supplemental data will be included in the Appendices as necessary. The testing is divided into the following segments:

1. Feasibility of Flowsheet (GF1 to GF8)
 - a. Flowsheet development GF1 to GF4 and GF8
 - b. Acid Stoichiometry Window (GF3, GF5 to GF7)
2. Ruthenium Catalyst Testing (GF9 to GF12). Data will not be presented as it is not pertinent to decision.
3. REDOX Target Testing (GF13 to GF16)
4. Optimum Glycolic-Formic Ratio (GF1, GF17, GF18, GF20, GF19, GF8)
5. Melter Feed Preparation (GF21 to GF25)

The focus of the study was on proving the glycolic/formic flowsheet could meet all current CPC processing objectives, most notably effective removal of mercury in the SRAT while simultaneously reducing hydrogen generation. Much of the data presented here will be a comparison between the two baseline flowsheet cases, GF1 and GF3. These are the only runs performed under the same conditions with both flowsheets and therefore the only direct point of comparison. Data for GF6, the 100% stoichiometry nitric/glycolic/formic run, will also be presented because it appears that running at lower acid stoichiometry is more appropriate for the new flowsheet.

3.1 Small-scale Laboratory Results (SRNL)

Twenty-two 4-L Laboratory Scale experiments (GF1 to GF22) were completed to develop the optimum glycolic-formic acid flowsheet for DWPF. Twenty-four 22-L Pilot Scale experiments (GF23A-H, GF24A-H and GF25A-H) were performed to prepare melter feed for VSL testing.

The testing was completed under very challenging conditions. First, the testing used a SB6 slurry produced for SRNL by Harrell Industries. This slurry was very rheologically viscous. During SRAT processing, the pH dropped from about 13 to pH 3 or 4. The slurry actually thickened as the pH dropped to near neutral (pH 7) so mixing of this slurry was very challenging. In addition, conservative concentrations of mercury and noble metals were added. This led to high hydrogen and ammonia generation along with the depletion of anion species (nitrate and formate) that are important to glass REDOX.

3.1.1 SRAT Offgas

Besides essentially eliminating hydrogen generation, the glycolic/formic acid flowsheet also appears to stop or significantly slow down other off-gas generating reactions. The graphs below compare N₂O (Figure 3-1) and CO₂ (Figure 3-2) generation rates for the two baseline flowsheet cases (GF1 for the nitric/formic flowsheet and GF3 for the glycolic-formic flowsheet. The rapid fluctuations, especially in the nitric/formic case, can be attributed to the mixing issues experienced during acid addition.

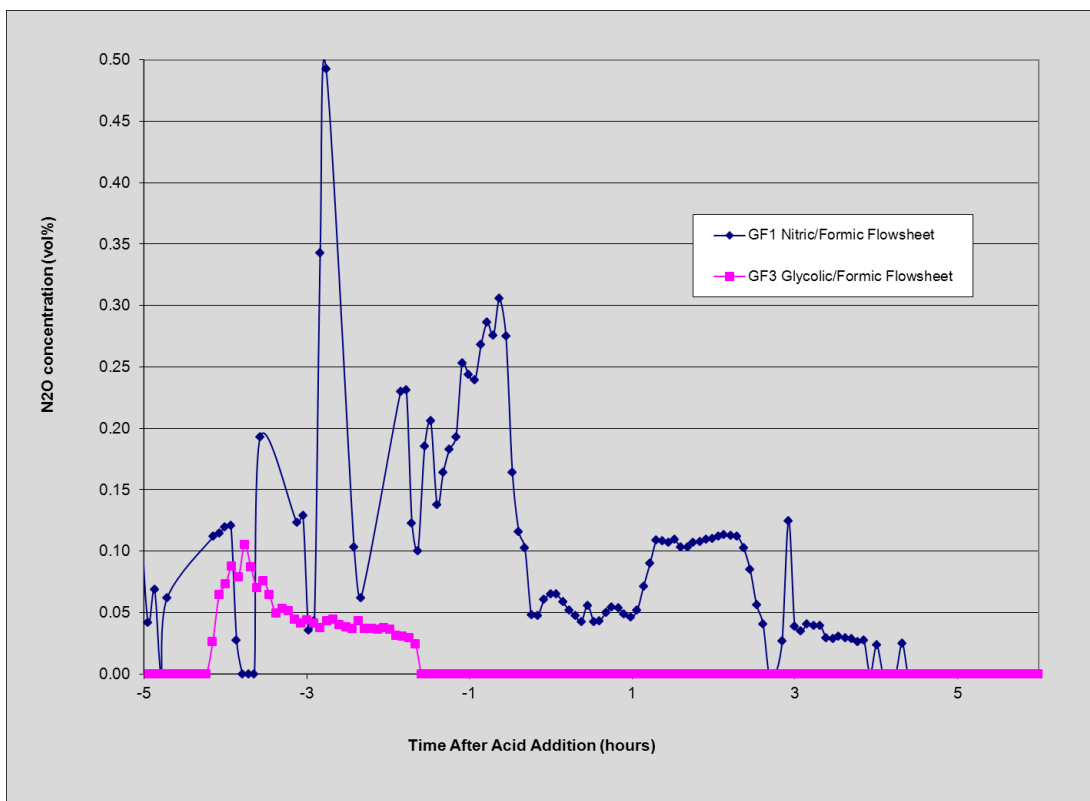


Figure 3-1. SRAT cycle N₂O generation

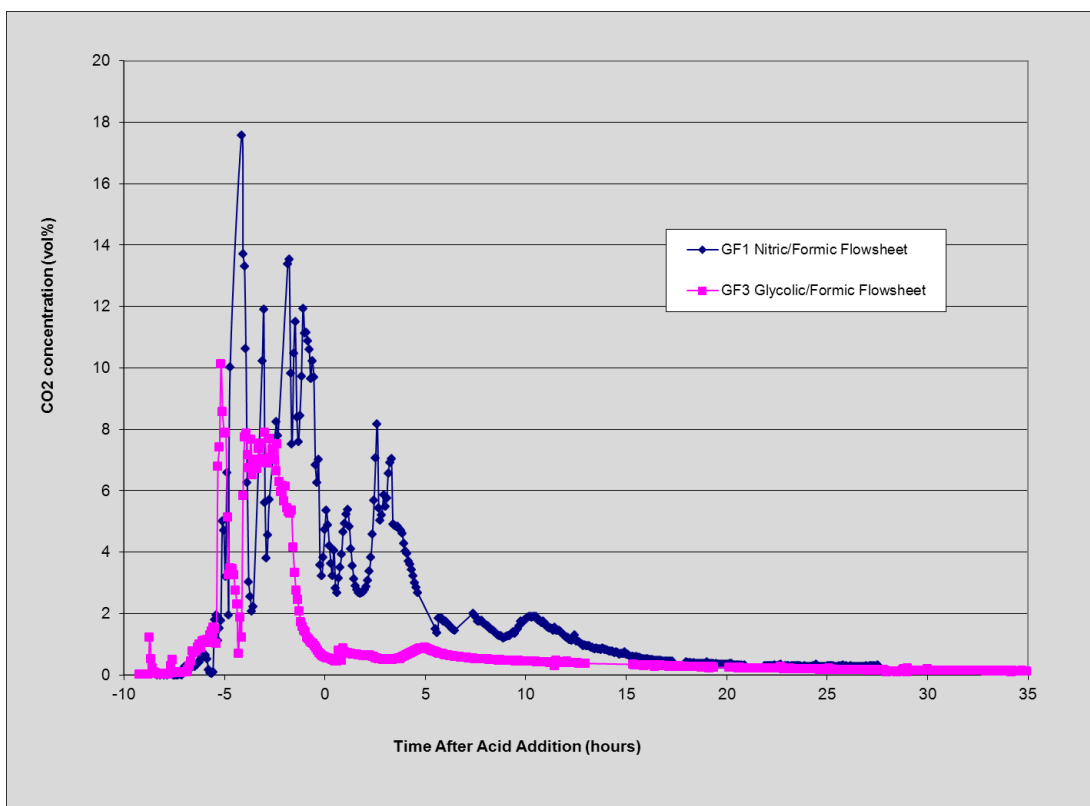


Figure 3-2. SRAT cycle CO₂ generation

It is worth noting that some of the GC data were impacted by mixing issues (meaning peaks on the DWPF flow versus time graphs were less intense than otherwise). Additional off-gas data for other GF simulations can be found in Appendix A3 or in the preliminary reports. Lower generation of N_2O and H_2 were noted in the nitric/glycolic/formic flowsheet runs. GF6 (Figure 3-3) is shown below as an example.

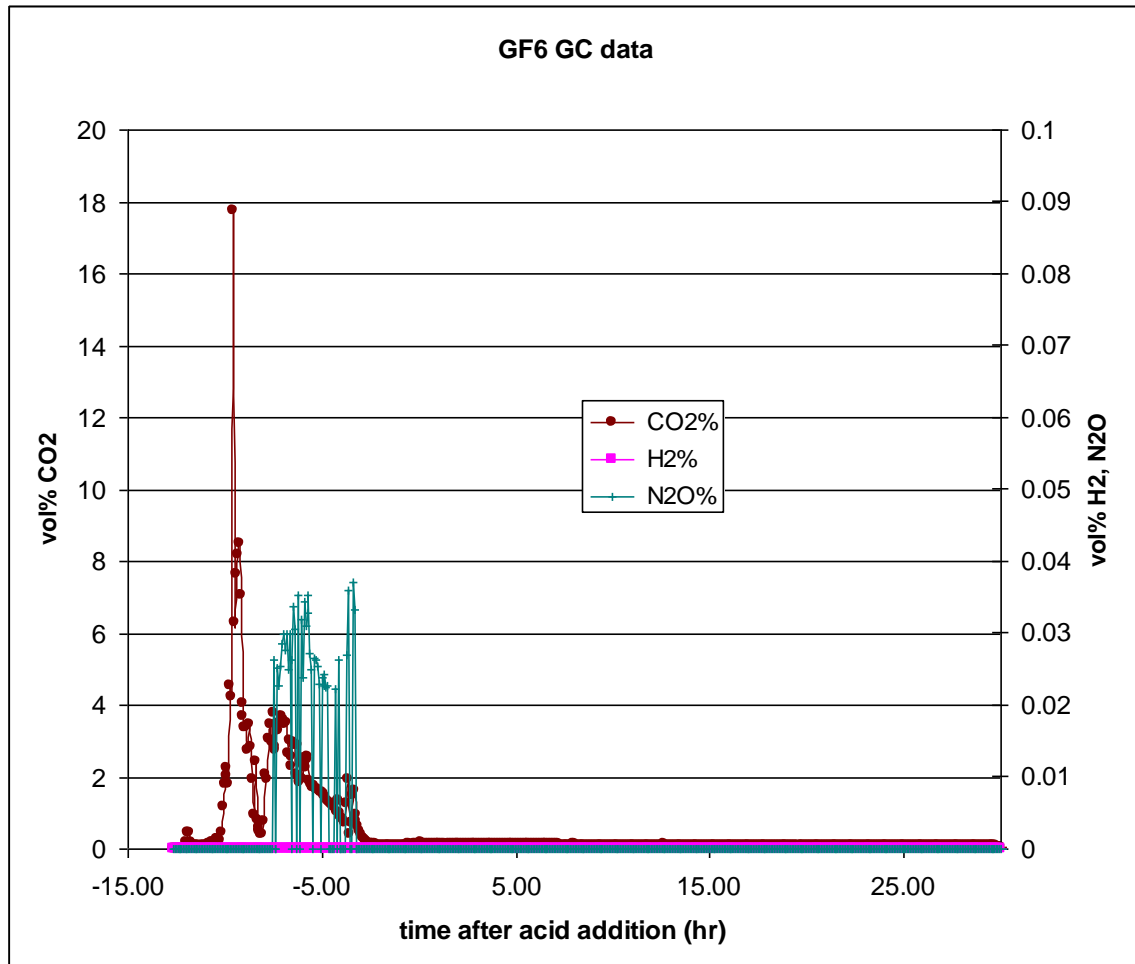


Figure 3-3. GF6 GC Data

3.1.2 SRAT Chemistry

The chemistry in the glycolic-formic SRAT cycle was very similar to the chemistry in the baseline flowsheet. However, there are a few areas where the chemistry is significantly different and these will be described below:

- The hydrogen generation in the glycolic-formic flowsheet was significantly lower compared to the baseline flowsheet. This will be discussed in Section 3.1.3.
- The formate destruction in the glycolic-formic flowsheet was significantly lower compared to the baseline flowsheet. This will be discussed in Section 3.1.2. This led to much lower carbon dioxide generation in the glycolic-formic flowsheet.
- The glycolic-formic flowsheet is much better at dissolving metals compared to the baseline flowsheet. This led to substantially lower yield stress SRAT and SME products but also led to significant dissolution of metals such as iron and gadolinium which have been used to provide criticality control. This will be discussed in Section 3.1.2.3.

- There are several flowsheet controls that could be useful in processing future sludge batches. First, a ratio of 4 moles of glycolic per mole of formic was used throughout much of the testing. However, this ratio could be adjusted as needed to optimize processing. For sludge batches with higher mercury or noble metals, using glycolic acid without formic acid would minimize the hydrogen generation while still reducing the mercury content of the SRAT product to meet target. In rheologically challenging slurries, higher acid stoichiometry and a higher glycolic ratio would produce a rheologically thinner product. However, since lower acid stoichiometries exhibited acceptable rheological products, targeting a lower acid stoichiometry (possibly lower than 100% Koopman Stoichiometry) likely will produce optimum processing conditions.

3.1.2.1 SRAT Product Data

General SRAT product data for the first eight runs are tabulated below (Table 3-1).

Table 3-1. SRAT Product Anions, Solids, **Density**, and pH Data

anions (mg/kg)	GF1	GF2	GF3	GF4	GF5	GF6	GF7	GF8
fluoride	<100	<100	<100	<100	<100	<100	<100	<100
chloride	1085	1040	976	839	1002	1230	890	1210
nitrite	<100	<100	<100	<100	<100	<100	<100	<100
nitrate	25000	51600	55950	53100	59900	42250	59900	56250
sulfate	1920	1680	1765	2120	3275	2565	3280	3485
glycolate	<100	53950	55400	56850	114500	65050	161500	118500
oxalate	296	649	2405	3910	2775	3395	1645	4680
formate	12900	2555	<100	<100	824	776	3750	<100
phosphate	<100	<100	<100	<100	<100	<100	<100	<100
wt% total solids	17.53%	21.77%	21.79%	22.32%	24.03%	25.59%	21.75%	24.62%
wt% calcined solids	12.19%	11.37%	11.36%	11.86%	12.02%	14.13%	10.20%	12.47%
wt% insoluble solids	11.01%	8.76%	8.98%	8.84%	10.23%	11.20%	5.96%	10.83%
wt% soluble solids	6.53%	13.01%	12.80%	13.48%	13.80%	14.39%	15.79%	13.80%
density (g/mL)	1.084	1.163	1.158	1.161	1.166	1.187	1.138	1.178
pH at 25°C	4.24	4.01	3.99	4.07	3.17	5.04	3.01	3.02

The oxalate results are of particular interest. The starting sludge contains about 800 mg/kg oxalate, which could be partially destroyed catalytically during the SRAT cycle. In the glycolic/formic flowsheet runs, however, oxalate is being created. It is possible that glycolic acid is oxidized to glyoxylic acid (HCOCO_2H) by nitrite or MnO_2 , which is further oxidized to oxalic acid by the reduction of mercury. This also would explain the lack of oxalate generation in the run without mercury, GF2.

These runs represent the first time that glycolate ion measurements were performed on actual SRAT/SME products, as opposed to spiked samples and simple solutions. A separate report has been drafted detailing the glycolate IC method development.²⁰ It appears from the data presented here that the second set of runs (GF5-8) may be biased high in glycolate. The 65,050 mg/kg

measured for GF6 represents 99.6% of the total moles of glycolate added during the SRAT. This is unrealistically high, especially if the proposed pathway for oxalate formation is correct. The results for GF5-8 show more glycolate in the SRAT product than was added. Resolving this issue so that reliable glycolate data is available will be especially important for refining the REDOX model as flowsheet development continues.

Anion balance data for nitrite, nitrate, formate and glycolate are presented in the table below for runs GF1-4 (Table 3-2).

Table 3-2. Anion Balance Data

	GF1	GF2	GF3	GF4	GF5	GF6	GF7	GF8
SRAT Formate Destruction (%)	78.7	71.4	100	100	94.0	92.1	71.3	N/A
SRAT Nitrite Destruction (%)	100	100	100	100	100	100	100	100
SRAT Glycolate Destruction (%)	N/A	9.3	11.7	4.5	-24	0.4	-85	-80
SRAT Nitrite to Nitrate Conversion (%)	18.9	44.4	51.4	46.4	-0.2	27.1	-3.2	73.5
SME Formate Destruction (%)	-3.5	44.3	100	41.5	61.8	42.6	62.2	N/A
SME Nitrate Destruction (%)	25.6	9.7	9.3	9.9	-2.5	10.1	21.8	N/A
SME Glycolate Destruction (%)	N/A	5.4	9.3	5.3	15.1	4.9	35.8	N/A

SRAT (Table 3-3) and SME (Table 3-4) product elemental data are summarized in the following tables.

Table 3-3. SRAT Product Elemental Data, wt % calcined solids basis

<i>element</i>	GF1	GF2	GF3	GF4	GF5	GF6	GF7	GF8
Al	16.5	16.3	16.1	14.2	16.4	16.3	16.7	16.6
B	<0.100	0.1	<0.100	<0.100	<0.100	<0.100	<0.100	<0.100
Ba	0.07	0.04	0.05	0.08	0.04	0.04	0.04	0.04
Ca	0.60	0.53	0.54	0.66	0.57	0.59	0.57	0.56
Cd	0.08	0.04	0.04	0.03	<0.010	<0.010	<0.010	<0.010
Ce	<0.010	<0.010	<0.010	<0.010	<0.010	<0.010	<0.010	<0.010
Cr	0.12	0.12	0.12	0.11	0.13	0.13	0.13	0.16
Cu	0.23	0.25	0.23	0.19	0.25	0.16	0.27	0.26
Fe	19.2	19.3	19.2	17.1	18.6	18.4	18.7	18.7
K	0.04	0.17	0.03	0.03	0.03	0.03	0.06	0.03
La	<0.010	<0.010	<0.010	<0.010	<0.010	<0.010	<0.010	<0.010
Li	<0.100	0.06	<0.100	<0.100	<0.100	<0.100	<0.100	<0.100
Mg	0.46	0.46	0.46	0.50	0.47	0.47	0.48	0.48
Mn	6.44	6.29	6.48	5.39	6.29	6.47	6.34	6.39
Mo	<0.010	<0.010	<0.010	<0.010	<0.010	<0.010	<0.010	<0.010
Na	15.55	15.45	15.60	16.45	15.69	16.44	16.03	15.99
Ni	2.68	2.70	2.69	2.16	2.63	2.65	2.66	2.68
P	<0.010	<0.010	<0.010	<0.010	<0.010	<0.010	<0.010	<0.010
S	0.43	0.46	0.48	0.53	0.46	0.47	0.46	0.42
Si	0.22	0.17	0.16	0.32	0.20	0.16	0.21	0.23
Sr	0.03	0.03	0.03	0.02	0.08	0.08	0.08	0.08
Ti	0.02	0.02	0.02	3.13	0.01	0.01	0.01	0.01
Zn	<0.010	<0.010	<0.010	<0.010	0.01	0.01	0.01	<0.010
Zr	0.25	0.24	0.24	0.23	0.26	0.25	0.26	0.23

Note – GF4 is the run with ARP/MCU and contains MST as a source of titanium

Table 3-4. SME Product Elemental Data, wt % calcined solids basis

<i>Element</i>	GF1	GF2	GF3	GF4	GF5	GF6	GF7
Al	6.17	6.02	5.87	5.13	6.03	5.71	6.08
B	1.44	1.52	1.45	1.48	1.26	1.22	1.20
Ba	0.03	0.01	0.02	0.03	<0.010	<0.010	<0.010
Ca	0.15	0.17	0.16	0.23	0.23	0.24	0.24
Cd	0.03	<0.010	<0.010	<0.010	<0.010	<0.010	<0.010
Ce	<0.010	<0.010	<0.010	<0.010	<0.010	<0.010	<0.010
Cr	0.06	0.05	0.05	0.05	0.05	0.05	0.05
Cu	0.11	0.09	0.09	0.09	0.07	0.05	0.15
Fe	7.27	6.77	7.04	6.08	7.35	6.86	6.78
K	0.06	0.12	0.05	0.05	0.06	0.05	0.10
La	<0.010	<0.010	<0.010	<0.010	<0.010	<0.010	<0.010
Li	2.15	2.28	2.19	2.21	2.22	2.15	2.12
Mg	0.19	0.19	0.18	0.20	0.20	0.20	0.20
Mn	2.31	2.26	2.22	1.83	2.58	2.41	2.32
Mo	<0.010	<0.010	<0.010	<0.010	<0.010	<0.010	<0.010
Na	9.71	9.78	9.37	10.15	9.39	9.53	9.69
Ni	0.87	0.75	0.75	0.60	0.80	0.81	0.93
P	0.02	<0.010	<0.010	<0.010	<0.010	<0.010	<0.010
S	0.16	0.14	0.14	0.14	0.16	0.15	0.14
Si	22.92	23.69	23.69	23.67	23.46	23.71	23.02
Sr	<0.010	<0.010	<0.010	<0.010	0.03	0.03	0.04
Ti	0.04	0.05	0.04	1.02	0.03	0.03	0.03
Zn	<0.010	0.01	<0.010	0.01	<0.010	<0.010	<0.010
Zr	0.17	0.17	0.16	0.24	0.20	0.19	0.19

3.1.2.2 SRAT Dissolution of Metals as a function of acid stoichiometry

Glycolic acid is currently used commercially to descale heat exchanger surfaces (DuPont uses a mixture of 2 parts glycolic acid and 1 part formic acid) and to dissolve rust. So it is not surprising that the glycolic acid dissolves a number of metals in sludge. Glycolic acid is added to paints and emulsions to give them “better flow properties”. Dissolution of metals can be a good thing as it can greatly lower the yield stress of the slurry and allow further concentration of the slurry. As a result, the use of glycolic acid has the potential to allow processing of slurries that could not be processed with the baseline flowsheet. In our testing, the glassware stayed much cleaner in the experiments with the glycolic-formic flowsheet. This was especially true in the melter feed preparation runs where four runs were completed sequentially in the same 22-L glass vessel with no cleaning between runs.

However, the higher the glycolic to formic ratio, the more metals were dissolved. The addition of glycolic acid in the glycolic-formic flowsheet runs caused some elements that are traditionally insoluble to become soluble. Al, Ca, Cu, Fe, Mg, Mn, Ni, Si, Sr, and Zr are much more soluble in the formic-glycolic flowsheet runs. Of particular concern is iron and gadolinium solubility because criticality control at DWPF is based on iron and plutonium not partitioning between the solids and supernate. The chart below (Figure 3-4) shows iron solubility as a function of acid stoichiometry for the nitric/glycolic/formic acid flowsheet (GF3) and the baseline nitric/formic run (GF1) as a point of comparison. It should be noted that metals such as Fe and Gd dissolve and reprecipitate during processing so the percent soluble can change throughout a run.

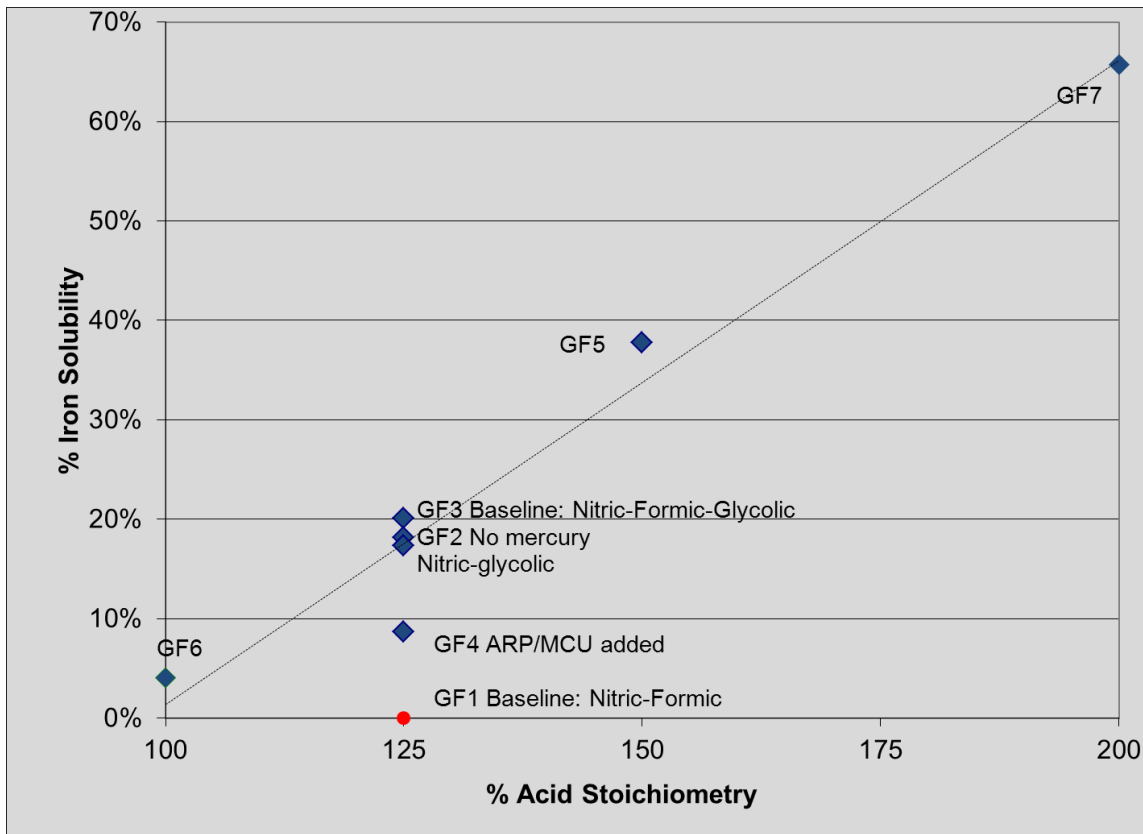


Figure 3-4. Iron solubility as a function of acid stoichiometry

Other elements also show significantly higher solubility in the glycolic/formic flowsheet runs. The table below shows the amount of each element found in the SRAT product supernate expressed as a percentage of the total element present. These data are calculated by dividing the supernate concentration by the total slurry fraction of each element. Numbers greater than 100% are not physically possible and are a result of error in one of the analytical measurements used in the calculation. Note that the table is grouped to put the acid stoichiometry in order to compare the solubility with stoichiometry. Also, the GF4 data (ARP run) and GF8 data (100% glycolic acid run) are grouped at the bottom of the table (Table 3-5).

Table 3-5. Acid Stoichiometry Study: SRAT Product Supernate % of Element Dissolved

Run	% Acid	Al	Ca	Cu	Fe	Mg	Mn	Ni	Si	Sr	Zr
Baseline	125	0.0%	8.8%	0.0%	0.0%	1.8%	0.0%	0.0%	22.6%	0.0%	0.0%
GF6	100	2.2%	116%	20.8%	4.1%	44.0%	99.0%	29.3%	39.1%	84.7%	17.7%
GF2	125	4.9%	131%	83.5%	18.1%	70.1%	82.6%	58.9%	42.1%	87.8%	45.7%
GF3	125	4.9%	128%	92.0%	20.1%	73.2%	82.1%	61.7%	45.2%	89.9%	47.7%
GF5	150	5.3%	130%	104%	37.7%	84.6%	72.0%	89.6%	51.0%	99.1%	55.7%
GF7	200	14.5%	138%	109%	65.7%	92.4%	91.2%	92.7%	117%	107%	82.0%
GF4 (ARP)	125	5.9%	97.6%	69.2%	8.7%	72.9%	62.4%	45.8%	31.1%	64.1%	9.8%
GF8	125	9.4%	129%	95.9%	17.3%	79.6%	71.2%	81.5%	39.2%	93.6%	60.7%

Data for the “baseline” case element dissolutions are not typical of most recent sludge batch testing. This difference is presumably due to the HM levels of noble metals that consumed over 70% of the formic acid in the SRAT and led to a SRAT product pH of about eight. These conditions are typically associated with significant absorption of the CO₂ by-product of formate destruction and subsequent reprecipitation of Ca, Mg, and Mn from the SRAT supernate during reflux.

The zirconium dissolution data in the GF flowsheet runs could impact future SRS accelerated closure projects, such as Small Column Ion Exchange, which use crystalline silicotitanate (CST) ion exchange resin. The binder material in CST contains zirconium, so the GF flowsheet might actively break down the CST binder material in the SRAT.

3.1.2.3 SRAT Dissolution of Metals as a *Function* of Glycolic-Formic Acid Ratio

Seven glycolic-formic flowsheet runs were completed to determine the optimum ratio of formic acid to glycolic acid for this flowsheet as this ratio was adjusted from 0% glycolic (baseline) to 100% glycolic (GF8). In earlier testing, glycolic did not reduce mercury. As a result, it was assumed that some formic acid was needed to reduce mercury. Elemental mercury can be steam stripped during SRAT processing so that the SRAT product mercury concentration would be less than the processing limit. However, the mercury target was met, even in the run with no added formic acid (GF8). Therefore any glycolic to formic ratio should be acceptable for mercury removal. Processing at a lower glycolic to formic ratio (more formic acid) leads to higher hydrogen generation. Processing at a lower acid stoichiometry and with a lower glycolic to formic ratio would cause fewer metals to become soluble.

In addition, most of the metals became at least partially soluble as the percentage of glycolic acid increased from 0 to 100%. For example, aluminum went from being essentially insoluble in the baseline flowsheet to dissolving almost 10% of the Al with 100% glycolic acid. Iron went from being essentially insoluble in the baseline flowsheet to dissolving almost 20% of the Fe with 100% glycolic acid. The solubility of many of the elements, including Ca, Cu, Mg, Mn, Ni and Zr increased as the % glycolic acid increased, approaching 100% solubility. As a result, the primary insoluble solids left in the SRAT product were aluminum and iron (Table 3-6, Figure 3-5). This data could be used to optimize the glycolic-formic ratio to minimize hydrogen and iron solubility.

**Table 3-6. Glycolic Ratio: SRAT Product Supernate % of Element Dissolved at 125%
Koopman Stoichiometry**

Run	% Glycolic	Al	Ca	Cu	Fe	Mg	Mn	Ni	Si	Zr
Baseline	0	0.0%	8.8%	0.0%	0.0%	1.8%	0.0%	0.0%	22.6%	0.0%
GF17	40	0.3%	113%	14.2%	0.2%	41.2%	44.1%	0.1%	16.0%	1.4%
GF18	50	0.7%	123%	4%	2.0%	64.8%	84.9%	10.4%	21.4%	3.9%
GF20	60	1.2%	122%	10%	9.4%	61.0%	94.1%	37.2%	25.4%	23.7%
GF19	70	3.0%	123%	62.1%	15.6%	65.8%	92.5%	52.0%	28.6%	42.4%
GF3	80	4.9%	128%	92.0%	20.1%	73.2%	82.1%	61.7%	45.2%	47.7%
GF8	100	9.4%	129%	95.9%	17.3%	79.6%	71.2%	81.5%	39.2%	60.7%

Note that the calcium data in tables 3-5 and 3-6 are quite unusual, but are typical of the results seen in the runs with glycolic acid. Calcium extents of dissolution in the 50-80% range are more typical of sludge batch testing with the formic acid flowsheet. It is not clear at this time whether slurry total calcium may be coming in artificially low or supernate calcium artificially high leading the percent dissolutions in the 120-130% range.

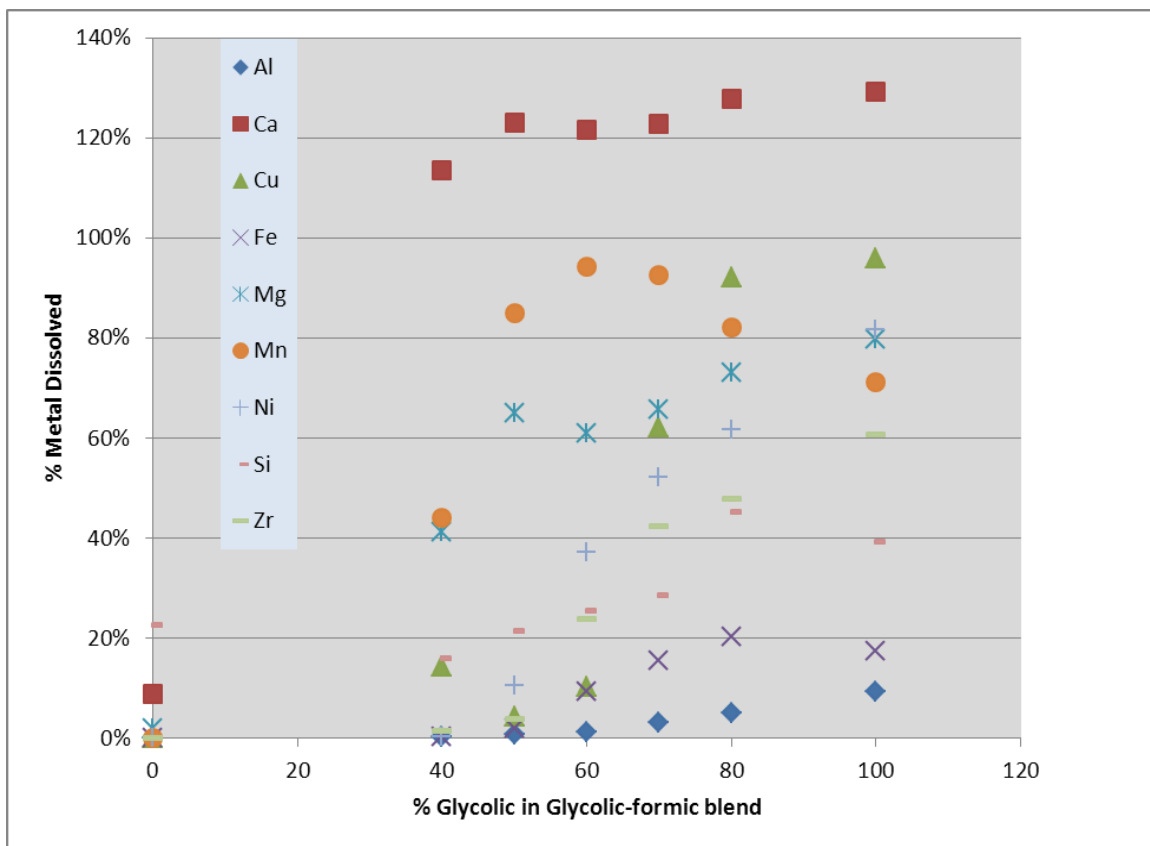


Figure 3-5. Metal solubility as a function of % glycolic acid in blend

Gadolinium may be used as a substitute neutron poison in the Tank Farm. This would allow the addition of Pu into the sludge batches without causing a potential criticality in DWPF. Testing

was completed using the baseline flowsheet and glycolic-formic flowsheet²¹ to determine the solubility of metals, including iron and gadolinium.

Gadolinium solubility is related to solution pH (the lower the pH the higher the gadolinium solubility). In the glycolic-formic flowsheet runs with simulant, the SRAT and SME product pH may be less than 4, so >80% of the gadolinium is soluble. Iron in the baseline nitric/formic acid simulant runs is approximately 20% soluble. In the one run with actual waste the iron solubility was close to zero, suggesting that the iron produced in simulant development is more readily solubilized than the iron in the actual waste. Thus, gadolinium may not be an effective neutron poison for the glycolic formic flowsheet. Figure 3-6 and 3-7 summarizes the iron and gadolinium solubility in simulant experiments for both flowsheets. Note that run SB6-29 is a baseline flowsheet run from another study. SB6-29 used the SB6-E sludge simulant, not the SB6-H sludge simulant used for all GF runs²¹.

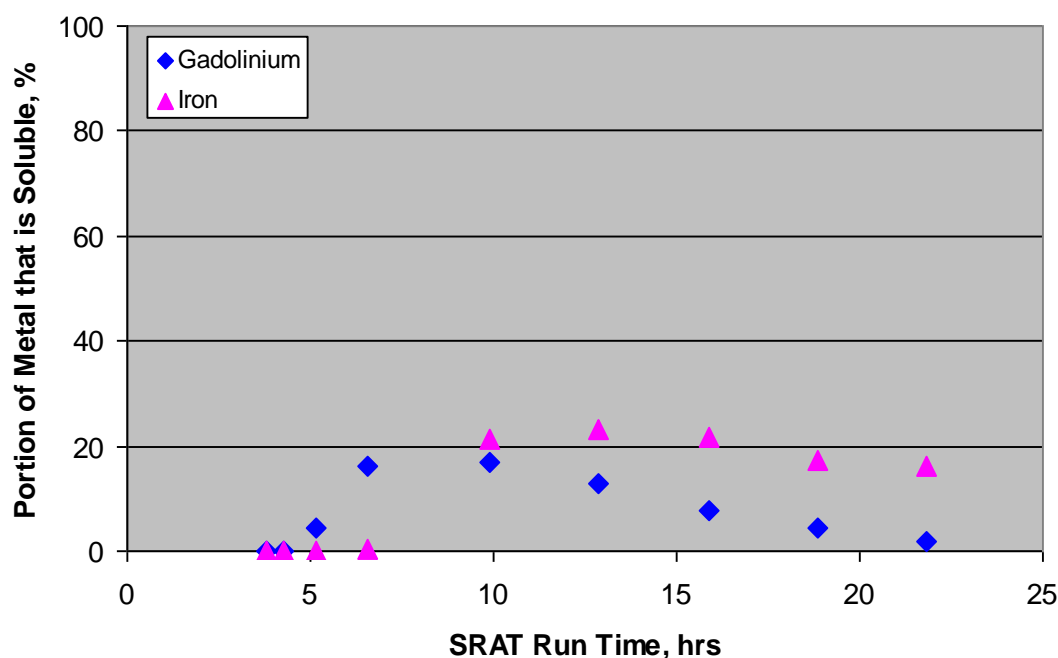


Figure 3-6. Iron and Gadolinium Solubility in SB6-29

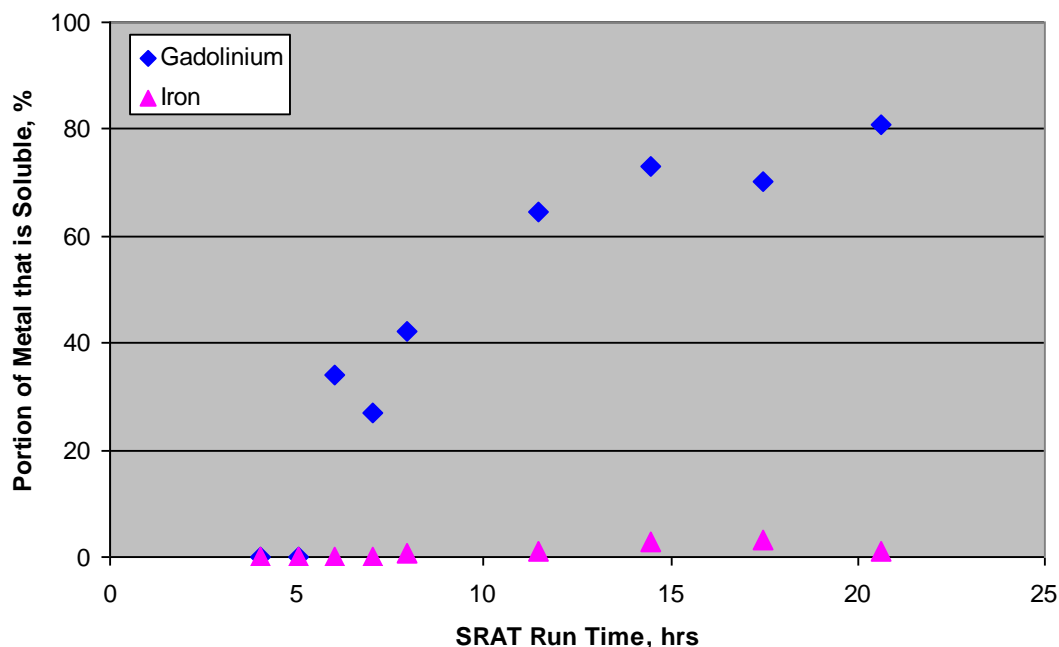


Figure 3-7. Iron and Gadolinium Solubility in GF13

3.1.2.4 SRAT Degradation Products

Condensate samples were analyzed by SRNL AD for volatile and semi-volatile organics to ensure that there are no new degradation products formed by glycolic acid that could present downstream issues to the Tank Farm. No semi-volatile organics were found in any of the samples. Small amounts (ranging from 5-15 mg/L) of siloxanes, primarily hexamethyldisiloxane, were found in all the samples. This is consistent with antifoam degradation and is not unique to the glycolic/formic acid flowsheet.

Irradiation testing is currently being completed on SRAT simulant supernate to determine whether polymerization of the glycolic acid occurs due to irradiation simulating storage in the DWPF SRAT and SME²². Introducing glycolic acid to high radiation doses may cause some polymerization of the glycolic acid in an oxygen depleted atmosphere. Results will be reported when complete.

3.1.3 SRAT Hydrogen Suppression

The main objective of this flowsheet testing was to show that hydrogen generation could be mitigated or eliminated by the use of the glycolic/formic flowsheet. In the first six simulations with the glycolic/formic flowsheet and mercury, hydrogen concentration in the off-gas never exceeded 0.03 volume percent in the SRAT cycle. When formic acid was added with the frit in the SME cycle, hydrogen generation on the order of 0.2 volume percent was noted in the 200% stoichiometry case, GF7. This can be compared to the baseline nitric/formic flowsheet run where hydrogen concentration in the SRAT exceeded the DWPF design basis limit of 0.65 lb/hr (>2 volume percent). Table 3-7 compares SRAT and SME cycle hydrogen on a DWPF scale. In the

one run with 100% glycolic acid (no formic acid), no hydrogen was detected at any time throughout the SRAT cycle. This run did not have a SME cycle.

Table 3-7. Hydrogen Generation

Run	% Acid Stoichiometry	Note	Glycolic: Formic	SRAT Hydrogen, lb/hr DWPF Scale	SME Hydrogen, lb/hr DWPF Scale
GF1	125	Baseline	0:100	1.614	0.007
GF2	125	No Hg	80:20	0.106	0.171
GF3	125	GF Baseline	80:20	0.006	0.004
GF4	125	ARP/MCU	80:20	0.004	0.003
GF5	150	GF Higher Acid	80:20	0.008	0.013
GF6	100	GF Lowest Acid	80:20	0.013	0.012
GF7	200	GF Highest Acid	80:20	0.024	0.049
GF8	125	100% Glycolic	100:0	0.000	NA
GF13	100	0 REDOX	80:20	0.000	NA
GF14	100	0.2 REDOX	80:20	0.008	NA
GF15	100	0.1 REDOX	80:20	0.005	NA
GF16	100	0.3 REDOX	80:20	0.006	NA
GF17	125	40 % Glycolic	40:60	0.547	NA
GF18	125	50 % Glycolic	50:50	0.198	NA
GF19	125	70 % Glycolic	70:30	0.021	NA
GF20	125	60 % Glycolic	60:40	0.068	NA

The highest hydrogen generation in the Glycolic-formic runs occurred in the runs with the highest formic acid ratio (Runs GF17-20 varied the glycolic-formic ratio). Run GF17 (40% glycolic, 60% formic acid blend) had the highest hydrogen generation at 0.547 lb/hr DWPF scale of any of the glycolic-formic acid runs. The data is summarized in Figure 3-8.

The peak hydrogen generation in the baseline run (GF1) was 260 times higher than in the glycolic-formic run with mercury and noble metals (GF3). The hydrogen profile in the SRAT cycles is summarized in Figure 3-9 for the SRAT cycle and Figure 3-10 for the SME cycle.

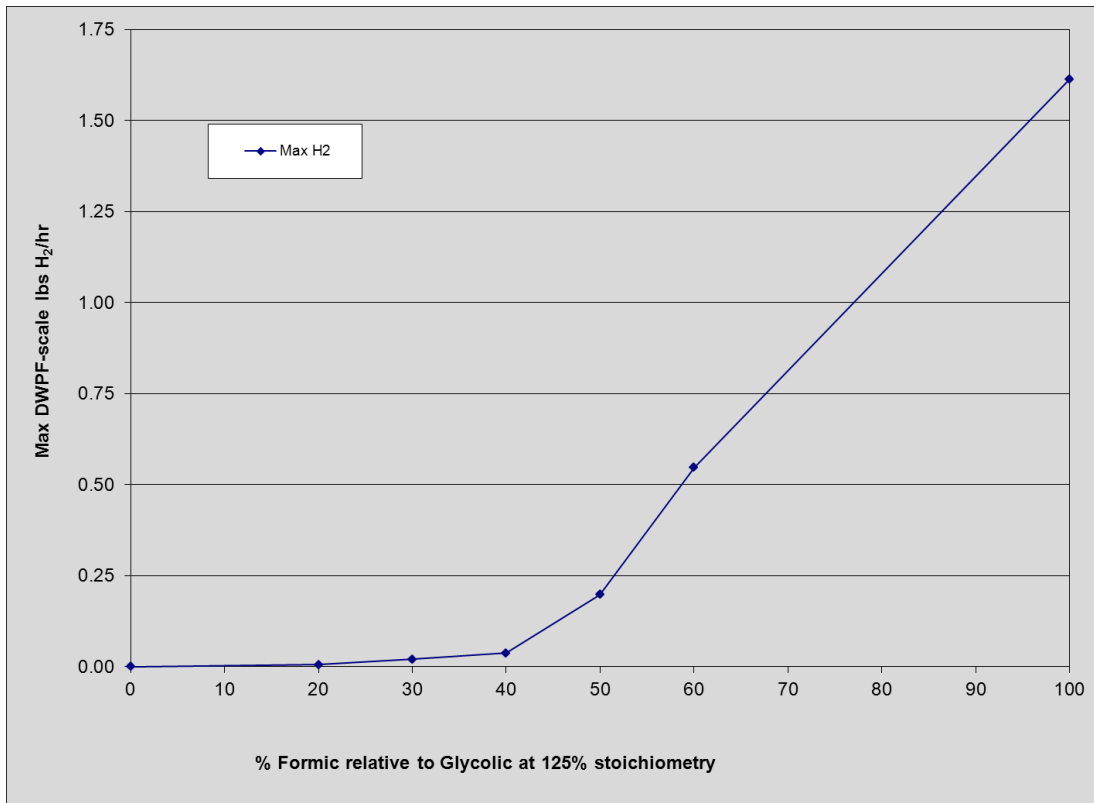


Figure 3-8. Max Hydrogen Generation Relative to mol% Formic in Formic/Glycolic blend

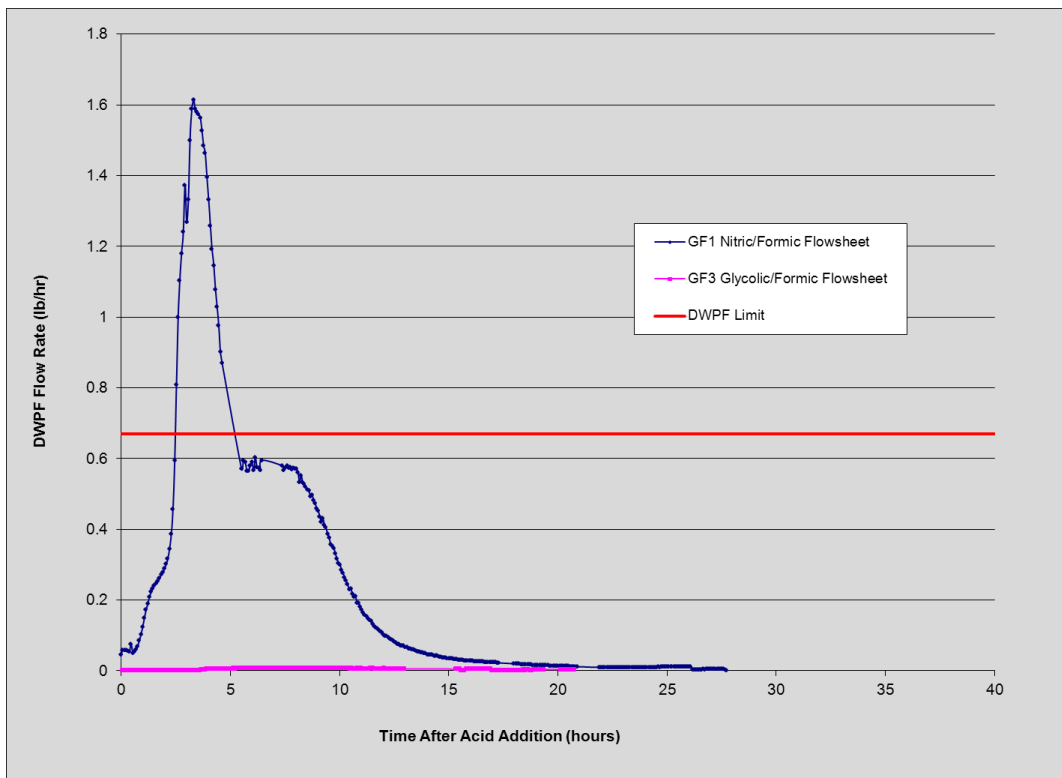


Figure 3-9. Baseline SRAT cycle hydrogen generation (GF1 vs. GF3)

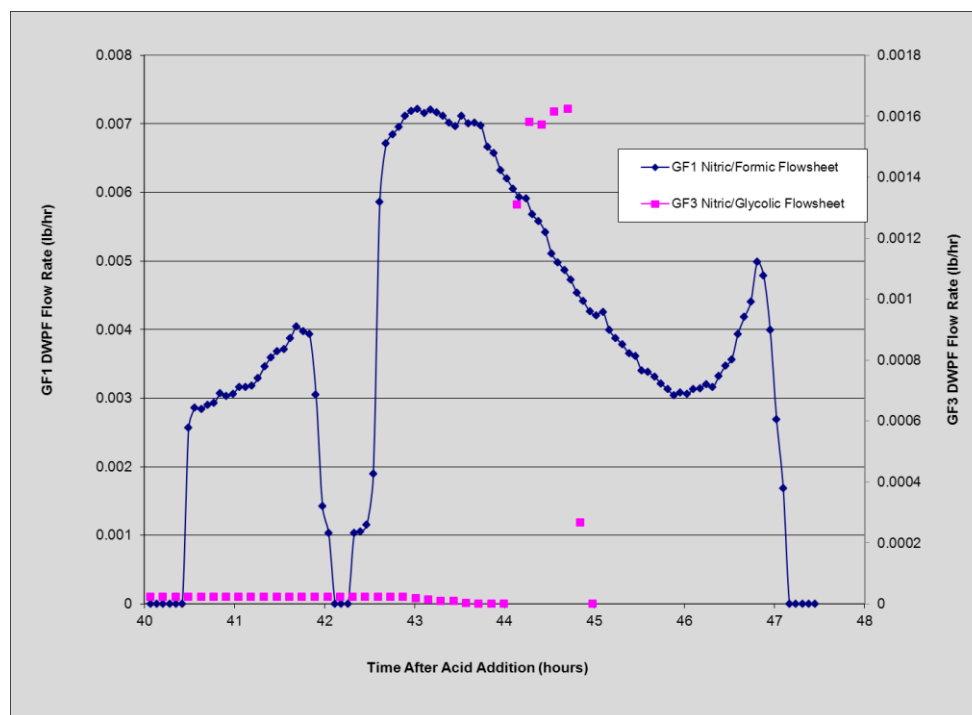


Figure 3-10. Baseline SME Cycle Hydrogen Generation (GF1 vs. GF3)

Without mercury present (GF2), more hydrogen was generated by processing with the glycolic/formic flowsheet (Figure 3-11). This is consistent with testing of the baseline flowsheet²³. Hydrogen generation was slowly increasing near the end of reflux and appeared to plateau at a maximum of about 0.14 volume percent at the end of the SRAT cycle (peak hydrogen was 17 times higher in run without mercury than in GF3). More hydrogen was generated in the SME cycle; with a maximum near 0.65 volume percent (peak hydrogen was 46 times higher in run without mercury). This is likely in part due to formic acid added with the frit. The hydrogen generation profile for the no mercury run is shown in the figure below.

Note that these runs were performed with HM levels of noble metals and mercury which leads to a high hydrogen generation rate. The maximum hydrogen generation rate is dependent on the noble metal and mercury concentration for a given sludge batch. Actual noble metal concentrations are likely to be significantly lower than were used in this testing.

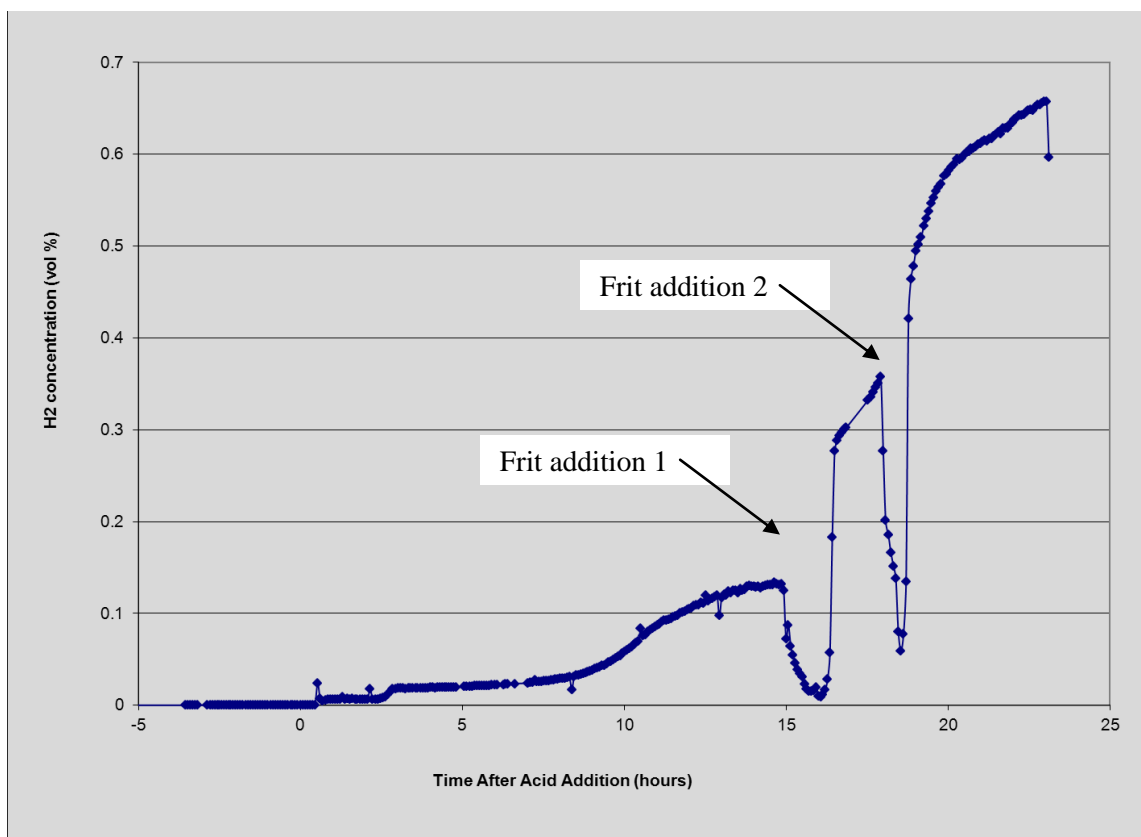


Figure 3-11. GF2 (no Hg) hydrogen generation

Other graphs of hydrogen, CO₂, and N₂O generation, can be found, i.e. in previously issued reports or in the Appendix A3 of this report.

3.1.4 SRAT Carbon and Nitrogen Balance

A carbon and nitrogen balance was completed. The results for runs GF1 (baseline formic flowsheet) and GF3 (Baseline Glycolic-formic Flowsheet) will be discussed and are included in Appendix A.4. After each run, a SRAT product, SME product and a composite condensate sample were pulled and analyzed for anions and ammonium. The ammonium concentration in the SRAT and SME products was less than the detectable limit (500 or 1000 mg/L). In addition, samples were submitted from the ammonia scrubber liquid (the condensate from the runs was not drained to the SMECT nor recirculated through the scrubber) and FAVC for ammonium analysis. Ammonium ion was found in the condensates and scrubber liquid samples although it was below the detection limit in the slurry samples due to sodium interferences. The inputs to the mass balance are summarized in the Tables 3-8 to 3-10 below.

Table 3-8. SRAT Carbon and Nitrogen Species in Offgas, g

Run	GF1	GF2	GF3	GF4	GF5	GF6	GF7	GF8
% Glycolic:% Formic	0:100	80:20	80:20	80:20	80:20	80:20	80:20	100:0
Acid Stoichiometry, %	125	125	125	125	150	100	200	125
Nitrous Oxide (N ₂ O)	1.15	0.50	0.13	0.19	0.14	0.49	0.01	0.00
Nitrogen Oxide (NO ₂)	93.4	44.7	84.4	52.7	25.0	35.2	45.5	NA
Nitric Oxide (NO)	0.08	0.99	0.05	1.06	0.07	2.63	1.60	14.6
Carbon Dioxide	105.0	33.4	38.5	35.7	40.7	37.4	62.4	0.076

Table 3-9. Carbon and Nitrogen Species in Sludge, g

Run	All Runs
TIC	2.82
Oxalate	2.30
Nitrate	17.33
Nitrite	47.32

Table 3-10. SRAT Carbon and Nitrogen added as Acids, g

Run	GF1	GF2	GF3	GF4	GF5	GF6	GF7	GF8
Formic Acid	182.71	26.74	26.51	24.09	30.64	23.01	41.36	0.00
Nitric Acid	41.38	112.85	112.66	94.00	143.16	77.76	187.45	125.82
Glycolic Acid	0.00	176.71	175.19	159.25	202.54	152.10	273.36	203.11

3.1.4.1 SRAT Cycle Carbon Balance

A number of carbon species are present in the sludge simulant (TIC, TOC, and oxalate). Carbon is added during SRAT processing as formic acid, glycolic acid, and antifoam. The carbon added with the antifoam will be ignored as it is a minor contributor. Carbon is also added during the SME processing as formic acid although this again is a minor contributor. The organic acids can decompose to smaller organic species such as formate, oxalate, carbonate, CO and CO₂. Instrumentation to quantify CO was not available for this testing. The primary source of carbon in both flowsheets is the formic and glycolic acid added. The overall carbon balance is summarized in Table 3-11.

Table 3-11. Carbon and Nitrogen Overall Balance

Run	GF1 C	GF3 C	GF1 N	GF3 N
Sludge, g	3.8	3.8	20.1	20.3
Acid, g	47.6	67.4	22.5	25.0
Total In, g	51.4	71.3	42.6	45.3
Offgas, g	29.7	11.0	19.1	11.7
Product, g	8.3	46.6	11.5	28.8
Condensate, g	0.2	0.2	0.1	0.1
Total Out, g	38.2	57.8	35.1	40.8
% Closure	74	81	82	90

3.1.4.2 SRAT Cycle Nitrogen Balance

A number of nitrogen species are present in the sludge (nitrite, nitrate). Nitrogen is added during SRAT processing as nitric acid. No nitrogen is added during the SME cycle. The major decomposition species of nitrate and nitrite include nitrous oxide, nitric oxide, nitrogen oxide, and ammonium. In addition, nitrogen gas could be produced but there is no way to quantify this using an air purge as this is a small quantity compared to the nitrogen present. In addition, NO₂ cannot be measured with the GC so its concentration was calculated by assuming that 2 moles of NO₂ were produced for each mole of oxygen consumed. It is obvious in these runs that a large quantity of NO₂ is produced since the offgas turns orange during acid driven nitrite destruction. However, there are other reactions that consume oxygen so this method may overestimate the NO₂ production. The overall carbon balance is summarized in Table 3-11. The baseline formic flowsheet (GF1) produces about 10 times as much nitrous oxide and ammonia and twice as much nitric oxide as the glycolic-formic flowsheet. The glycolic-formic flowsheet produces almost exclusively NO₂.

3.1.5 SRAT and SME Rheology

The rheology of the sludge simulant made testing very challenging. The initial sludge has a yield stress of 31.5 Pa and a consistency of 11.8 cP. This feed slurry exceeds the DWPF SRAT receipt design basis of 1-10 Pa. The high yield stress feed was expected to impact the yield stress values of the SRAT and SME products. During acidification in the SRAT, the slurry yield stress increases and reaches a maximum at approximately pH 7 (Figure 3-12). During all testing, this was a challenging processing segment and often required periodically turning the agitator off and back on to prevent the acids from pooling in the vessel. A software tool was added to the 4-L control computer to allow the automated turning off and turning on of agitation. In the 22-L vessels, a second agitator blade was added. In addition, the acid is fed below the liquid surface in the 22-L kettles so no pooling of acids was apparent.

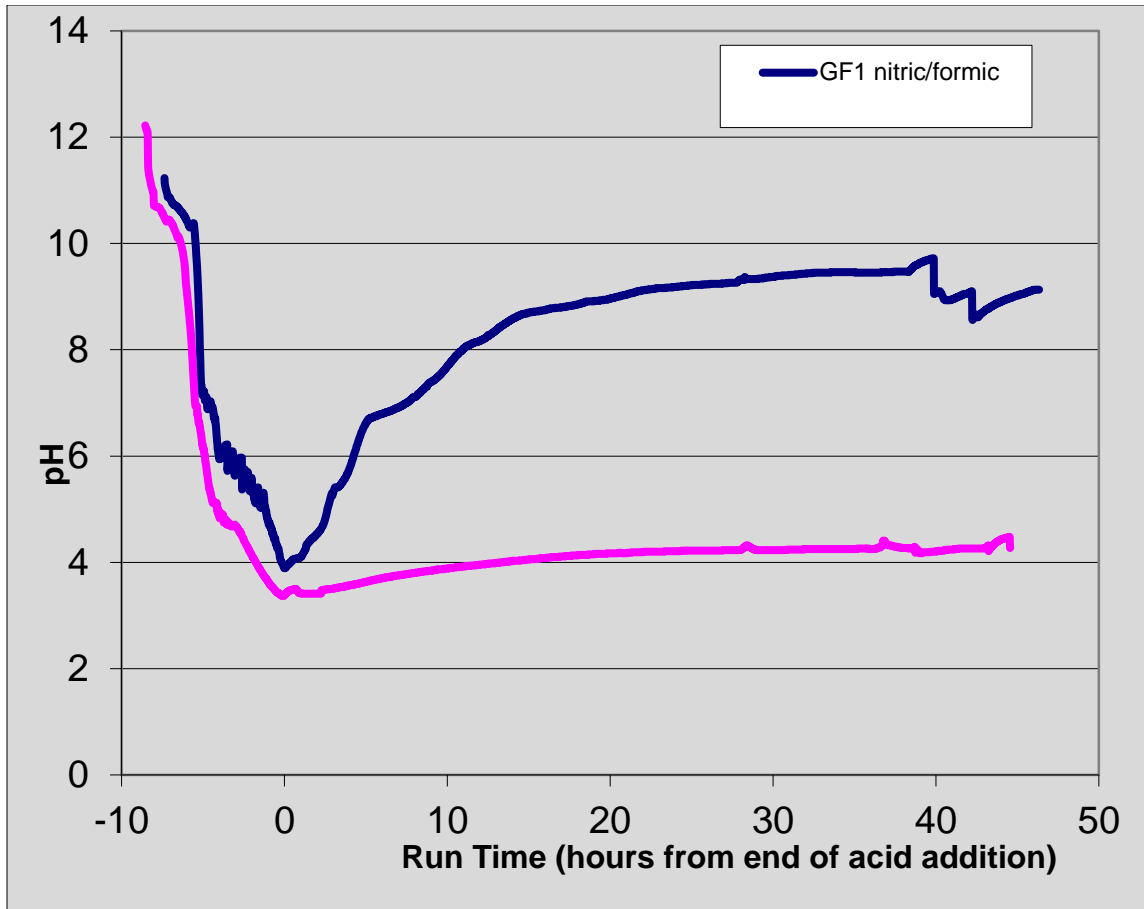


Figure 3-12. pH trends for baseline SRAT/SME runs with mercury and noble metals

Once the pH of slurry dropped below 6, the slurry thinned considerably. In the baseline formic flowsheet, as was noted in Figure 3-12, the pH slowly increased during SRAT processing until it reached a pH of 9.5 at the end of the SRAT cycle. The SRAT product had a yield stress of 33 Pa and a consistency of 22 cP, exceeding DWPF SRAT design bases for both yield stress and consistency. The glycolic-formic flowsheet pH did not change appreciably after acid addition during SRAT processing. The SRAT product had a yield stress of 1.6 Pa and a consistency of 7.1 cP. These properties constitute a relatively low viscosity SRAT product. Flow curves for the SRAT and SME products were obtained by using a Haake RS600 rheometer and the current DWPF simulant rheology protocol²⁴. The up and down curves (Figure 3-12) were fit to a Bingham plastic model to determine yield stress and consistency. Down flow curve data are the generally preferred choice for comparisons between systems. The data for all runs are tabulated below for the SRAT (Table 3-12) and SME (Table 3-13) along with a graphical comparison of the SRAT product yield stress (Figure 3-14) for the first seven runs.

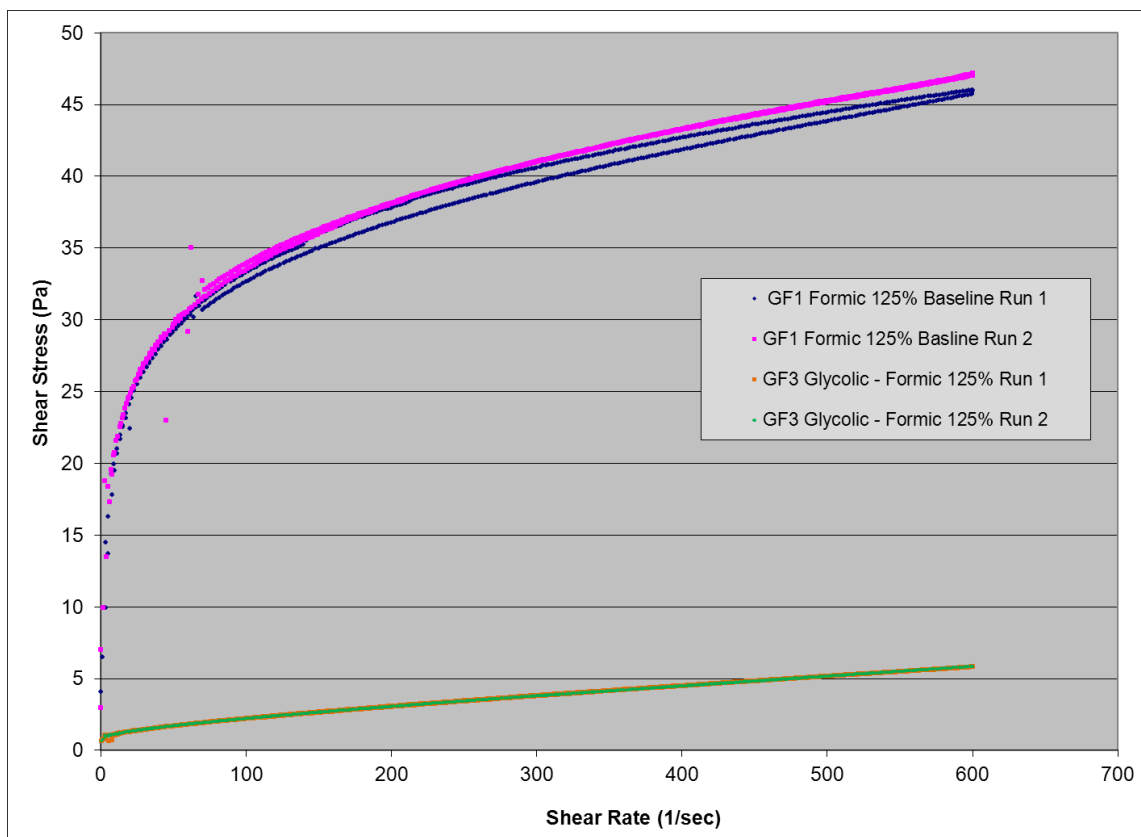


Figure 3-13. SRAT Product flow curve comparison for GF1 and GF3

Table 3-12. SRAT Product Rheology Summary

Rheology	GF1	GF2	GF3	GF4	GF5	GF6	GF7	GF8
Up yield stress, Pa	33.8	1.3	1.6	0.9	2.8	6.1	7.7	1.5
Up consistency, cP	22.2	6.6	7.1	5.0	10.1	14.8	10.3	6.4
Down yield stress, Pa	33.1	1.3	1.6	0.9	2.9	6.0	6.9	1.5
Down consistency, cP	22.8	6.6	7.1	5.0	10.0	14.7	11.0	6.4

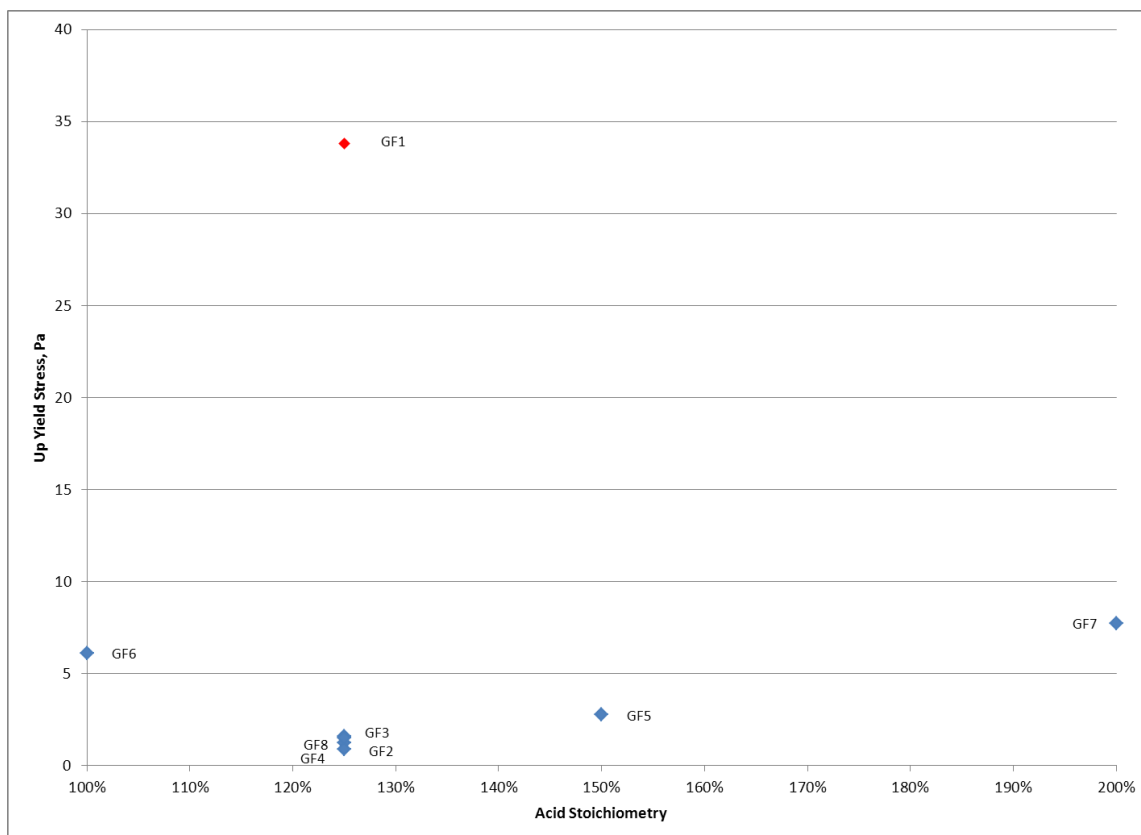


Figure 3-14. SRAT Product Rheology

Table 3-13. SME Product Rheology Summary

Rheology	GF1	GF2	GF3	GF4	GF5	GF6	GF7
Up yield stress, Pa	334.4	6.1	6.7	3.5	22.1	32.0	44.0
Up consistency, cP	-63.6	22.5	24.5	17.3	58.3	85.4	60.9
Down yield stress, Pa	223.0	6.8	7.2	3.3	23.9	30.2	41.4
Down consistency, cP	289.0	21.7	24.1	18.3	51.9	89.2	69.2

The lower yield stress was initially believed to be the result of the SRAT product differences of the two flowsheets. However, in producing melter feed for melt rate testing, shortened SRAT cycles were used to produce melter feed (runs GF23, baseline flowsheet, GF24, glycolic-formic flowsheet, GF25, sugar flowsheet). Each of these feeds was produced to target total solids of 45 wt% after the addition of frit. The final pH was 4.1 for the baseline flowsheet and 3.1 for the glycolic-formic flowsheet. In spite of similar pH profiles and SRAT product pH, the glycolic-formic flowsheet was much thinner rheologically than the baseline flowsheet. The yield stress of the glycolic-formic flowsheet is about one-third that of the other flowsheets. The rheology is summarized in Table 3-14. It is likely that the dissolution of metals, not pH is the major factor in the lower rheology for the glycolic-formic flowsheet. However, it should also be noted that there were higher yield stresses at higher acid stoichiometry.

Table 3-14. Melter Feed Rheology Summary

Flowsheet	Baseline		Glycolic-formic		Sugar	Rheology
Run	GF21	GF23	GF22	GF24	GF25	Limits
Up yield stress, Pa	103	93	35	37	101	2.5-15
Up consistency, cP	44	41	43	27	38	10-40
Down yield stress, Pa	87	81	27	26	89	2.5-15
Down consistency, cP	62	56	49	40	55	10-40

The baseline nitric/formic flowsheet run far exceeds both the SRAT and SME design basis limits for yield stress and consistency. The formic/glycolic flowsheet run was also higher than limits but still fluid. The negative value for SME consistency in the baseline run indicates a large hump in the up curve; therefore the values for the down curve are more representative. Yield stress for GF7 is higher than that for GF5 or GF6 despite having more acid added and lower insoluble solids. This could be because the slurry chemistry is different at such a high acid stoichiometry or it could be sampling or analytical error. Additional rheology graphs are included in Appendix A2.

3.1.6 SRAT Acid Stoichiometry

Four glycolic-formic flowsheet runs were completed to develop an operating window for this flowsheet. Note that with the baseline formic flowsheet, no window was found. A wide acid stoichiometry window allows processing flexibility during DWPF operations. The stoichiometry window for the glycolic-formic flowsheet is at least from 100% to 200% of Koopman minimum acid demand. This is wider than any flowsheet that SRNL has developed for DWPF since sludge batch 1A (125-300). Generally the window for the formic acid flowsheet is limited by hydrogen and rheology, while the glycolic-formic flowsheet was not. The data are summarized in Table 3-15. Nitrite was successfully destroyed in all of these runs.

Table 3-15. Acid Stoichiometry, Hydrogen Generation and Rheology

Run	Limit	GF6	GF3	GF5	GF7
Acid Stoichiometry	NA	100%	125%	150%	200%
SRAT Hydrogen, lb/hr DWPF Scale	0.65	0.013	0.006	0.008	0.024
SME Hydrogen, lb/hr DWPF Scale	0.23	0.012	0.004	0.013	0.049
SRAT product yield stress, Pa	1.5-5	6.1	1.6	2.9	7.3
SRAT product consistency, cP	5-12	14.8	7.1	10.3	10.6
SME product yield stress, Pa	2.5-15	31.1	6.9	23.0	42.5
SME product consistency, cP	10-40	87.3	24.3	55.1	65.1

3.1.7 SRAT/SME REDOX

SME product samples were vitrified in nepheline sealed crucibles and the resulting glasses measured for REDOX ($\text{Fe}^{2+}/\Sigma\text{Fe}$)²⁵. The REDOX target for all the simulations in this study was 0.2 (except for runs GF13 to GF16 discussed below). The target is achieved by predicting the SME product anion concentrations and adjusting the split of acids between nitric and

glycolic/formic. Therefore the ability to hit a REDOX target is highly dependent on being able to accurately predict anion behavior in the SRAT and SME cycles. Inserting the SME product data into the latest REDOX correlation gives a “predicted” REDOX that is different than the targeted REDOX of 0.2.

The REDOX prediction equation used in this study with an added term for glycolate is²⁶:

$$\text{Fe}^{2+}/\Sigma\text{Fe} = 0.2358 + 0.1999 * (2[\text{F}] + 4[\text{C}] + 6 [\text{G}] + 4[\text{O}_\text{T}] + 5[\text{N}] - 5[\text{Mn}])45/\text{T}$$

Where
 [F] = formate (mol/kg feed)
 [C] = coal (carbon) (mol/kg feed)
 [O_T] = oxalate_{Total} (soluble and insoluble) (mol/kg feed)
 [G] = glycolate (mol/kg feed)
 [N] = nitrate + nitrite (mol/kg feed)
 [Mn] = manganese (mol/kg feed)

Values less than zero or greater than one can be calculated with the REDOX equation, because it is a linear regression equation fit to experimental data. Values outside the range of zero to one, however, are physically impossible. A number less than zero can be interpreted as fully oxidized and likewise a number greater than one as fully reduced.

Analysis of these data leads to two conclusions. First, predicted REDOX based on SME product data vary significantly from the targeted 0.2. Secondly, measured REDOX does not agree well with predicted REDOX.

The first conclusion points to errors in predicting anion conversion factors. This is not entirely unexpected for runs with a previously untested sludge and a new flowsheet. The results from these runs and in particular the 100% acid run can be used to generate new predictions for future work. It is easy to understand how it would be hard to predict redox if the reported anion concentrations vary substantially.

The second conclusion indicates error in either the applicability of the REDOX model (error in Mn or glycolate term) in this compositional space, the IC data, or the REDOX test method itself. The SRAT products were reanalyzed for anions (see Table 3-16). SRAT product samples were used since many of the runs were SRAT cycles only. The reanalysis of both the glycolate and nitrate were significantly different than the first analysis for many of the samples. The data was also used to predict the TOC concentration in the SRAT product, since no TOC analysis was requested of the SRAT or SME products.

Table 3-16. SRAT product anions, mg/kg

	1 st	2 nd	1 st	2 nd	1 st	2 nd	1 st	2 nd
Run	Nitrate	Nitrate	Glycolate	Glycolate	Formate	Formate	Calculated TOC	Calculated TOC
GF1	25,000	20,600	<100	<1000	12,900	12,250	3,520	3,350
GF2	51,600	54,500	53,900	68,500	2,555	2,495	18,300	23,100
GF3	55,950	52,650	54,700	56,400	<100	<1000	18,400	19,000
GF4	53,100	49,000	57,300	48,100	<100	<1000	19,700	16,700
GF5	59,900	68,800	115,000	85,500	824	<1000	38,300	28,700
GF6	45,250	51,500	66,300	51,300	776	<1000	22,600	17,800
GF7	59,900	71,650	161,000	130,000	3,750	3,245	53,700	43,500
GF8	56,250	62,100	118,000	75,700	<100	<1000	39,600	25,800
GF13	64,100	63,400	44,500	47,900	485	<1000	15,400	16,500
GF14	39,500	53,550	52,600	47,500	997	<1000	18,000	16,400
GF15	58,950	59,550	49,600	48,800	509	<1000	16,400	16,200
GF16	62,400	54,050	56,300	53,700	753	<1000	18,600	17,800
GF17	42,800	45,000	58,000	44,700	7,845	7,865	20,900	16,600
GF18	48,600	51,100	65,300	41,300	5,125	4,640	22,600	14,700
GF19	56,900	56,500	94,600	63,200	1,870	1,325	31,500	21,200
GF20	50,600	46,300	85,300	44,800	3,885	3,365	28,900	15,700

Table 3-17 below shows the appropriate SME product data with the corresponding predicted REDOX values as well as the REDOX as measured.

Table 3-17. SME product data for REDOX calculations

<u>anions (mg/kg)</u>	GF1	GF2	GF3	GF4	GF5	GF6	GF7
Nitrite	<100	<100	<100	<100	<100	<100	<100
Nitrate	25,350	54,950	53,100	47,150	64,750	42,900	69,600
Glycolate	0	57,000	52,550	58,100	102,000	65,250	154,000
Oxalate	519.5	737	2690	4185	3500	4105	2175
Formate	22200	3470	<100	937	1700	2525	3455
<u>Other properties</u>							
Mn (gmol/kg slurry)	0.167	0.140	0.136	0.115	0.172	0.181	0.141
wt% total solids	46.28%	44.95%	44.66%	45.18%	49.73%	52.70%	47.04%
predicted REDOX*	0	0.159	0.108	0.336	0.654	0.432	1
measured REDOX	0.000	0.661	0.750	0.612	0.751	0.528	0.877
stoichiometry (% Koopman minimum)	125	125	125	125	150	100	200

* Predicted REDOX used existing REDOX prediction equation with Mn term

The initial formic-glycolic flowsheet runs (GF2 to GF7) all had very high glass REDOX results (0.5 to 0.8). This is much higher than the typical 0.2 target and outside the 0.1 to 0.33 REDOX limits. As a result, four runs (GF13 to GF16) were performed to target a glass REDOX of 0.0 to 0.3. The results are summarized in Table 3-18

Table 3-18. Glass REDOX

Sample	GF13	GF15	GF14	GF16
REDOX Target, $\text{Fe}^{2+}/\sum\text{Fe}$	0.0	0.1	0.2	0.3
Predicted REDOX Calc without Mn term, $\text{Fe}^{2+}/\sum\text{Fe}$	0.03	0.08	0.16	0.22
Measured REDOX, $\text{Fe}^{2+}/\sum\text{Fe}$	0.00	0.08	0.20	0.45

In the REDOX series runs, the initial REDOX equation and estimates of anion conversion were used to develop the acid mix. Two issues had been noted. First the concentration of the anions is high so any error in the estimate of either glycolate or nitrate would skew that REDOX prediction. Second, the new glycolate method was being improved, and the PSAL analysts were getting more comfortable with the method. As a result, all of the anion analyses were repeated for the first twenty runs. However, even using new analyses, the REDOX equation prediction was much lower than the measured REDOX.

But if glycolic acid is completely reducing the Mn to +2 (the Mn is completely dissolved) and it stays reduced throughout the SRAT and SME processing, then there is no need for the Mn term.

A plot of measured REDOX against acid stoichiometry indicates that increasing acid led to linearly increasing REDOX in the test program, Figure 3-16 below. This strong correlation means that once the appropriate anion predictions for processing are determined, the REDOX should be predictable. The ability to control REDOX once it can be accurately predicted depends on the quality of the SME product glycolate predictions and the amount of acid added. The less acid added, the smaller the effect conversion factor errors will have on the final REDOX.

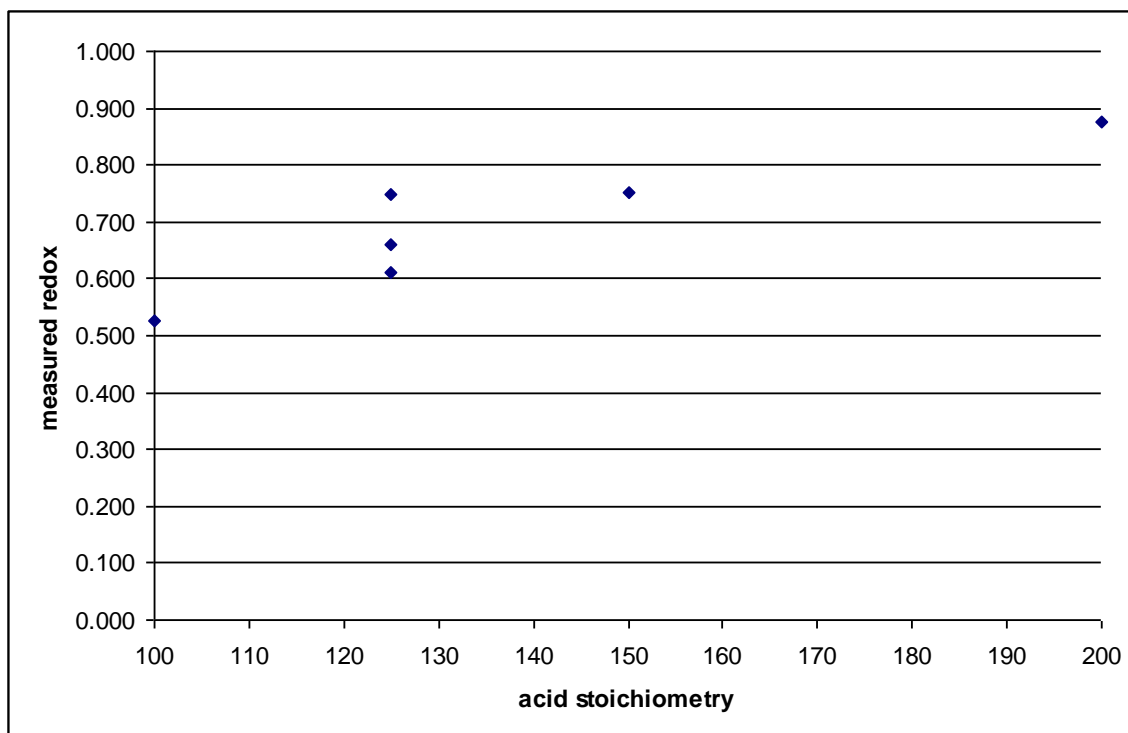


Figure 3-15. Measured REDOX dependence on acid stoichiometry

One last note on REDOX is that the REDOX target does impact hydrogen generation. In the four runs targeting a REDOX of 0, 0.1, 0.2 and 0.3, the hydrogen generation increased with REDOX target. The run with the REDOX target of 0 had no detectable hydrogen. As the REDOX target increases, more reducing acid (glycolic-formic mixture) is added and less nitric acid is added. This leaves more formic acid present post acid addition for producing hydrogen. These runs all had low hydrogen generation as the runs were performed at a Koopman acid stoichiometry of 100%. The hydrogen profile for these runs is summarized in Figure 3-17.

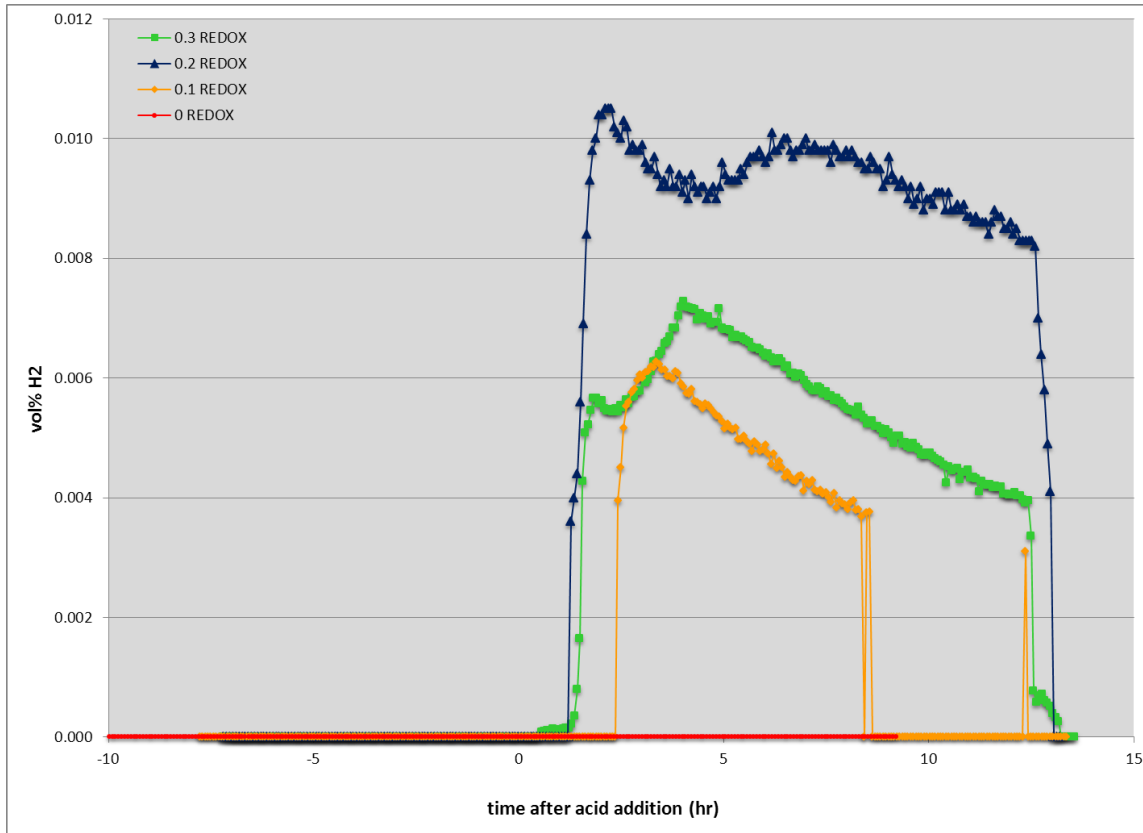


Figure 3-16. Hydrogen Generation Dependence on REDOX

An attempt was made to find an equation to better predict REDOX. One of the problems with this dataset is only one sludge was used. In addition, in targeting a REDOX of 0.2, the reducing anions (formate and glycolate) increased together with the oxidizing anions (primarily nitrate) as stoichiometry is increased. The REDOX equation assumes that the manganese is in a +5 oxidation state and must be reduced to +2 in the melter. But if glycolic acid is completely reducing the Mn to +2 (the Mn is completely dissolved) and it stays reduced throughout the SRAT and SME processing, there is no need for the Mn term.

Eliminating the Mn term increases the REDOX prediction by 0.1-0.2, giving the following revised REDOX equation.

$$\text{Fe}^{2+}/\Sigma\text{Fe} = 0.2358 + 0.1999 * (2[\text{F}] + 4[\text{C}] + 6[\text{G}] + 4[\text{O}_\text{T}] + 5[\text{N}])45/\text{T}$$

Although the new Mn Free REDOX predictions agree better with the measured REDOX, it still can and should be improved. The results for all REDOX measurements are summarized in Figure 3-15. The three circled runs are the first three glycolic-formic runs (GF2 to GF4). The use of the REDOX data from the in-progress matrix study would be useful in improving the REDOX equation for the glycolic-formic flowsheet.

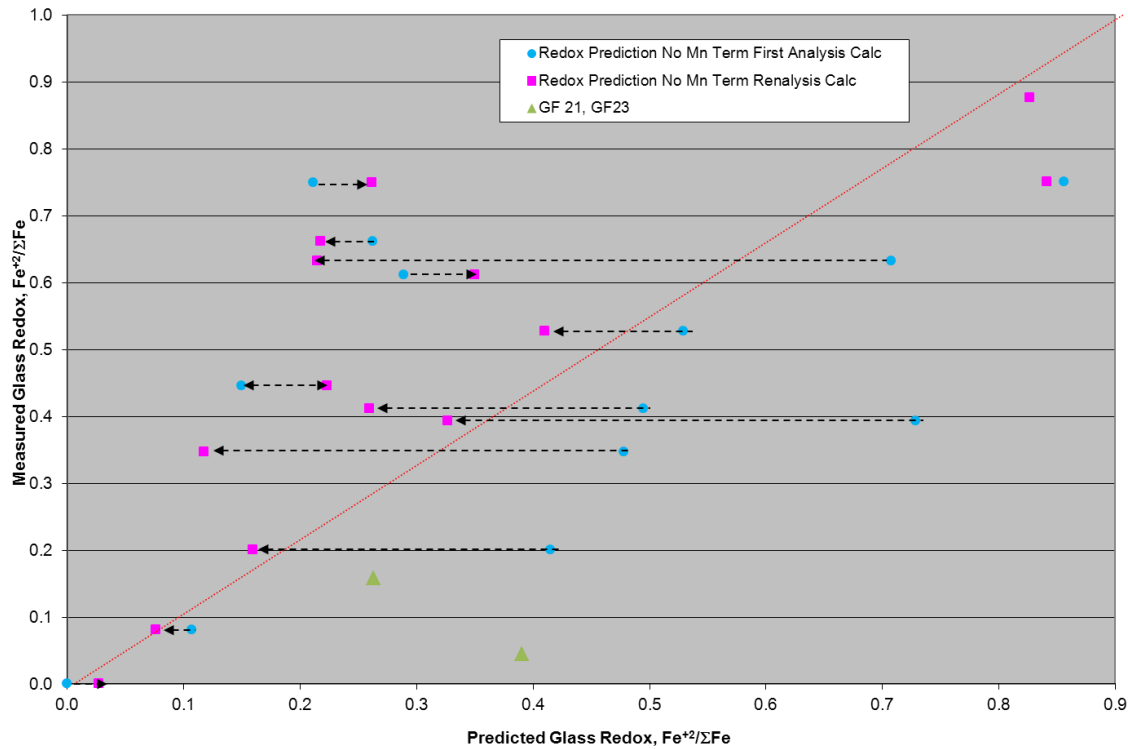


Figure 3-17. SRAT Product REDOX comparison

3.1.8 SRAT Gd Solubility

Six SRAT runs were performed to compare the partitioning behavior of gadolinium to that of iron. This work was done to support potential use of gadolinium as a supplemental neutron poison²⁷. Four of the SRAT runs were performed under typical baseline flowsheet conditions utilizing a combination of nitric and formic acids. The four baseline SRAT runs were SB6-27, -28, -29, and -30. In contrast, the other two SRAT runs were performed under alternative reductant flowsheet conditions utilizing a combination of nitric, formic, and glycolic acids. The two alternative reductant SRAT runs were GF-13 and -14.

In each of these runs, gadolinium was added to the sludge in order to determine the impact of the baseline flowsheet (SB6 runs) and the glycolic-formic flowsheet (GF Runs) on Gd solubility. The two GF runs were part of the REDOX series, GF13 having a REDOX target of 0 and GF14 having a REDOX target of 0.2. Both of these tests were at an acid stoichiometry of 100%. These tests are described in more detail in a report summarizing all of the Gd testing performed by Reboul²⁸. For the baseline runs, the Gd and Fe became somewhat soluble (both peaked at about 20% soluble) and slowly declined to near zero by the end of the SRAT cycle (Figure 3-18). For the GF runs (Figure 3-19), the Fe remained insoluble but the Gd solubility continued to increase until almost 80% of the Gd was soluble. Thus Gd may not be as effective a neutron poison in the glycolic-formic flowsheet as it is in the baseline flowsheet, especially at higher acid stoichiometry..

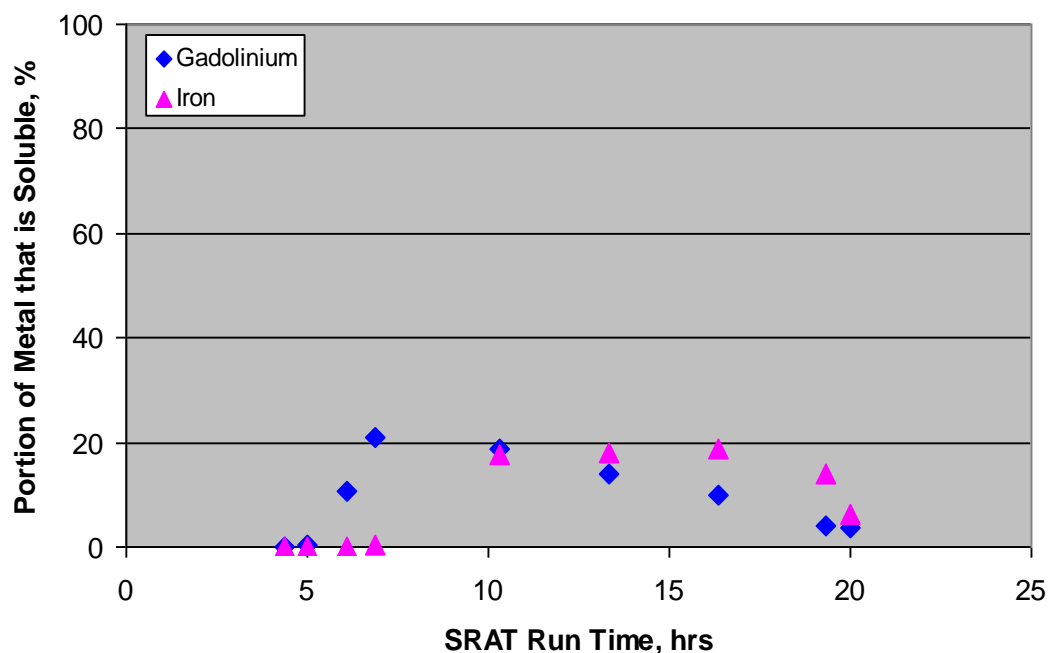


Figure 3-18. SB6-29 Fe and Gd Solubility during SRAT Cycle

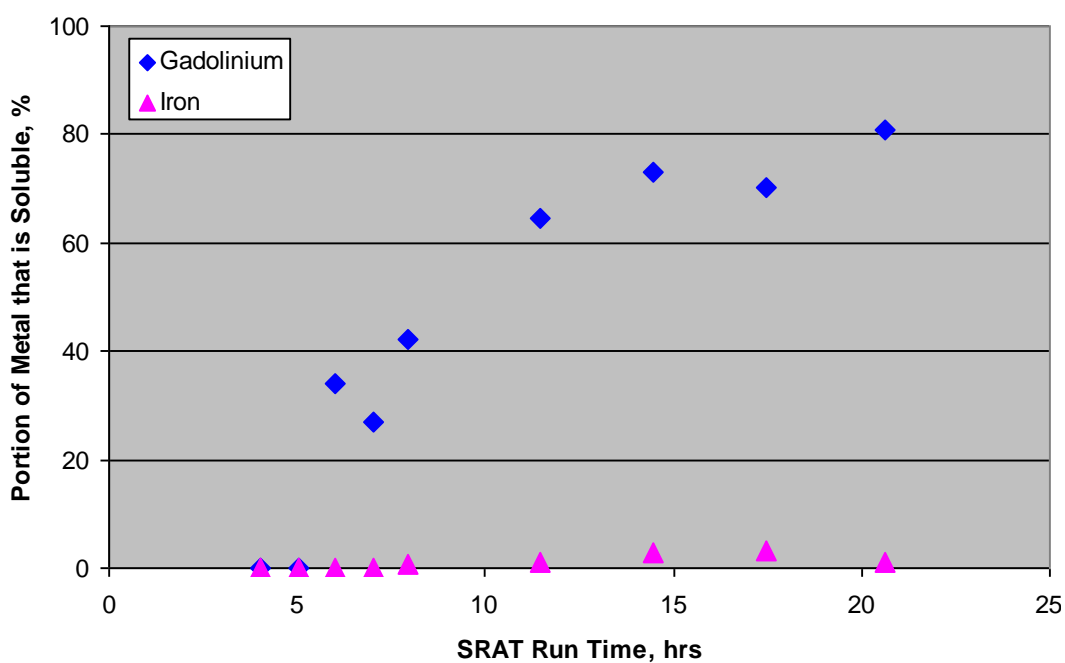


Figure 3-19. GF13 Fe and Gd Solubility during SRAT Cycle

3.1.9 SRAT Mercury Reduction

One of the most important questions to resolve concerning the glycolic/formic flowsheet is whether mercury could be effectively reduced and steam stripped in the SRAT cycle. The starting sludge was trimmed to 3.263 wt% Hg in the total solids. (HM basis). This required a theoretical boiling time of nearly 36.5 hours to remove mercury to less than 0.60 wt% in the SRAT product total solids using lab-scaled DWPF design basis boil-up rates and a stripping efficiency of 750 g steam/g Hg. Note that DWPF has increased their mercury limit from 0.6 to 0.8 wt% in the SRAT product on a total solids basis.

Samples were taken periodically throughout the runs for mercury analysis. The chart below (Figure 3-20) shows the concentration of mercury in the slurry as a function of time for the two baseline flowsheet cases, GF1 (nitric/formic) and GF3 (nitric/glycolic/formic).

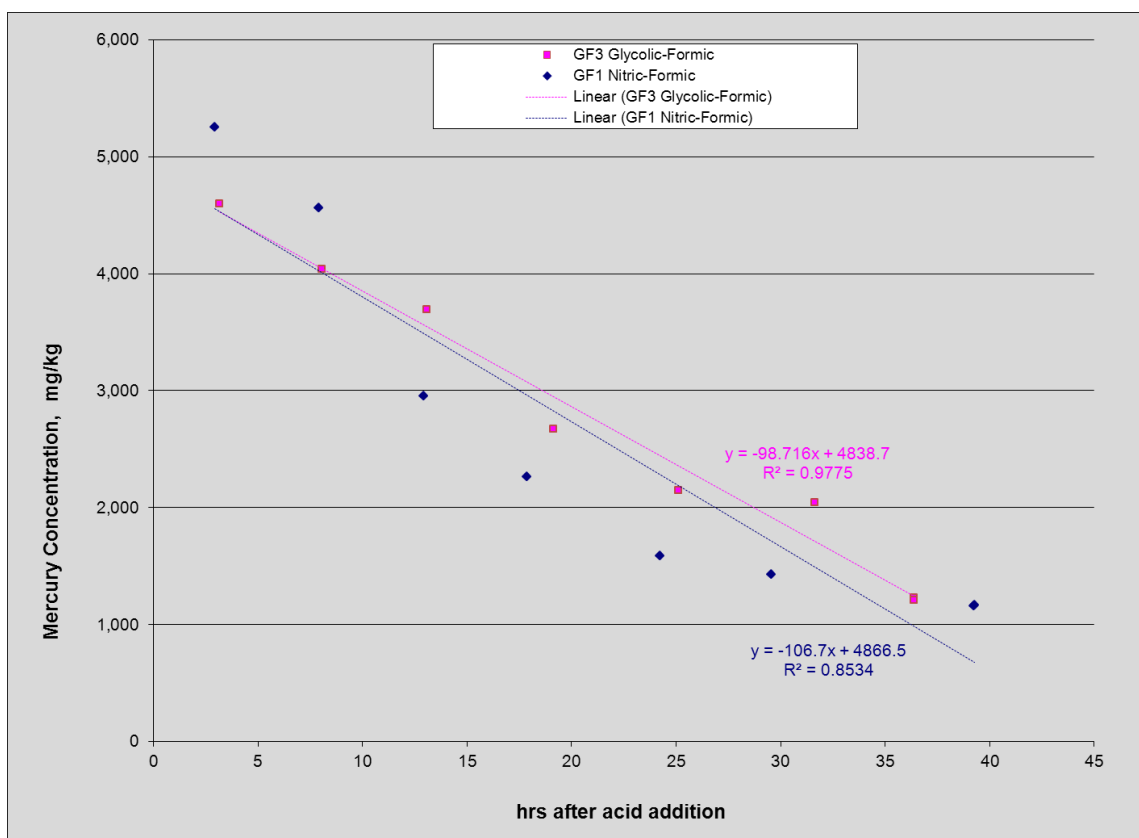


Figure 3-20. Mercury concentration with time in baseline SRAT cycles

This plot shows actual sample data along with a calculated linear trend line for the two baseline flowsheets. The rate of mercury removal appears to be nearly identical for both flowsheets. On a total solids basis, the SRAT product Hg concentration in the glycolic/formic flowsheet was 0.56 wt% while the SRAT product for Hg concentration in the nitric/formic flowsheet measured 0.66 wt%. The next plot shows the mercury removal rate for the 100% stoichiometry run, GF6 (Figure 3-21). The rate of removal in this run GF6, the lowest acid stoichiometry tested, also matches well with the two baseline cases. The final SRAT product mercury concentration was slightly above the limit in this run, 0.61 wt% in the total solids. There are additional mercury graphs in appendix A1.

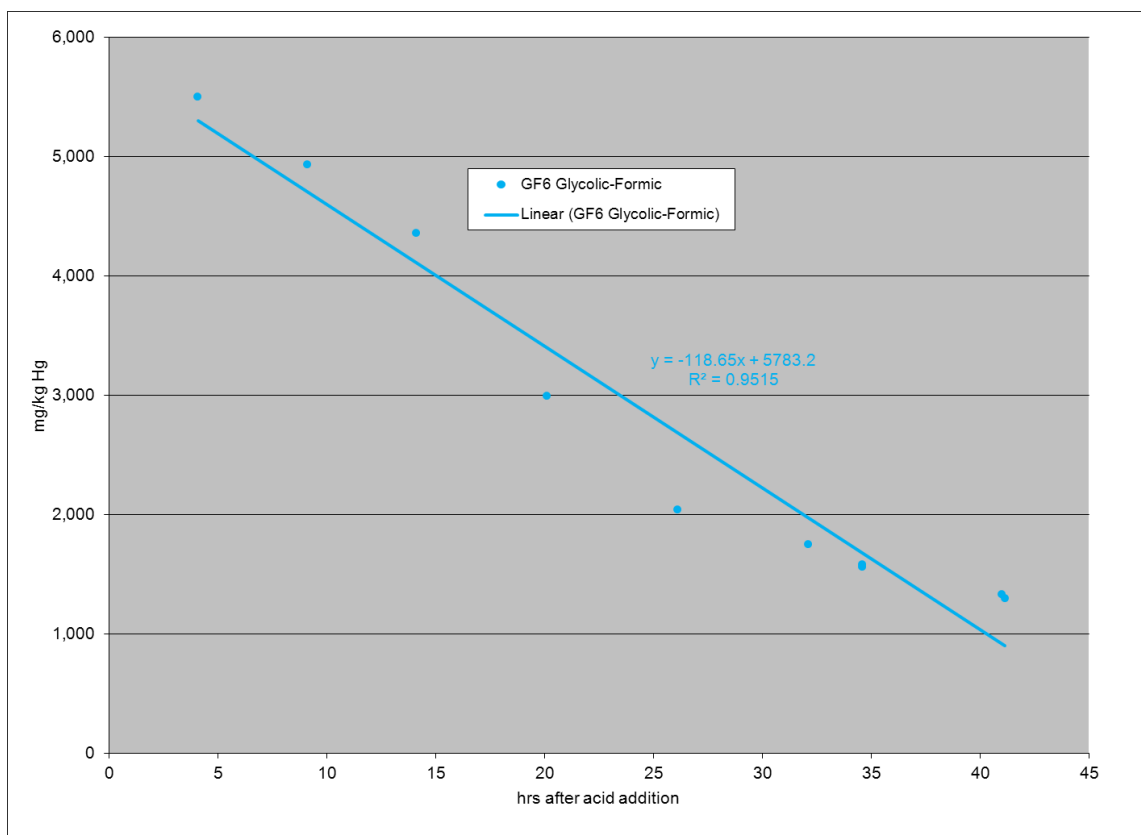


Figure 3-21. Mercury concentration with time for 100% stoichiometry run

Table 3-19 below shows the SRAT and SME product mercury results for all of the runs in this series.

Table 3-19. Comparison of SRAT and SME Product Hg results

Run	Acid Stoichiometry	SRAT Product Hg (wt% TS)	SME Product Hg (wt% TS)
GF1	125	0.66	0.29
GF3	125	0.56	0.25
GF4	125	0.97	0.39
GF5	150	0.41	0.15
GF6	100	0.61	0.25
GF7	200	0.31	0.37
GF8	125	0.39	no SME

All of the runs with the exception of the ARP/MCU run (GF4) had SRAT product mercury results near or below the limit of 0.60 wt% in the total solids. Note that in SRNL testing, the Hg was

added after the ARP caustic addition was complete to prevent the formation of dimethyl mercury. In DWPF, some mercury is stripped during caustic boiling. However, since mercury is not added until caustic addition is complete; no mercury stripping was completed during caustic boiling.

It is of particular interest that mercury was successfully removed in GF8, a run with no formic acid. Glycolic acid did not show the ability to reduce mercury in earlier screening studies, which is why testing has focused on using the formic/glycolic blend. It is proposed that glycolic acid ($\text{H}_2(\text{OH})\text{CCO}_2\text{H}$) is reacting with nitrite (or other species, e.g. MnO_2) to form glyoxylic acid (HCOCO_2H), the aldehyde form of glycolic acid. Glyoxylic acid then reacts with mercury oxide to form elemental mercury. The final form of the glycolic acid after these reactions is oxalic acid. This result potentially opens the door to completely removing formic acid from the flowsheet.

During the SRAT/SME process, mercury was collected in the Mercury Water Wash Tank (MWWT). The mercury tended not to coalesce into a single liquid phase, but instead come over as small beads. These beads would stick to the sides of the SRAT condenser drain tube rather than flowing to the sump in the MWWT. The mercury was dull in color. The sticking behavior qualitatively increased with increasing acid stoichiometry. The overall behavior of the mercury seemed to be consistent with previous observations of high acid runs in SB6 flowsheet studies.²⁹ One possibility is that the antifoam degradation is increased in higher acid runs (lower pH) and those degradation products form compounds with mercury, including calomel (Hg_2Cl_2). The photo below (Figure 3-22) was taken during the 200% acid stoichiometry run.



Figure 3-22. Mercury collection in SRAT condenser drain tube

All of the mercury removed and collected during these runs was retained for potential future analysis. Mercury stripping efficiency appears similar for the other runs. Plots of mercury concentration with time for all runs are included in Appendix A.

The mercury produced in the high acid runs was very different looking than the elemental liquid that was produced in the low acid runs. This is consistent with what is being produced in the baseline flowsheet runs for SB7. The mercury produced in the low acid runs is reduced and steam stripped easily, and it is easy to quantify the amount by weighing the mercury collected in the MWWT. The mercury produced in the high acid runs looks darker and more crystalline, collects in the tubing between the condenser and the MWWT, and mass-wise is much smaller than that collected in the low acid runs. Pictures of the mercury collected in the low stoichiometry and high stoichiometry runs are shown in Figure 3-23.

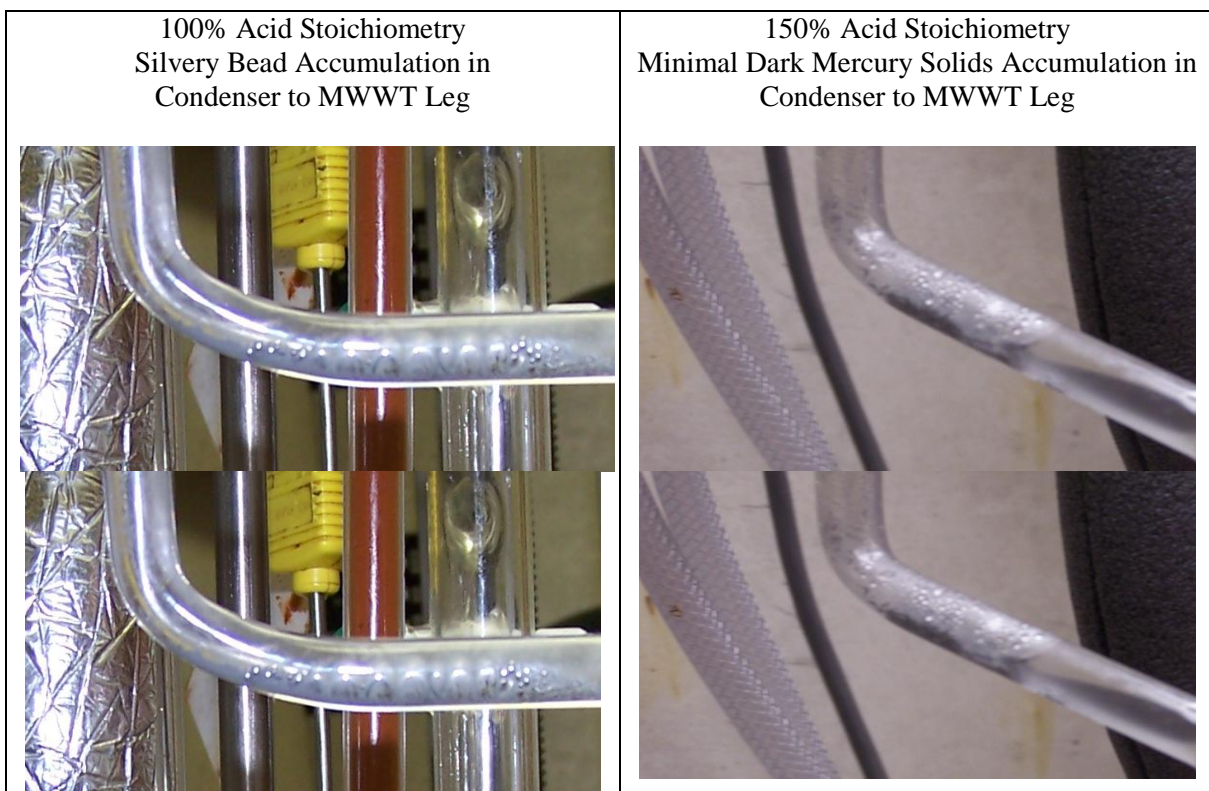


Figure 3-23. Mercury collection in SRAT condenser drain tube

Because of the problems DWPF is experiencing with mercury recovery, a special study is being completed to understand the mercury mass balance. In several of the completed runs (GF17 to GF20), very careful cleaning of vessels with nitric acid and drying of the SRAT product to recover elemental mercury was completed. Table 3-202020 summarizes the data collected. At present the mass balance data from Run GF20 is complete and the data from Runs GF17-GF19 will be added when available. Small amounts of Hg were recovered in acid rinses of the glassware, but the major change was the recovery of about 45% of the mercury from the SRAT product that was not found in analysis of the SRAT product sample pulled from the SRAT vessel during cooldown.

Table 3-20. Mercury Balance

Run	GF17		GF18		GF19		GF20	
	Mass, g	%	Mass, g	%	Mass, g	%	Mass, g	%
Hg Added	NA	NA	NA	NA	NA	NA	12.12	100
SRAT Product Sample	NA	NA	NA	NA	NA	NA	1.75	14.4
SRAT Product Recovered	NA	NA	NA	NA	NA	NA	5.51	45.4
MWWT Hg	NA	NA	NA	NA	NA	NA	2.06	17.0
Condensate Hg	NA	NA	NA	NA	NA	NA	0.11	0.9
Total Hg Out	NA	NA	NA	NA	NA	NA	9.42	77.8

3.1.10 SRAT pH profile

Time dependent SRAT/SME pH data were collected throughout the first twenty-two runs. The graph below shows the pH trends of the two baseline runs with mercury and noble metals. The noise through the 5-7 pH region further illustrates the mixing difficulties experienced during acid addition. The data is summarized in Figure 3-24.

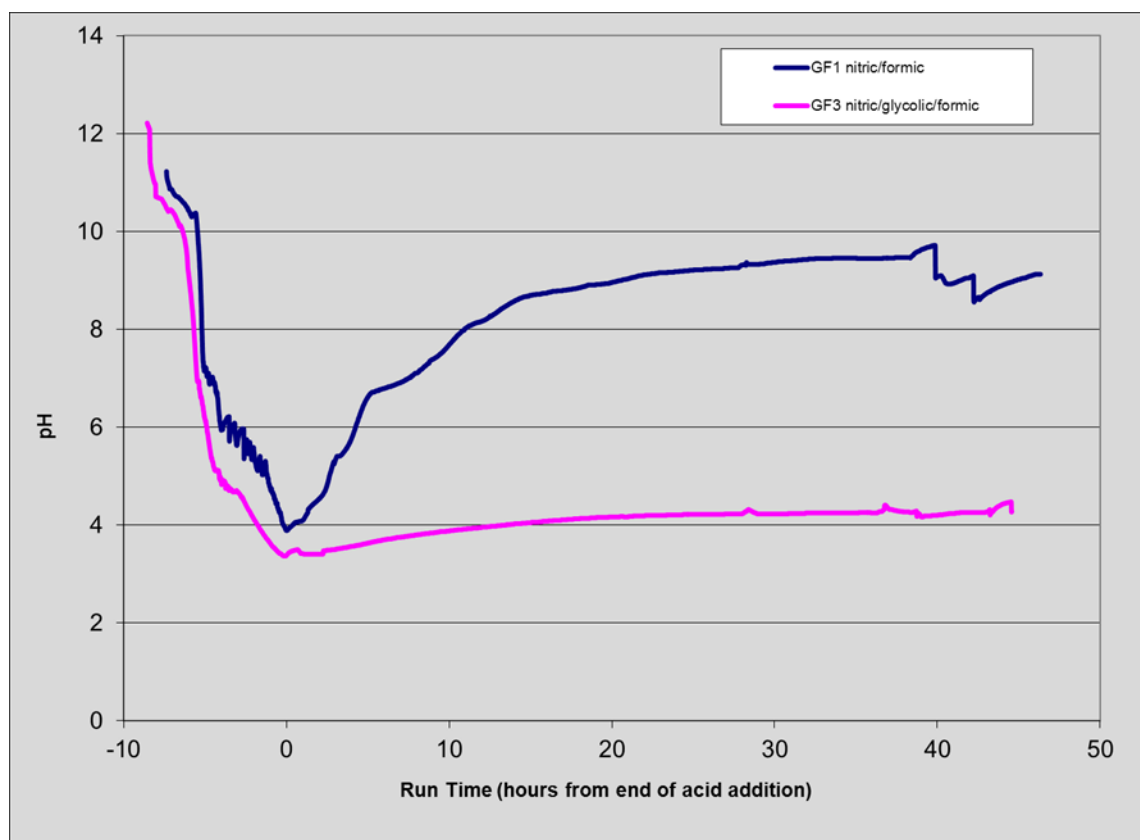


Figure 3-24. pH trends for baseline SRAT runs with mercury and noble metals

The additional nitric acid needed for REDOX balancing the glycolic/formic acid flowsheet runs causes the pH to be lower at the end of acid addition. During reflux, the catalytic destruction of formic acid which causes hydrogen generation in the current DWPF flowsheet causes the pH to increase as formic acid is consumed. Since this does not happen to nearly the same extent in the glycolic/formic flowsheet, the pH tends not to rebound as much during reflux. This leads to low pH SRAT and SME products which presents some additional concerns related to metal solubility that will be discussed later. A positive result of the low pH with the alternate flowsheet is that yield stress both during the process and of the products is low compared to the baseline flowsheet.

The pH increase in the runs with noble metals and mercury is caused by the catalytic decomposition of formic acid. Note in two runs performed without mercury or noble metals (GF21 and GF22); there was no significant pH increase during the SRAT cycle for either flowsheet. The data is summarized in Figure 3-25.

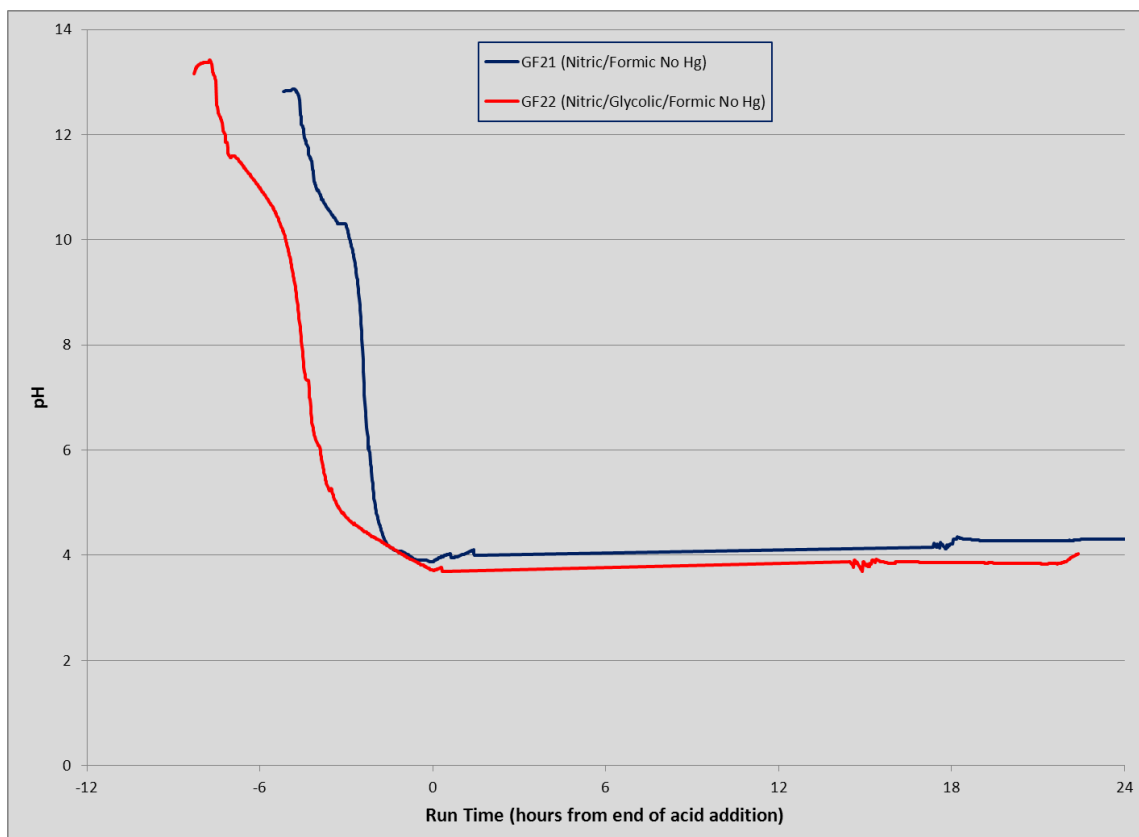


Figure 3-25. pH trends for baseline SRAT runs without mercury and noble metals

3.1.11 SRAT Foaming Issues

One observation that could be made for all of the simulations is that maintaining a well-mixed vessel was very challenging with this particular sludge feed and was independent of the flowsheet testing objective. The sludge prepared at Harrell Industries measured 31.5 Pa yield stress. Because of the rheology of the sludge, it is possible that some of the problems noted in this testing would not be observed in actual DWPF processing. With a typical 4-L SRAT vessel, air entrainment becomes a serious concern during periods of significant off-gas generation, that is, from early in acid addition through the entire period of NO_x generation. A pocket of gas was

found to build up around the agitator blades which prevented the bulk slurry from mixing. The agitator motor was stopped to allow the trapped gas to escape, followed by restarting the mixer. This method was effective for getting through acid addition without stopping acid flow, however, the mixer would need to be stopped and restarted at least once a minute. It is important to note that trapped air in the slurry caused by the unusually high yield stress is not the same as foaming in a classical sense. The trapped air caused an increase in slurry level, but no foam lamella was observed. Antifoam was added during one of the runs, but no decrease in slurry level was noted as a result of the addition. Again, this was common to all of the demonstrations with this simulant, not just the baseline run.

Another overall observation for these runs is that foaminess was not really a concern other than in the ARP/MCU test. The ARP/MCU run foamed extensively during ARP addition while caustic boiling and antifoam was added as necessary. Foaming during caustic boiling has been a minor issue with simulants, though it is known to be a problem with real waste.

3.1.12 SRAT Condensate Data

A composite sample was prepared for each of the first 8 runs by combining the condensate from the MWWT, FAVC, and SMECT to produce an “average” condensate sample. The sample was analyzed for elementals via ICP-AES, anions via IC, pH and density. The results are summarized in Tables 3-21 and 3-22.

The main difference in the flowsheets was the pH of the condensate samples and the amount of formate, glycolate and nitrate in the composite samples. In the glycolic-formic flowsheet runs, the condensate pH was 1-2.4. For the baseline formic-nitric flowsheet, the pH was 6.5. In the run with glycolic acid, no glycolate was measured in the condensate but was present in glycolic-formic flowsheet runs. One other observation is that the higher acid stoichiometry runs had higher Si in the condensate. This is likely due to antifoam degradation products in the condensate. It should also be noted that GF3 had almost 2X higher Si than GF1 indicating that the antifoam may degrade faster in the glycolic-formic flowsheet.

Table 3-21. Comparison of Composite Condensate Data, ICP-AES, mg/L

Sample ID	GF1	GF2	GF3	GF4	GF5	GF6	GF7	GF8
Lab ID	10-0978	10-0979	10-0980	10-0981	10-0982	10-0983	10-0984	10-0985
Ag	<0.010	<0.010	<0.010	<0.010	<0.010	<0.010	<0.010	<0.010
Al	0.094	0.077	0.082	0.085	0.087	0.094	0.088	0.099
B	<0.100	<0.100	<0.100	<0.100	<0.100	<0.100	<0.100	<0.100
Ba	<0.010	<0.010	<0.010	<0.010	<0.010	<0.010	<0.010	<0.010
Ca	0.112	0.110	0.108	0.098	0.161	0.163	0.124	0.135
Cr	<0.010	<0.010	<0.010	<0.010	<0.010	<0.010	<0.010	<0.010
Cu	0.032	0.028	0.031	0.031	0.035	0.035	0.029	0.033
Fe	<0.010	<0.010	<0.010	<0.010	<0.010	<0.010	0.058	<0.010
K	0.262	0.211	0.223	0.215	0.243	0.302	0.212	0.208
Li	0.160	0.161	0.161	0.161	0.161	0.161	0.161	0.161
Mg	<0.010	<0.010	<0.010	<0.010	<0.010	<0.010	<0.010	<0.010
Mn	<0.010	<0.010	<0.010	<0.010	<0.010	<0.010	<0.010	<0.010
Na	<0.100	<0.100	<0.100	<0.100	<0.100	<0.100	<0.100	<0.100
Ni	<0.010	<0.010	<0.010	<0.010	<0.010	<0.010	<0.010	<0.010
P	0.095	0.085	0.096	0.047	0.082	0.096	0.103	0.078
Pb	<0.010	<0.010	<0.010	<0.010	<0.010	<0.010	<0.010	<0.010
S	<0.100	<0.100	<0.100	<0.100	<0.100	<0.100	<0.100	<0.100
Si	84.1	118.7	155.1	163.5	125.8	99.8	354.5	185.6
Ti	0.011	0.011	0.011	0.014	0.012	0.011	0.011	0.011
Zn	<0.010	<0.010	<0.010	<0.010	<0.010	<0.010	<0.010	<0.010
Zr	<0.010	<0.010	<0.010	<0.010	<0.010	<0.010	<0.010	<0.010

Table 3-22. Comparison of Composite Condensate Data, IC (mg/L), Density (g/mL), pH

Sample ID	GF1	GF2	GF3	GF4	GF5	GF6	GF7	GF8
Lab ID	10-0978	10-0979	10-0980	10-0981	10-0982	10-0983	10-0984	10-0985
Fluoride	<100	<100	<100	<100	<100	<100	<100	<100
Chloride	<100	<100	<100	<100	<100	<100	<100	<100
Nitrite	<100	<100	<100	<100	<100	<100	<100	<100
Nitrate	156	224	132	132	1520	2230	4460	4180
Sulfate	<100	<100	<100	<100	<100	<100	<100	<100
Glycolate	<100	61.9	62.8	62.8	80.5	64.6	60.2	180
Oxalate	<100	<100	<100	<100	<100	<100	<100	<100
Formate	322	612	293	293	948	169	2310	<100
Phosphate	<100	<100	<100	<100	<100	<100	<100	<100
Density	0.998665	0.99878	0.998615	0.99882	0.999545	0.99974	1.00149	1.000885
pH	6.45	2.22	2.4	1.99	1.53	1.35	1.07	1.11

3.1.13 SME Offgas

Because of the long processing time in the SRAT cycle due to the stripping of mercury, there was no significant chemistry in the SME cycles (low carbon dioxide, hydrogen generation). Table 3-23 and Figure 3-26 summarizes the hydrogen and carbon dioxide generation in the SME cycle. The small generation of CO₂ and H₂ (Figure 3-26) is triggered by the addition of formic acid with

the frit in the frit-slurry. This could be eliminated by not adding formic acid with frit in the SME cycle.

Table 3-23. Comparison of SME Offgas Generation Data

SME Offgas	GF1 SME	GF3 SME
Nitrous Oxide (N ₂ O), g	0.00	0.00
Nitric Oxide (NO), g	0.00	0.00
Carbon Dioxide, g	3.6	1.7
Hydrogen, g	0.00	0.00

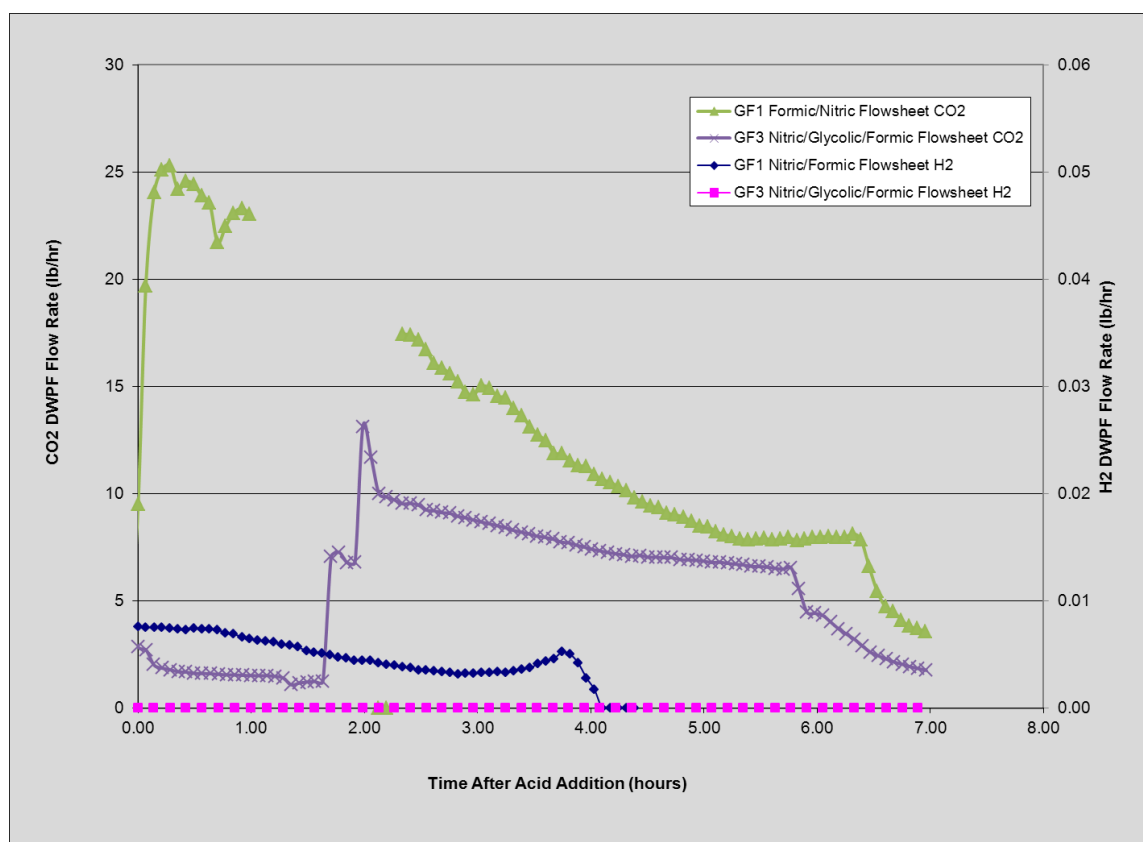


Figure 3-26. Carbon Dioxide Generation in GF1 and GF3 SME cycles, lb/hr DWPF Scale

3.1.14 Ruthenium Testing

Four runs (GF9-GF12) were completed to understand the hydrogen generation in low and high acid stoichiometry runs with two forms of ruthenium. This was due to differences in hydrogen generation between the SRNL and VSL testing as the result of using different forms of Ru in the two labs. These tests are not pertinent to the flowsheet decision so will not be reported here.

3.2 Melter Feed Preparation

Two 4-L runs were completed to ensure the processing parameters were defined to produce a REDOX of 0.2 before the melter feed preparation began. This was needed since no runs without mercury, with 110% Koopman acid stoichiometry, had been completed. Run GF21 was the baseline flowsheet and Run GF22 was the glycolic-formic flowsheet run. A 4-L run with the sugar flowsheet was not completed as there was no REDOX target for this run (sugar was added later to control REDOX). The conditions for these runs was then used as the inputs for the GF23 (baseline flowsheet) and GF24 (glycolic-formic flowsheet).

Three melter runs were performed at VSL to evaluate the performance of three flowsheets, baseline, glycolic-formic and sugar. The feed for these melter runs was prepared by SRNL in 22-L SRAT Simulant Equipment. Eight SRAT cycles were performed for each flowsheet to produce approximately 100 kg of SRAT product for melter testing. No frit was added at SRNL. The baseline flowsheet runs were designated as GF23A to GF23H. The glycolic-formic flowsheet runs were designated as GF24A to GF24H. The sugar flowsheet runs were designated as GF25A to GF25H.

3.2.1 Flowsheet Calculations of Acid Requirement

SRNL specified the conditions for the melter feed runs under the baseline and glycolic-formic flowsheets. VSL specified the conditions for the melter feed run for the sugar flowsheet. The run conditions are summarized in Table 3-24. The processing assumptions are summarized in Table 3-25, 3-26 and 3-27.

Table 3-24. SRAT Cycle Additions and Dewater Targets, grams

Addition or Removal	GF23	GF24	GF25
Sludge Simulant	16,620	16,620	16,620
Other trim chemicals	5.7561	5.7561	5.7561
Water to dilute/rinse trim chemicals	500.00	500.00	500.00
Total Slurry	17,126	17,126	17,126
1:20 by mass Antifoam	266.48	266.48	266.48
50 wt% Nitric Acid solution	276.65	1,309.91	1,476.06
90 wt % Formic Acid solution	1,139.50	0.00	221.81
80:20 mole fraction Glycolic/Formic Acid solution	0.00	1,281.15	0.00
Water added to flush Acid Lines	20.00	20.00	20.00
Total Dewater	6,742.00	6,815.07	7,038.93

Table 3-25. Sludge Composition for Melter Feed Preparation

Input	GF23, -25	Units
Fresh Sludge Mass without trim chemicals	16,620	g slurry
Fresh Sludge Weight % Total Solids	16.46	wt%
Fresh Sludge Weight % Calcined Solids	12.37	wt%
Fresh Sludge Weight % Insoluble Solids	8.45	wt%
Fresh Sludge Density	1.108	kg / L slurry
Fresh Sludge Supernate density	1.070	kg / L supernate
Fresh Sludge Nitrite	16,750	mg/kg slurry
Fresh Sludge Nitrate	6,135	mg/kg slurry
Fresh Sludge Formate	0	mg/kg slurry
Fresh Sludge Sulfate (mg/kg)	2,310	mg/kg slurry
Fresh Sludge Chloride (mg/kg)	776	mg/kg slurry
Fresh Sludge Phosphate (mg/kg)	0	mg/kg slurry
Fresh Sludge Oxalate	815	mg/kg slurry
Fresh Sludge Slurry TIC (treated as carbonate)	1,000	mg/kg slurry
Fresh Supernate TIC (treated as carbonate)	1,000	mg/L supernate
Fresh Sludge Hydroxide (Base Equivalents) pH = 7	0.643	Equiv Moles Base/L slurry
Fresh Sludge Coal/Carbon source	0.000	wt% dry basis
Fresh Sludge Manganese (% of Calcined Solids)	6.230	wt % calcined basis
Fresh Sludge Mercury (% of Total Solids in untrimmed sludge)	0.0000	wt% dry basis
Fresh Sludge Magnesium (% of Calcined Solids)	0.380	wt % calcined basis
Fresh Sludge Sodium (% of Calcined Solids)	19.500	wt % calcined basis
Fresh Sludge Potassium (% of Calcined Solids)	0.031	wt % calcined basis
Fresh Sludge Cesium (% of Calcined Solids)	0.000	wt % calcined basis
Fresh Sludge Calcium (% of Calcined Solids)	0.583	wt % calcined basis
Fresh Sludge Strontium (% of Calcined Solids)	0.000	wt % calcined basis
Fresh Sludge Nickel (% of Calcined Solids)	2.510	wt % calcined basis
Fresh Sludge Supernate manganese	0	mg/L supernate

Table 3-26. SRAT Processing Assumptions for Melter Feed Preparation

SRAT Processing Assumptions	GF23	GF24	GF25	Units
mol % Glycolic Acid	0.00	80.00	0.00	mol glycolic acid/100 mol total acid
Conversion of Nitrite to Nitrate in SRAT Cycle	20.00	0.00	NA	gmol NO ₃ ⁻ /100 gmol NO ₂ ⁻
Destruction of Nitrite in SRAT and SME cycle	100.00	100.00	NA	% of starting nitrite destroyed
Destruction of Formic acid charged in SRAT	20.00	90.00	NA	% formate converted to CO ₂ etc.
Destruction of Glycolic acid charged in SRAT	0.00	0.00	NA	% glycolate converted to CO ₂ etc.
Conversion of Glycolic acid to Oxalate	NA	3.00	NA	% glycolate converted to C ₂ O ₄
Destruction of Oxalate charged	0.00	0.00	NA	% of total oxalate destroyed
Percent Acid in Excess Stoichiometric Ratio	110	110	72.7	%
SRAT Product Target Solids	27.84	29.39	28.31	%
Nitric Acid Molarity	9.444	10.005	10.005	Molar
Formic Acid Molarity	23.610	NA	23.385	Molar
Glycolic Acid Molarity	NA	11.826	NA	Molar
DWPF Nitric Acid addition Rate	4.6	4.6	4.7	gallons per minute
DWPF Formic Acid addition Rate	2.0	4.1	2.0	gallons per minute
REDOX Target	0.220	0.170	NA	Fe ⁺² / ΣFe
SRAT air purge	230	230	230	scfm

Table 3-27. SME Processing Assumptions for Melter Feed Preparation

SME Processing Assumptions	GF23	GF24	GF25	Units
Sludge Oxide Contribution in SME (Waste Loading)	36.00	36.00	36.00	%
Target SME Solids total Wt%	45.0	45.0	45.0	wt%

3.2.2 Run Details

Eight duplicate 22-L batches of melter feed were completed to produce enough SRAT product for the VSL melter testing of each of the flowsheets. Processing conditions for these runs were modified to produce the batches as quickly as possible. For example, the acids were added at the same molar flowrate as formic acid so the nitric and glycolic-formic mixture were both added about 2x what is achieved in DWPF. Also, the SRAT boiling time was limited to the time needed to destroy nitrite and complete dewater to the target needed for added frit (36 wt % waste loading) to produce a 45 wt% total solids SME product. For the baseline and sugar flowsheet, this was too concentrated to feed to the melter so was diluted by VSL. Once the SRAT cycle was complete, the slurry was cooled down and transferred to the product drum. No cleaning of the processing equipment was completed between runs although the equipment was cleaned and reassembled before starting production of each flowsheet melter feed. Subsequent runs for each flowsheet were labeled with the run number and a letter designating which of the eight batches was produced. For example, Run 23A was the first run using the baseline flowsheet and Run 25H was the eighth run produced using the sugar flowsheet.

3.2.3 Product Results

The SRAT product from the first run for each flowsheet was analyzed, plus a composite sample from the drum was analyzed for each flowsheet. The composite results are summarized in Tables 3-28 to 3-32.

There are several analyses that are significant and will be discussed. First, the glycolic-formic flowsheet slurry is rheologically much thinner than the baseline or sugar flowsheet. Once the pH drops below 7 in the SRAT, the glycolic-formic flowsheet is much easier to mix. Second, the slurry soluble solid concentration is much higher for the glycolic-formic flowsheet. This is one of the reasons (pH is the other) for the lower yield stress for the glycolic-formic flowsheet. Third, the anions are very different for the three flowsheets. The baseline flowsheet is high in formate and nitrate. The formic-glycolic flowsheet is high in glycolate and nitrate. The sugar flowsheet is high in nitrate and will be high in sugar once added. Note that the sugar was added by VSL after all processing was complete and was not involved in SRAT or SME processing.

Table 3-28. SRAT Product ICP-AES results, wt % calcined solids basis

Sample ID	10-GF-23-4501	10-GF-24-4519	10-GF-25-4512
Lab ID	11-0001	11-0002	11-0003
Al	16.1	15.75	15.95
Ba	<0.010	<0.010	<0.010
Ca	0.564	0.546	0.541
Cd	0.0455	<0.010	0.0580
Cr	0.122	0.125	0.127
Cu	0.269	0.250	0.269
Fe	20.9	20.65	20.4
K	0.0545	0.05	0.0545
Mg	0.450	0.445	0.449
Mn	6.29	6.21	6.23
Mo	<0.010	<0.010	<0.010
Na	16.5	16.2	16.3
Ni	2.69	2.64	2.69
P	<0.100	<0.100	<0.100
S	0.459	0.461	0.453
Si	0.157	0.158	0.173
Ti	0.0260	0.0250	0.0265
Zn	0.0120	0.0120	0.0135
Zr	0.252	0.254	0.262

Please note that the sugar flowsheet managed to get some nitrite destruction without any reducing agent although it did not meet the DWPF SRAT product specification. Consequently, it might be possible to get hydrogen generation in the SME cycle once the frit formic acid was added and the residual nitrite was destroyed. Also, the sulfate concentrations, as measured by the IC varied significantly for the three flowsheets. It would be expected that the sulfate concentration would be approximately equal in all three flowsheets. A row was added to Table 3-29, with a calculated sulfate concentration from the ICP-AES S analysis. As can be seen, the calculated sulfate concentrations were much more consistent than IC sulfate values.

Table 3-29. SRAT Product Anion results, mg/kg

Sample ID	10-GF-23-4501	10-GF-24-4519	10-GF-25-4512
Lab ID	11-0001	11-0002	11-0003
Fluoride	<100	<100	<100
Chloride	1,090	515	965
Nitrite	<100	<100	1,170
Nitrate	27,050	68,600	79,200
Glycolate	<100	54,200	<100
Oxalate	<100	351	<100
Formate	71,400	9,520	12,700
Phosphate	<100	<100	<100
Sulfate	800	2,610	1,260
Sulfate from ICP S	2,380	2,170	2,300

Table 3-30. SRAT Product Solids Results, wt % Total Solids Basis and pH

Sample	GF-23-4501	GF-24-4519	GF-25-4512
Lab ID	11-0001	11-0002	11-0003
Total Solids	27.1	28.4	26.6
Insoluble Solids	15.8	11.5	13.7
Calcined Solids	17.3	15.7	16.9
Supernate Solids	13.4	19.0	14.9
Soluble Solids	11.3	16.8	12.9
pH	4.2	3.0	4.7

Table 3-31. SRAT Product Rheology results

Sample ID	GF23-4501	GF24-4518	GF25-4512
Upcurve Yield Stress, Pa	93.5	36.9	101
Downcurve Yield Stress, Pa	80.6	25.8	89.0
Upcurve Consistency, cP	40.7	26.8	38.4
Downcurve Consistency, cP	56.2	39.7	55.1

The eight GF23 nitric/formic flowsheet runs were completed after first completing a 4-L run (GF21) to determine the processing parameters (REDOX being critical). The eight GF24 glycolic/formic flowsheet runs were completed after first completing a 4-L run (GF23) to determine the processing parameters. Results are summarized in Table 3-32. Note that runs GF23 and GF24 were shorter in duration than GF21 and GF22 as nitrite was <1000 mg/kg in four hours of boiling so the GF23 and GF24 were shortened to the time it took to dewater.

Table 3-32. SRAT Product REDOX, Inputs and Outputs

analyte	GF21	GF22	GF23	GF24
nitrite, mg/kg	<100	<100	<100	<100
nitrate, mg/kg	34,500	70,750	27,050	68,600
glycolate, mg/kg	<100	54,800	<100	54,200
oxalate, mg/kg	<100	802	<100	351
formate, mg/kg	68,400	9,550	71,400	9,520
wt% total solids	28.94	29.34	27.06	28.37
wt% calcined solids	18.22	16.25	17.27	15.69
Predicted REDOX, $\text{Fe}^{2+}/\Sigma\text{Fe}$	0.26	0.09	0.39	0.11
Measured REDOX, $\text{Fe}^{2+}/\Sigma\text{Fe}$	0.16	0.23	0.04	0.17

Note: REDOX was not measured for GF25, since it would have been completely oxidized prior to sugar addition (completed by VSL).

3.3 Recommended Flowsheet

The recommended Glycolic-Formic Flowsheet is very similar to the baseline flowsheet in most ways. The main change is to replace formic acid with an 80:20 molar blend of glycolic acid. It has been demonstrated that process was acceptable with all blends from 100% formic to 100% glycolic, so other acid blends might be preferable for some sludge batches. Glycolic acid is more dilute on a molar basis than formic acid (11.7 M for the mixture versus 23.6 M for 90 wt % formic acid), so it is recommended that glycolic acid is fed at the same molar flowrate as formic acid to keep from extending the SRAT processing time. Using the same basis for nitric acid would also be important as the nitric acid volume is larger in the glycolic-formic flowsheet so the acid feed time will be longer unless the acid addition rates are increased. The acid addition rate controls the production of process gases (CO_2 , N_2O , NO_x , etc.) produced during acid addition.

The data in hand following the above studies indicate that the glycolic-formic acid flowsheet is technically feasible subject to additional progress in just one or two areas such as REDOX control. The existing formic acid cold feed preparation and handling equipment could be adapted for blend acid addition. Additional reduction in cycle time could be accomplished by increasing the nitric acid and formic acid feed pump capacity to four gallons per minute, but such modifications would not have to delay the implementation of the flow sheet. Few other facility modifications appear to be needed to implement this flowsheet in DWPF (some process instrumentation might need to be rearranged or modified), so the process could be deployed quickly once the necessary analytical methods, operating procedures, etc. were in place. Few downstream impacts have been identified. A low concentration of glycolate would be recycled to the tank farm (about a tenth of the formate concentration currently being recycled).

The acid stoichiometry needed will be specific to each sludge batch, but it is expected that a Koopman stoichiometry of 100% would be acceptable for most sludge batches. Higher acid stoichiometry might be needed if DWPF wants to target higher solids loading in the SRAT and SME or if the rheology of the sludge is challenging at lower acid stoichiometry. Hydrogen generation was minimal even at 200% acid stoichiometry and hydrogen generation can be virtually eliminated by using only glycolic acid. Lower acid stoichiometry led to more accumulation of elemental mercury in the MWWT.

The addition of glycolic acid in DWPF will require the analysis of the glycolate anion using ion chromatography. A new method has been developed for this analysis which allows the

characterization of the current DWPF anions (nitrate, nitrite, formate, sulfate, phosphate, chloride, fluoride, and glycolate). Properties of the glycolic acid:formic acid blend fed to the SRAT will also need to be tracked in order to determine the correct volume to add.

3.4 Physical Properties

A document was issued summarizing the glycolic acid's physical properties, impurities, and radiation effects³⁰. It concluded, "Blends of formic acid in glycolic acid were prepared and their physical properties tested. Increasing amounts of glycolic acid led to increases in blend density, viscosity and surface tension as compared to the 90 wt% formic acid that is currently used at DWPF. These increases are small, however, and are not expected to present any difficulties in terms of processing."

The main impurities in the glycolic acid are formic acid and sulfur. As long as it is being blended with formic acid, the formic impurity is not an issue. However, sulfur could impact glass quality. The report concluded, "The effect of sulfur impurities in technical grade glycolic acid was studied for its impact on DWPF glass quality. While the glycolic acid specification allows for more sulfate than the current formic acid specification, the ultimate impact is expected to be on the order of 0.03 wt% sulfur in glass. Note that lower sulfur content glycolic acid could likely be procured at some increased cost if deemed necessary."

Communication with DuPont after the issuing of the above report led to the discovery of DuPont data relating density and glycolic acid concentration at 50°C. This data was developed by titrating the acids, measuring the density and relating acid concentration to molarity. The data was used to calculate the concentration of the pure glycolic acid wt % and the resulting concentration of the glycolic/formic acid m. Based on this data, the as purchased glycolic acid concentration was 71.1 wt% versus the 70 wt % assumed throughout the first 20 tests. The data is summarized in Table 3-33 below.

Table 3-33. Glycolic Acid Determination Using Density Measurement

Density, g/ml @50 °C	wt% Glycolic
1.196373	60.7346
1.222427	67.3276
1.229959	69.0459
1.238992	71.2213
1.253999	75.3670
1.274718	80.2045
1.288263	83.4646

3.5 Degradation Issues

A document was issued summarizing glycolic acid's physical properties, impurities, and radiation effects³⁰. It concluded "A paper study on the effects of radiation on glycolic acid was performed. The analysis indicates that substitution of glycolic acid for formic acid would not increase the radiolytic production rate of H₂ and cause an adverse effect in the SRAT or SME process. It has been cited that glycolic acid solutions that are depleted of O₂ when subjected to large radiation doses produced considerable quantities of a non-diffusive polymeric material. Considering a

constant air purge is maintained in the SRAT and the solution is continuously mixed, oxygen depletion seems unlikely, however, if this polymer is formed in the SRAT solution, the rheology of the solution may be affected and pumping of the solution may be hindered.” The proposed test is in progress and will be reported when complete.

3.6 Analytical Issues

As was discussed in section 2.3, a new analytical method was developed for the glycolic-formic flowsheet. The method has a long analytical time due to the current necessity to analyze for phosphate. Measuring phosphorus by ICP-AES and remove phosphate from the list of requested anions could decrease analytical time significantly. The method is also sensitive to the potential degradation of standard solutions so it is recommended that all organic anion standards (manufacturer and calibration) be kept refrigerated and in the dark. Analytical QC will be needed on the glycolic acid-formic acid blend in the SRAT acid feed tank so that the molarity and acid proportions are known in order to determine the acid volume and acid mix to control REDOX.

3.7 Unresolved Technical Issues

The primary unresolved technical issue is the inability to predict REDOX based on anion measurements. This could lead to a new REDOX model for the glycolic-formic flowsheet or could be caused by inaccuracies in measuring anion concentrations. One of the hindrances to predicting the REDOX was the use of the same sludge for all testing. At present, a series of eight runs are being completed to study the glycolic-formic flowsheet using a matrix of four sludges (Hi Fe, Hi Al, Hi Mn, and Lo Mn). The variability in the composition of the sludge should help to refine or improve the REDOX model for the glycolic-formic flowsheet. The four REDOX runs (GF13, GF14, GF15, and GF16) demonstrated that melter feed could be produced to target the expected REDOX range of 0 to 0.35.

4.0 Conclusions

Flowsheet testing was performed to develop the nitric/glycolic/formic acid flowsheet as an alternative to the nitric/formic flowsheet currently being processed at the DWPF. This new flowsheet has shown that mercury can be removed in the Sludge Receipt and Adjustment Tank (SRAT) with minimal hydrogen generation. All other processing objectives were also met, including greatly reducing the Slurry Mix Evaporator (SME) product yield stress as compared to the baseline nitric/formic flowsheet. Forty-six runs were performed in total, including the baseline run and the melter feed preparation runs. Significant results are summarized below:

Constraint	Limit	Baseline Flowsheet GF1	Glycolic-formic Flowsheet GF3
SRAT hydrogen, lb/hr	<0.65	1.62	0.03
SME hydrogen, lb/hr	<0.23	0.0072	0.0017
SRAT carbon dioxide, lb/hr	NA	375	200
SRAT nitrous oxide, lb/hr	NA	0.75	1.93
SRAT product Hg, wt %	0.8	0.66	0.56
SRAT product nitrite, mg/kg	<1000	<100	<100
SRAT product down yield stress, Pa	1.5 to 5	33.1	1.6
SRAT product down consistency, cP	5 to 12	22.8	7.1
SME product down yield stress, Pa	2.5 to 15	223	7.2
SME product down consistency, cP	10 to 40	289	24.1
Glass REDOX $\text{Fe}^{+2}/\Sigma\text{Fe}$	0.1-0.33	0.00	0.22 ²
SME product total solids, wt %	>45	46.28	44.66
Minimal foaming	NA	No	Yes

The baseline nitric/formic flowsheet run was extremely difficult to process successfully under existing DWPF acceptance criteria with this simulant at the HM levels of noble metals. Certain baseline results were not considered typical of normal flowsheet processing. While nitrite was destroyed and mercury was removed to near the DWPF limit, the rheology of the SRAT and SME products are well above design basis and hydrogen generation far exceeded the DWPF limit. In addition, mixing during the SME cycle was very poor. In this sense, the nitric/glycolic/formic acid flowsheet represents a significant upgrade over the current flowsheet. Mercury was successfully removed with almost no hydrogen generation and the SRAT and SME products yield stresses were within process limits or previously processed ranges.

The glycolic-formic flowsheet has a very wide processing window. Testing was completed from 100% to 200% of acid stoichiometry and using glycolic-formic ratios from 40% to 100% glycolic acid. The testing met all processing requirements throughout these processing windows. This should allow processing at an acid stoichiometry of 100% and a glycolic-formic ratio of 80% glycolic acid with minimal hydrogen generation. It should also allow processing endpoints in the SRAT and SME at significantly higher total solids content. The flowsheet should be easy to implement using the existing formic acid equipment with at most minor modifications. A

² REDOX of GF14.

modified IC method will be needed in DWPF to quantify glycolate in the SRAT and SME product samples. Such a method has been developed and implemented in SRNL.

5.0 Recommendations

The glycolic/formic flowsheet is recommended as a viable flowsheet alternative to the baseline DWPF flowsheet. In the testing that has been performed to date, this flowsheet meets or outperforms the current flowsheet in minimizing off-gas generation, mercury removal, thinner product rheology and having a wide processing window regarding both the glycolic-formic ratio and acid stoichiometry. The addition of glycolic acid leads to SRAT and SME products that are rheologically much thinner which means that more concentrated products can be produced, leading to potentially larger batches and higher throughput. Recommended SRAT processing conditions are summarized below:

- Hsu Acid Stoichiometry: 107.7% (100% Koopman Stoichiometry)
- Nitric Acid Concentration: 10.4 M (50 wt %)
- Nitric Acid Addition Rate: 4.5 gallon per minute (178.7 mole/minute)
- Glycolic/Formic Acid Concentration: 13.1 M (73.1 wt %)
- Glycolic-Formic Acid Addition Rate: 3.6 gallon per minute (178.7 mole/minute)
- 4 mols glycolic acid:mol formic acid
- Glycolic-formic Acid Density: 1.2576 g/mL at 50° C
- If needed, add glycolic acid in place of formic acid in frit slurry
- Targeting higher solids loading in SRAT and SME products

Two tests in progress should be completed and the results documented to provide additional data which may be important to making a decision on the best flowsheet for DWPF.

- Complete irradiation testing to determine whether irradiation of SRAT simulant supernate causes polymerization of the glycolic acid. Introducing glycolic acid to high radiation doses may cause some polymerization of the glycolic acid in an oxygen depleted atmosphere. Results will be reported when complete.
- Complete glycolic-formic flowsheet testing of the four matrix sludges to demonstrate the viability to process the very different sludge compositions of these four extreme simulants. This knowledge will provide additional confidence of the robustness of the glycolic-formic flowsheet if it is able to successfully process four sludge extremes planned in this testing matrix.

Based on the additional testing above, the REDOX equation should be modified or a new REDOX equation should be developed for predicting the melter REDOX for the glycolic-formic flowsheet.

The glycolate IC method could benefit from further refinement. Shortening the method cycle time and an overall improvement of accuracy would be very beneficial for both continued SRNL testing and eventual DWPF implementation. The run time is significantly long due to the request for phosphate. Measuring phosphorus by ICP-AES and remove phosphate from the list of requested anions could decrease analytical time significantly.

The glycolic-formic flowsheet should be demonstrated with actual waste in SRNL Shielded Cells SRAT and SME processing, including the production of glass and measurement of the glass REDOX.

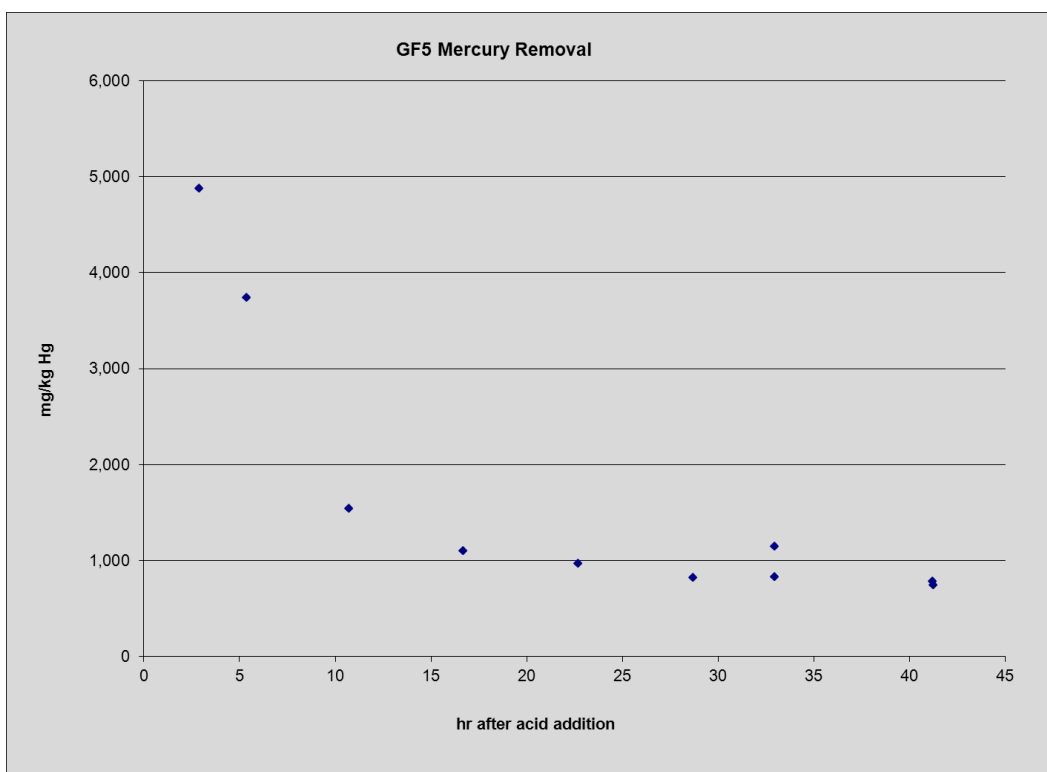
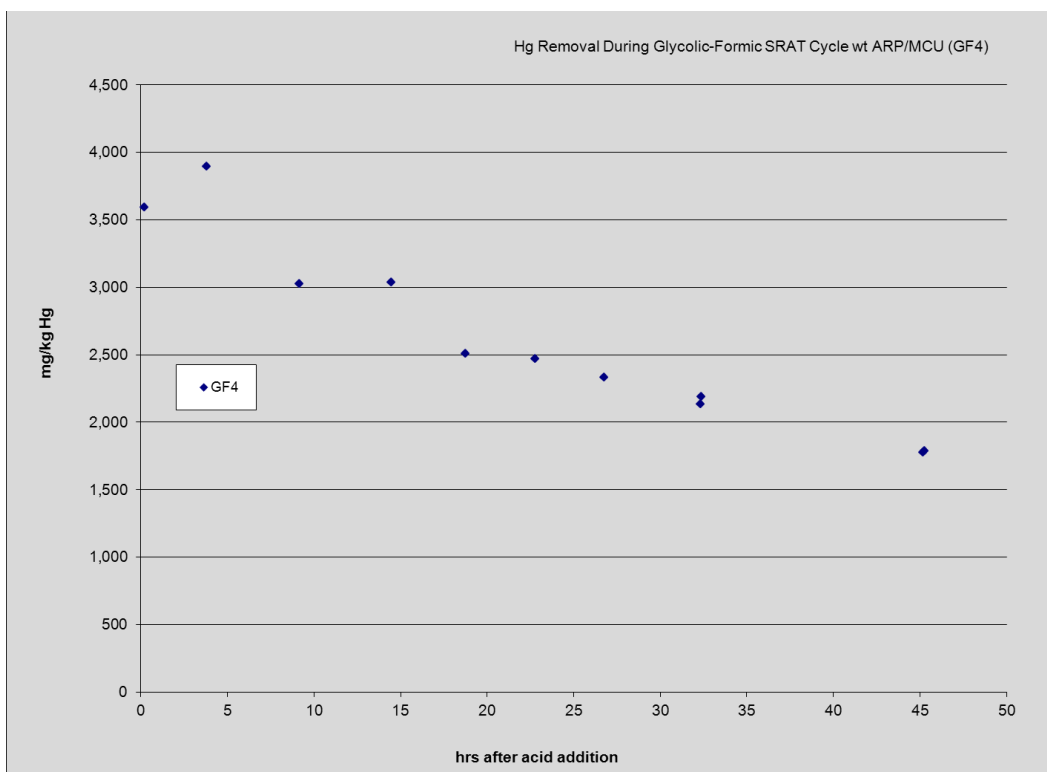
6.0 References

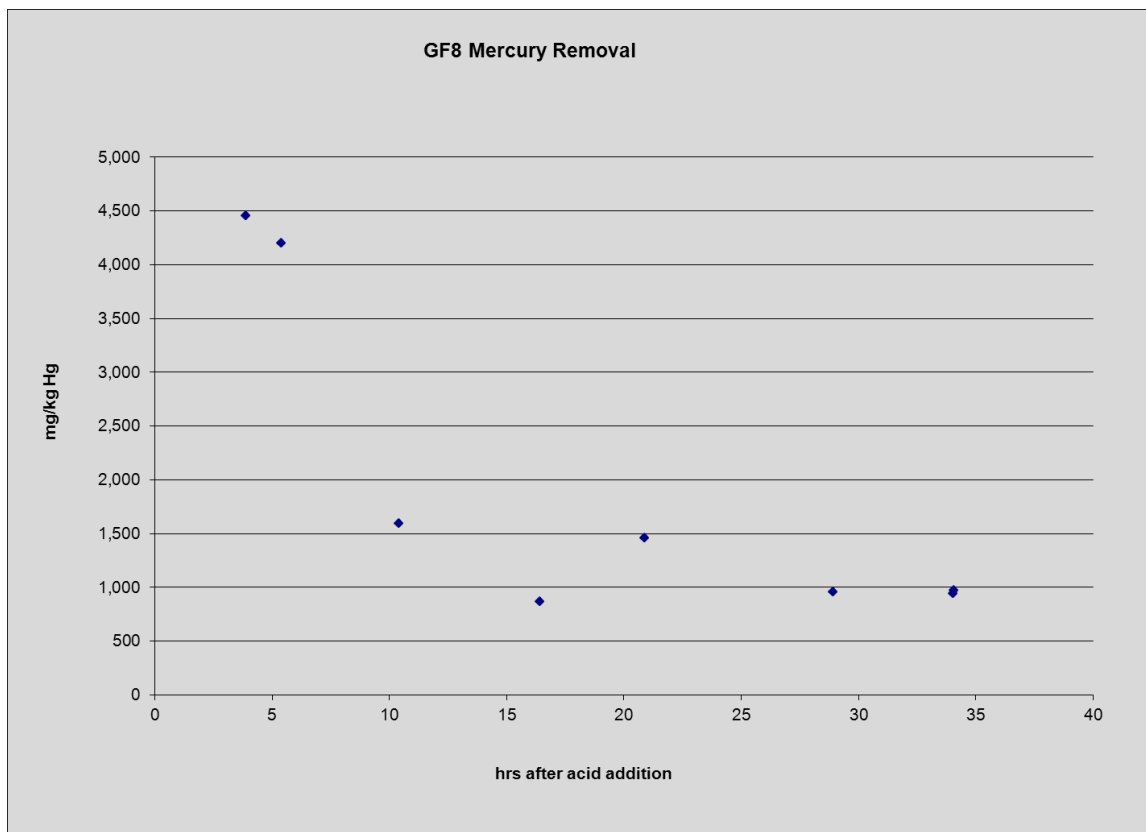
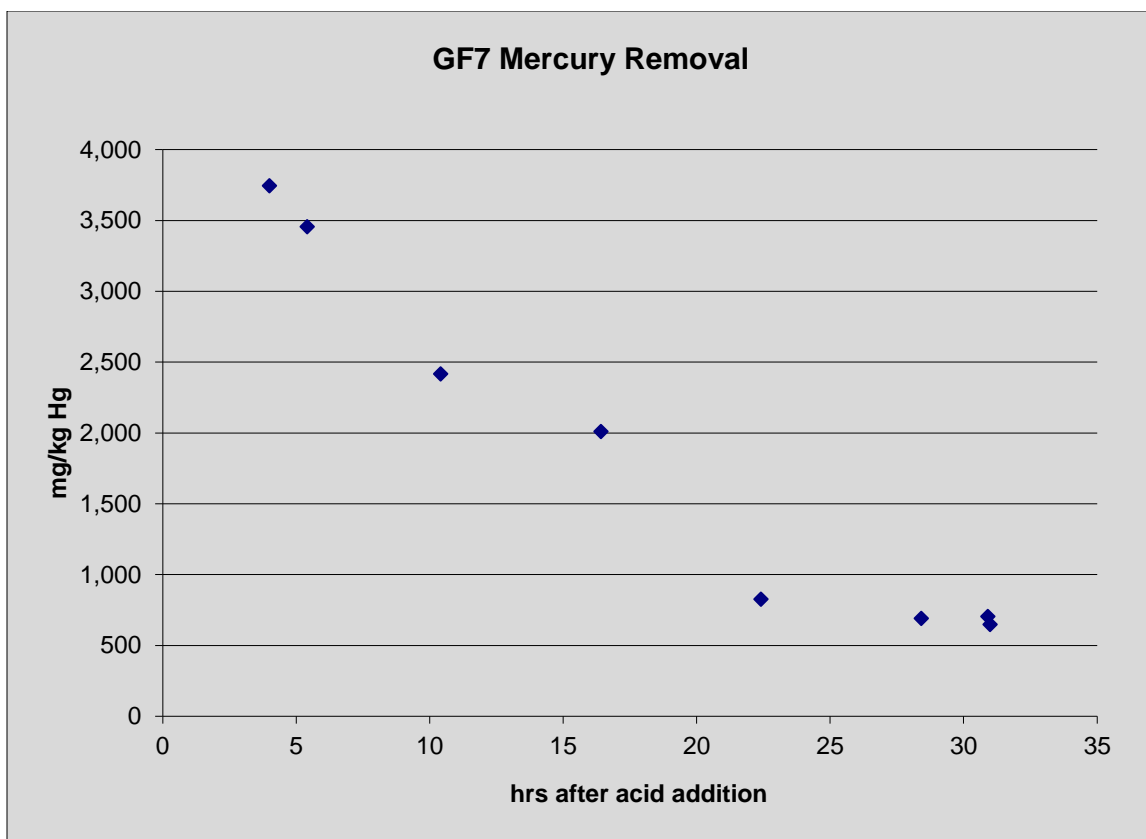
- ¹ Pickenheim, B.R., M.E. Stone, D.K. Peeler, Selection and Preliminary Evaluation of Alternative Reductants for SRAT Processing, SRNL-STI-2009-00120, Savannah River National Laboratory, Aiken, SC, June 2009.
- ² Pickenheim, B.R., M.E. Stone, SRAT Alternative Reductant Feasibility Assessment – Phase I, SRNL-STI-2009-00120, Savannah River National Laboratory, Aiken, SC, February 2009.
- ³ Holtzscheiter, E. W. Technical Task Request – Slurry Receipt and Adjustment Tank (SRAT) Alternative Reductant Assessment, HLW-DWPF-TTR-2008-0039, Washington Savannah River Company, Aiken, SC, 2008.
- ⁴ Holtzscheiter, E. W. Technical Task Request – Perform Glycolic-Formic Acid Flowsheet Development, Definition, and Demonstration, HLW-DWPF-TTR-2010-0003, Savannah River Remediation, Aiken, SC, December 2009.
- ⁵ Holtzscheiter, E. W. Technical Task Request – Perform Glycolic-Formic Acid Flowsheet Development, Definition, and Demonstration, HLW-DWPF-TTR-2010-0003, Revision 1, Savannah River Remediation, Aiken, SC, September 2010.
- ⁶ Pickenheim, B.R., Task Technical and Quality Assurance Plan for Glycolic-Formic Acid Flowsheet Development, Definition and Demonstration Tasks 1-3, SRNL-RP-2010-00105, Savannah River National Laboratory, Aiken, SC, Add Date.
- ⁷ Pickenheim, B.R., Task Technical and Quality Assurance Plan for Glycolic-Formic Acid Flowsheet Development, Definition and Demonstration Tasks 4-5, SRNL-RP-2009-00484, Savannah River National Laboratory, Aiken, SC, April 2010.
- ⁸ Pickenheim, B.R., Choi, A.S., Task Technical and Quality Assurance Plan for Glycolic-Formic Acid Flowsheet Development, Definition and Demonstration Tasks 4-7A, SRNL-RP-2009-00484, Revision 2, Savannah River National Laboratory, Aiken, SC, October 2010.
- ⁹ Fernandez, A.I., SB6-H Simulant Development: Evaluation Memo, SRNL-L3100-2010-00159, Savannah River National Laboratory, Aiken, SC, August 2010.
- ¹⁰ Pickenheim, B.R., M.E. Stone, J.D. Newell, Glycolic-Formic Acid Flowsheet Development, SRNL-STI-2010-00523, Rev 0, Savannah River National Laboratory, Aiken, SC, November 2010.
- ¹¹ Koopman, D.C., A.I. Fernandez and B.R. Pickenheim, Preliminary Evaluations of Two Proposed Stoichiometric Acid Equations, SRNL-L3100-2009-00146, Savannah River National Laboratory, Aiken, SC, 2009
- ¹² VSL Recipe for Sugar Flowsheet Melter Slurry Prep,
- ¹³ Stone, M. E., Lab-Scale CPC Equipment Set-up, SRNL-ITS-2006-00074, Savannah River Site, Aiken, SC 29808 (2008).
- ¹⁴ Manual L29, Procedure ITS-0094, Rev. 3, Laboratory Scale Chemical Process Cell Simulations, Savannah River Site, Aiken, SC 29808 (2006)
- ¹⁵ Glycolic-Formic Flowsheet Development, Part I, WSRC-NB-2011-00021.
- ¹⁶ Glycolic-Formic Flowsheet Development, Part II, WSRC-NB-2011-00022.
- ¹⁷ Koopman, D.C., A.I. Fernandez, B.R. Pickenheim, Preliminary Evaluations of Two Proposed Stoichiometric Acid Equations, Revision 0, Savannah River Site, Aiken, SC 29808 (2009).
- ¹⁸ Jantzen, C.M., J.R. Zamecnik, D.C. Koopman, C.C. Herman, and J.B. Pickett, Electron Equivalents Model for Controlling Reduction-Oxidation (REDOX) Equilibrium during High Level Waste (HLW) Vitrification, WSRC-TR-2003-00126, Savannah River Site, Aiken, SC 29808 (2003).
- ¹⁹ Jantzen, C.M. and M.E. Stone, Role of Manganese Reduction/Oxidation (REDOX) on Foaming and Melt Rate in High Level Waste Melters, WSRC-STI-2006-00066, Savannah River Site, Aiken, SC, March 2007.
- ²⁰ Best, D.R., Anion Analysis by Ion Chromatography for the Alternate Reductant Program for the Defense Waste Processing Facility, SRNL-STI-2010-00389, Savannah River National Laboratory, Aiken, SC, June 2010.
- ²¹ S. H. Reboul, D. R. Best, M. E. Stone, D. R. Click, Partitioning of Gadolinium in the Chemical Processing Cell, SRNL-STI-2010-00804, Savannah River National Laboratory, Aiken, SC, January 2010.

- ²² Grant, P.M. and Ward, R.B., Effects of Radiation, Part II. Characterization of the Products from Glycolic Acid, J. Chem. Soc, p 2554, (1959).
- ²³ Koopman, D.C., D.P. Lambert, M.A. Baich, Review Of Catalytic Hydrogen Generation in the DWPF Chemical Processing Cell, Part II, WSRC-TR-2005-00206, Savannah River National Laboratory, Aiken, SC, August 2005.
- ²⁴ Koopman, D. C., Rheology Protocols for DWPF Samples, WSRC-RP-2004-00470, Savannah River Site, Aiken, SC, 29808 (October 2004).
- ²⁵ Manual L29, Procedure ITS-0052, Rev. 2, Heat Treatment of Waste Slurries for REDOX ($\text{Fe}^{2+}/\Sigma\text{Fe}$) and Chemical Composition Measurement.
- ²⁶ Jantzen, C. M. and M. E. Stone, Role of Manganese Reduction/Oxidation (REDOX) on Foaming and Melt Rate in High Level Waste Melters, WSRC-STI-2006-00066, Savannah River Site, Aiken, SC, 29808, March 2007.
- ²⁷ S. H. Reboul, Task Technical and Quality Assurance Plan for Quantifying the Partitioning of Gadolinium in the Chemical Processing Cell, SRNL-RP-2010-00931, Savannah River National Laboratory, Aiken, SC, June 2010.
- ²⁸ S. H. Reboul, D. R. Best, M. E. Stone, D. R. Click, Partitioning of Gadolinium in the Chemical Processing Cell, , SRNL-STI-2010-00804, Savannah River National Laboratory, Aiken, SC, in draft.
- ²⁹ Koopman, D.C., Sludge Batch 6/Tank 40 Simulant Chemical Process Cell Simulations, SRNL-STI-2010-00212, Savannah River National Laboratory, Aiken, SC, April 2010.
- ³⁰ Pickenheim, B.R. and Bibler, N.E, Glycolic Acid Physical Properties, Impurities, and Radiation Effects Assessment, SRNL-STI-2010-00314, Savannah River National Laboratory, Aiken, SC, May 2010.

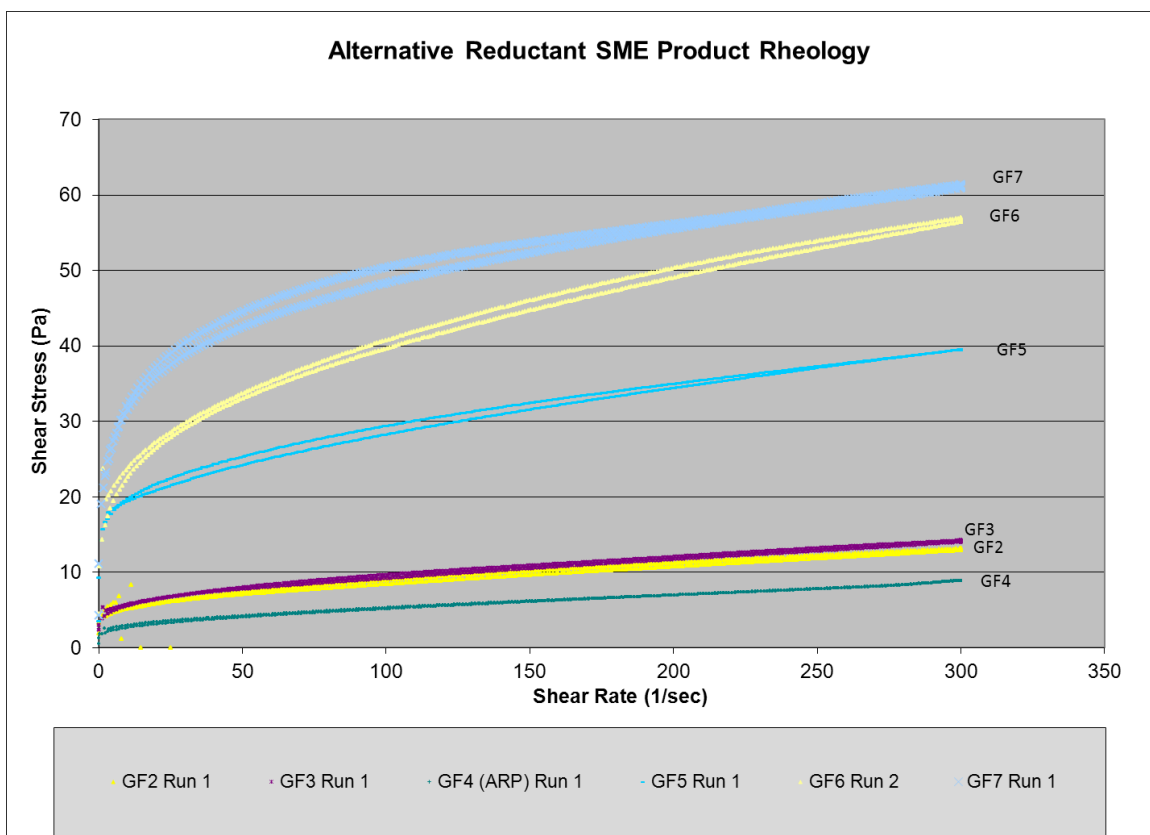
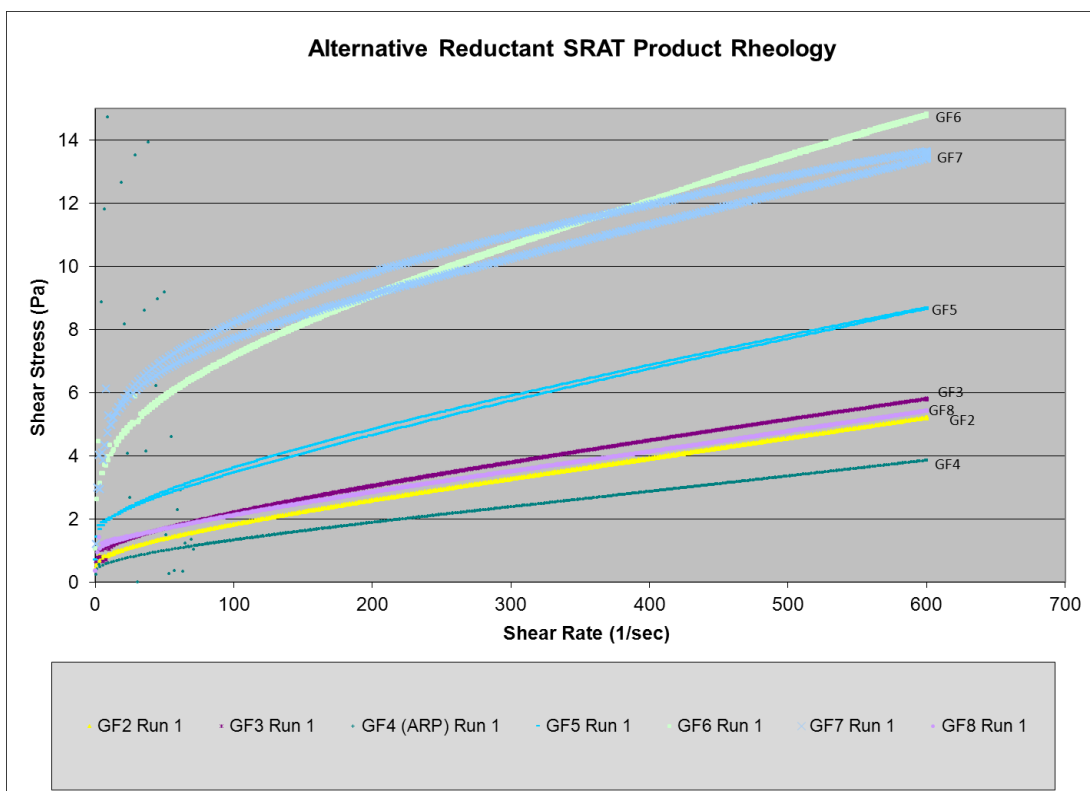
Appendix A

A.1 Mercury Removal Plots

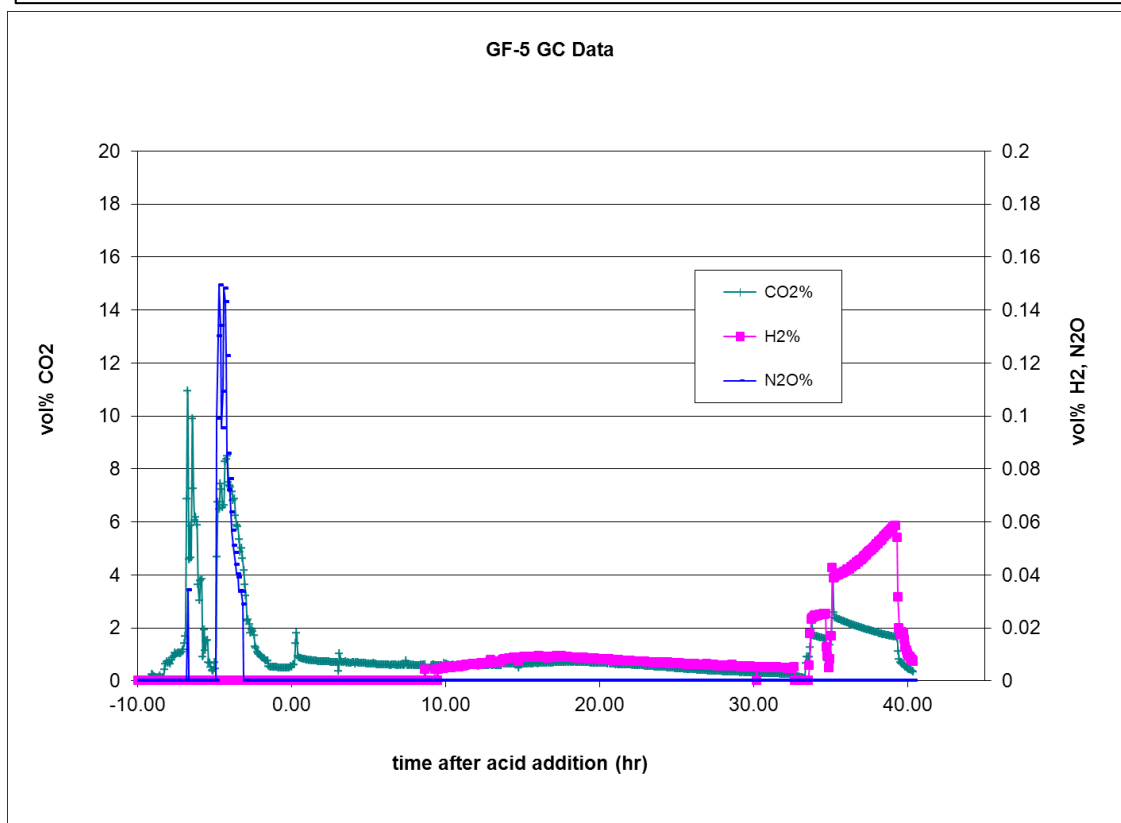
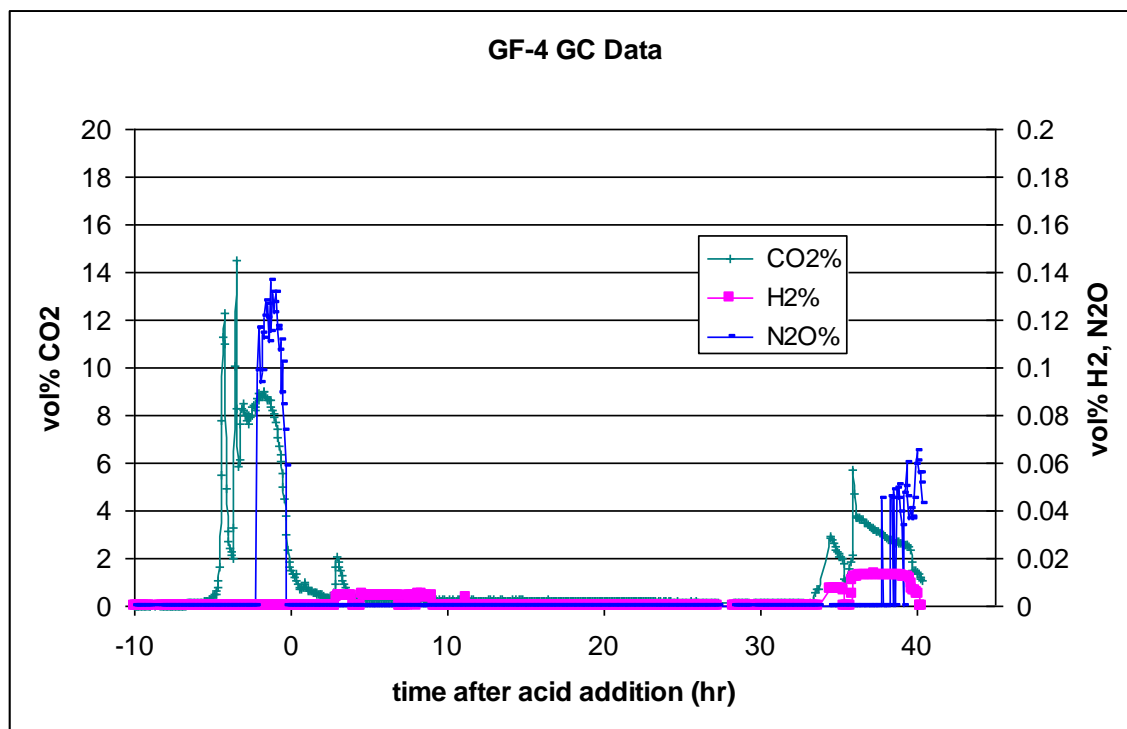


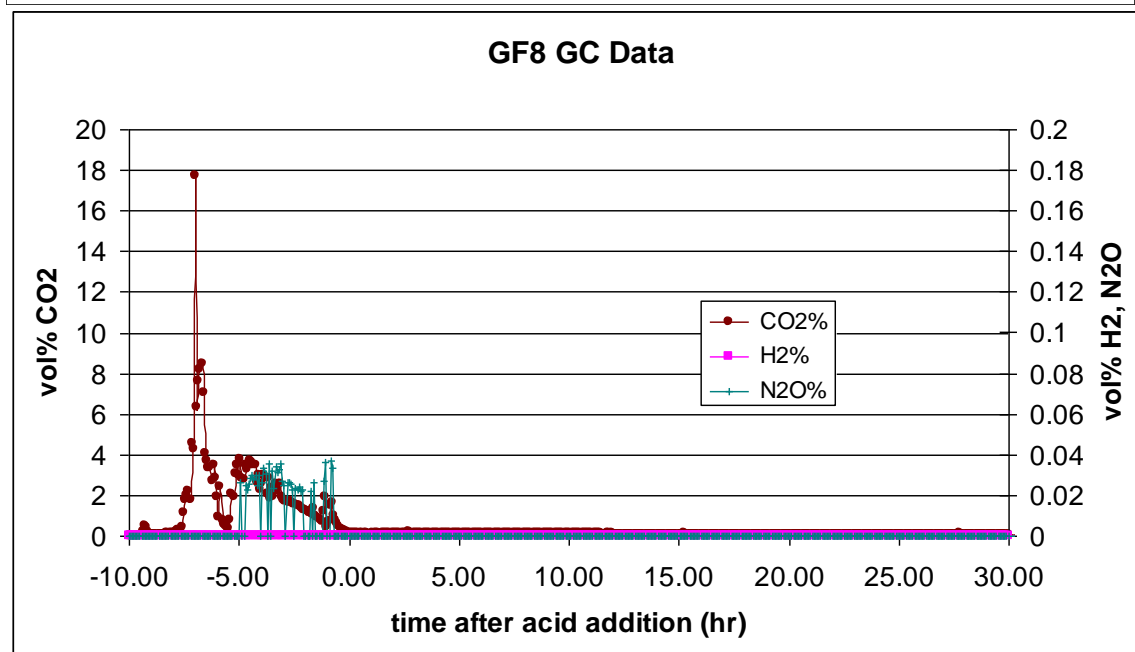
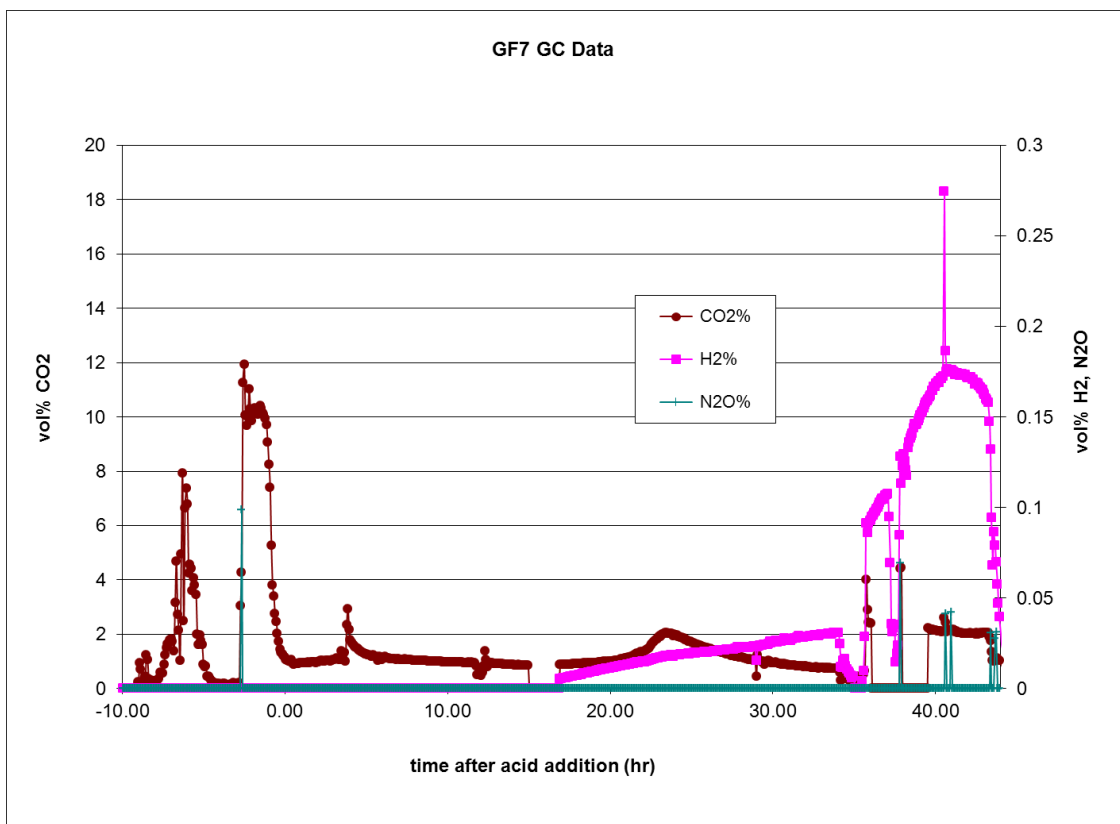


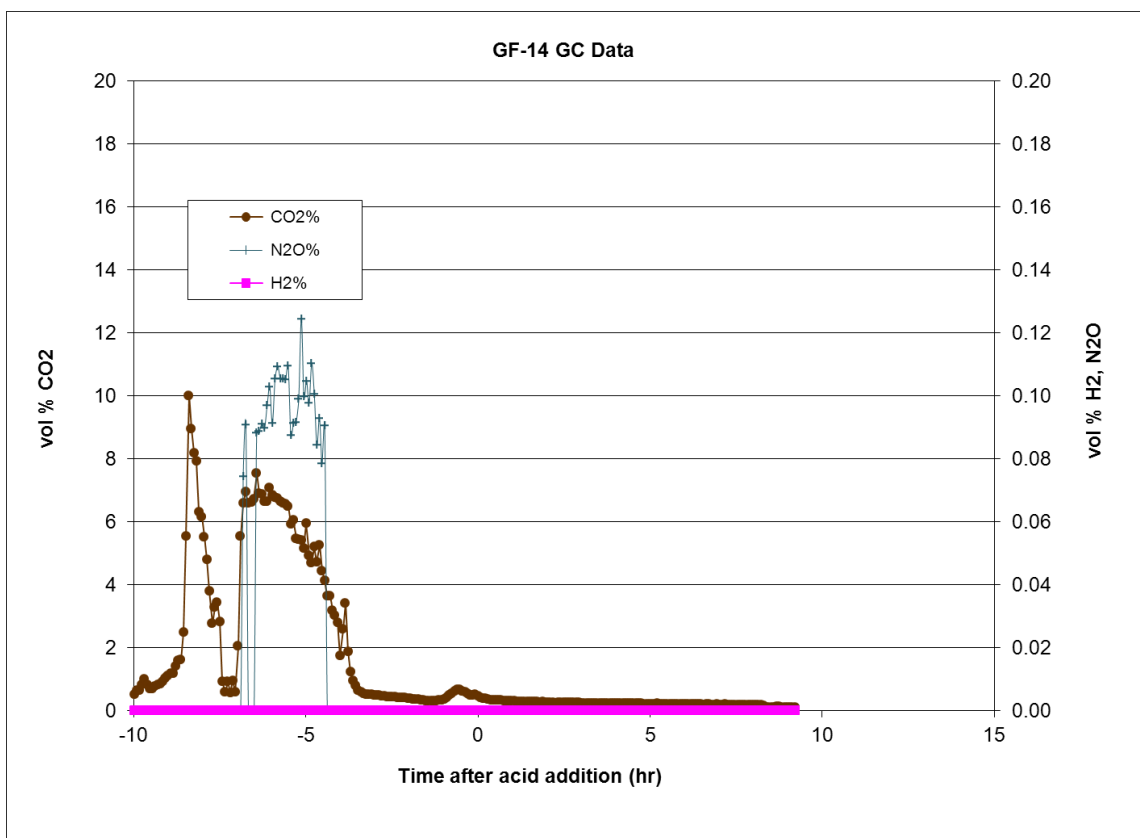
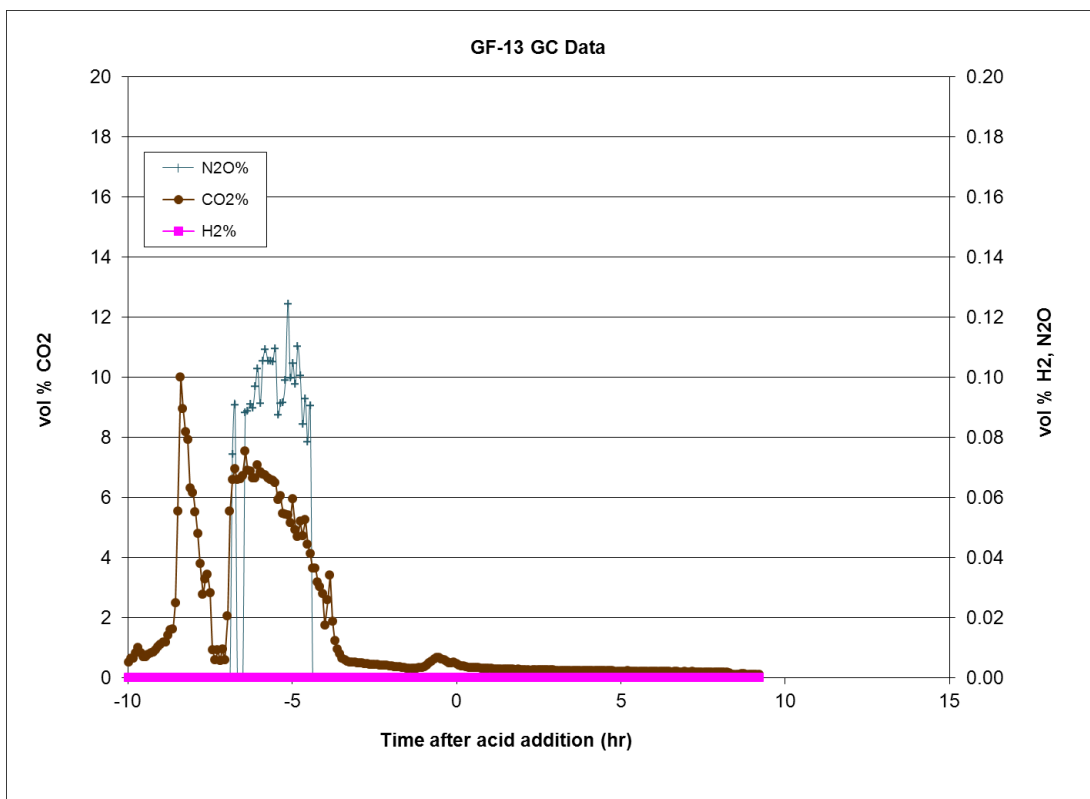
A.2 Rheology Flow Curves

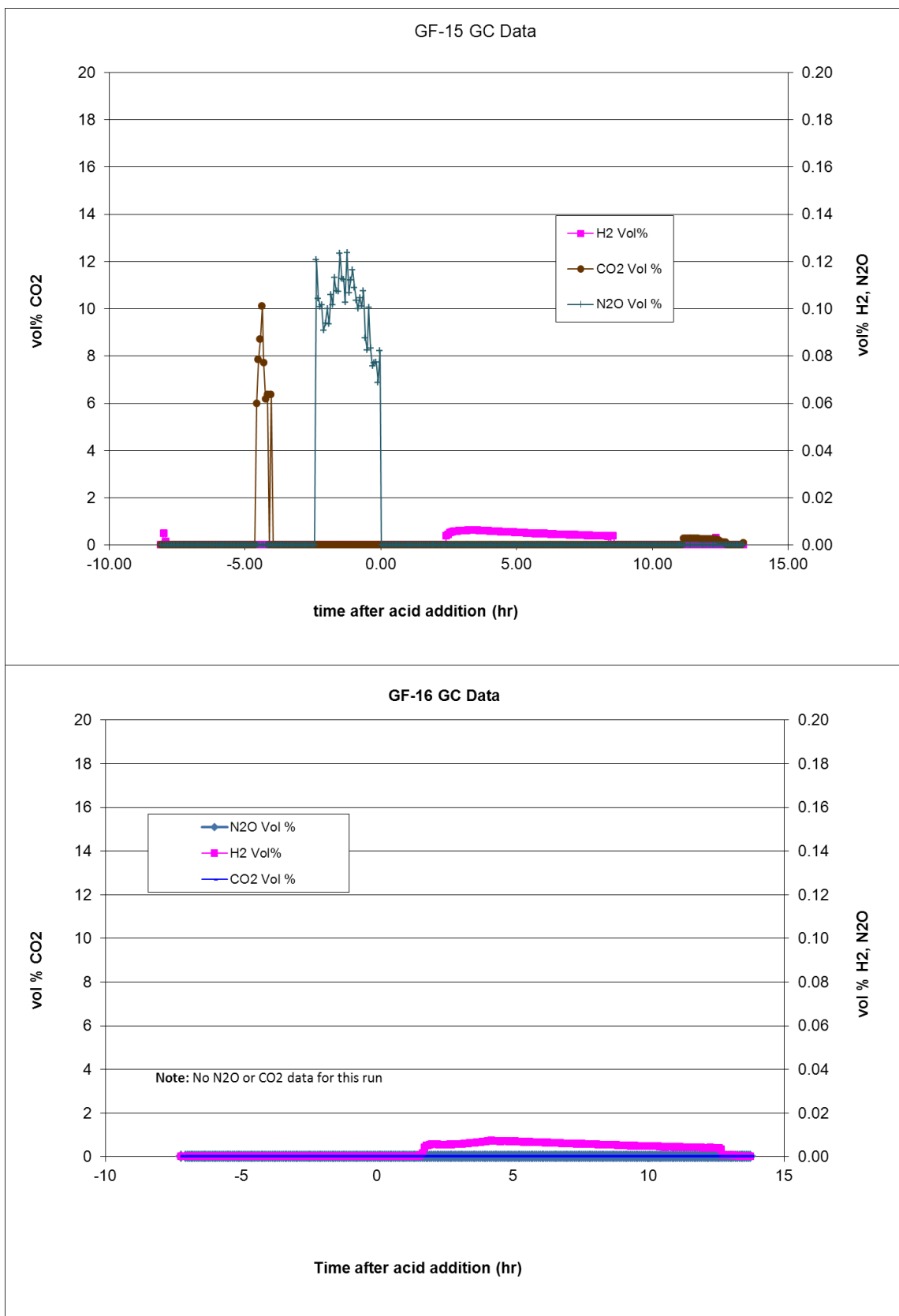


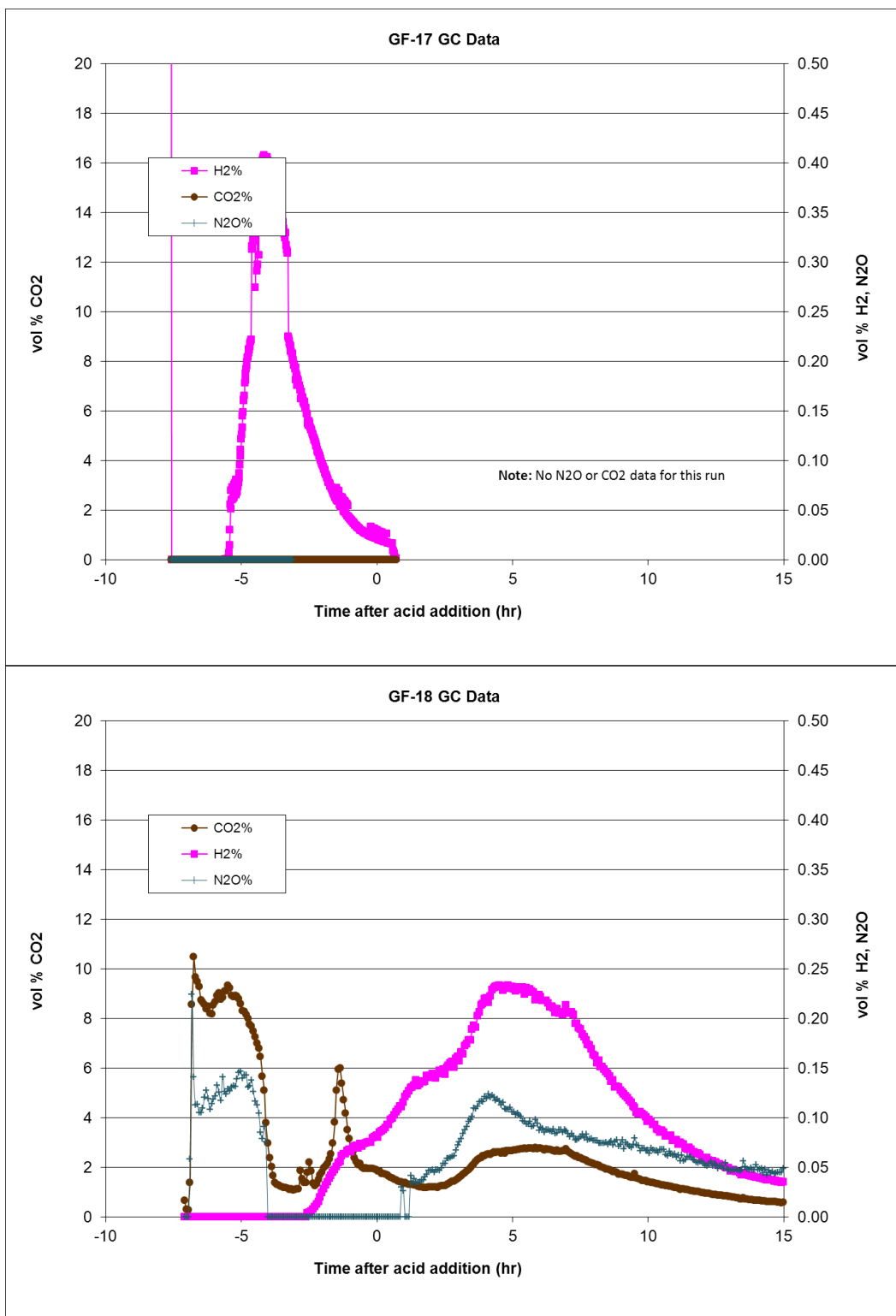
A.3 Additional GC Data

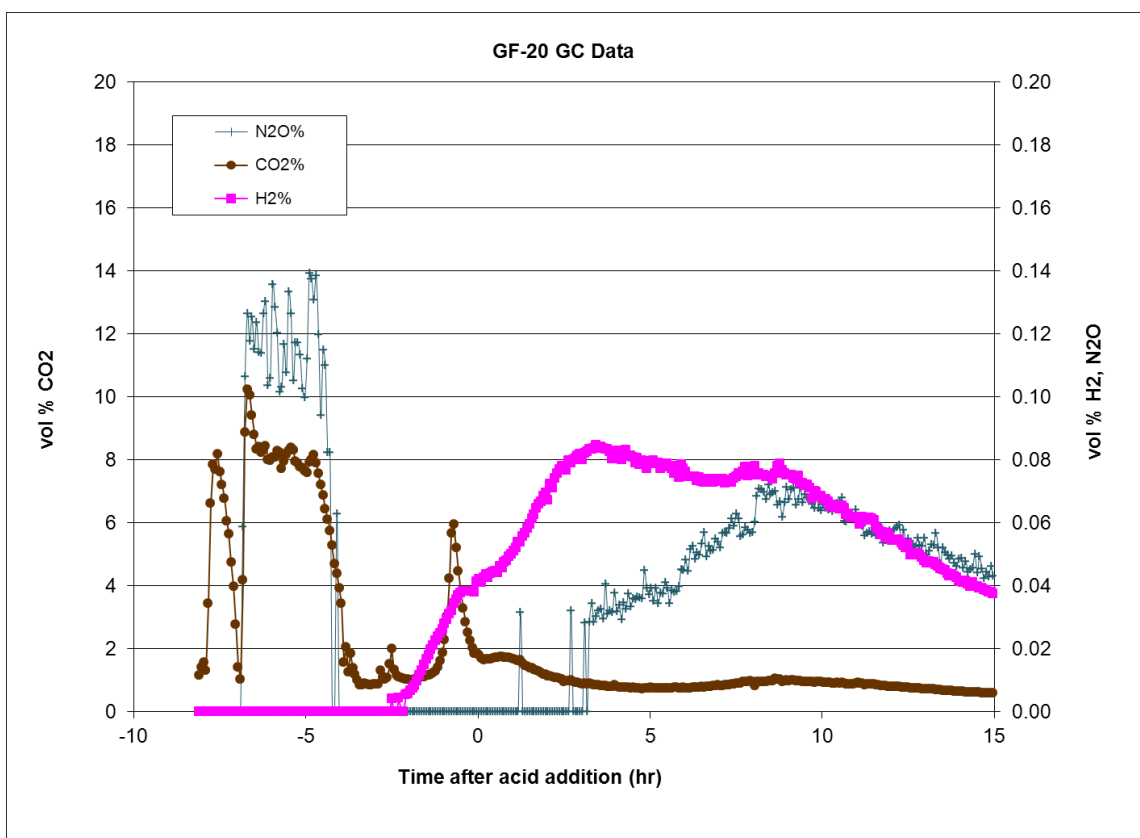
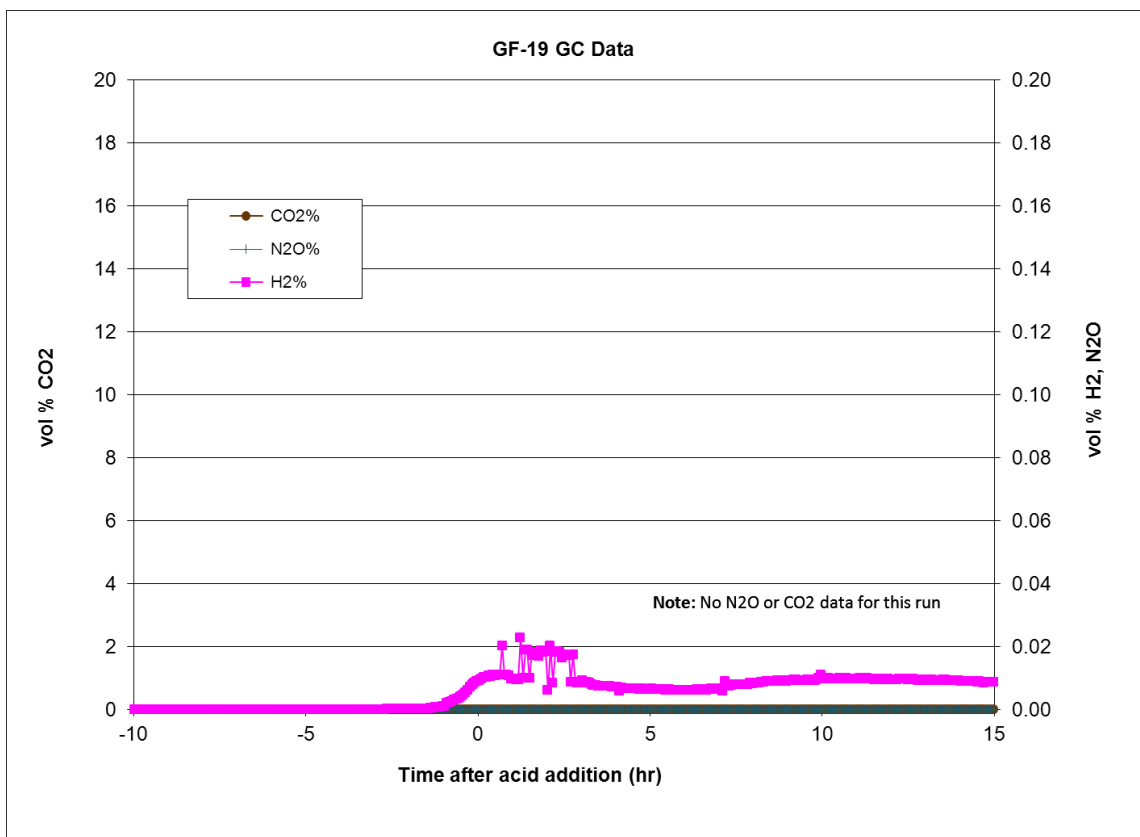












A.4 Mass Balance Data

GF1 SRAT Carbon Balance

	Input					Calculation						
	Mass, g	TIC, mg/kg	Oxalate, mg/kg	Glycolic Acid, wt %	Formic Acid, wt %	TIC, g	Oxalate, g	Glycolate, g	Formate, g	CO, g	CO2, g	Total C, g
MW						12.0107	88.019	74.03548	45.01744	28.0101	44.0095	12.0107
Number of Carbons						1	2	2	1	1	1	1
SRAT Receipt	3,102.64	1000	815			3.103	2.529	0.000	0.000			3.793
Added Acid	202.20			0.00	90.16			0.000	178.316			47.575
Total In						3.103	2.529	0.000	178.316	0.000	0.000	51.36769
	Mass, g	Carbonate, mg/kg	Oxalate, mg/kg	Glycolate, mg/kg	Formate, mg/kg	TIC, g	Oxalate, g	Glycolate, g	Formate, g	CO, g	CO2, g	Total C, g
Offgas											108.96	29.736
SRAT Product	2,481.38		296	0	12250	0.000	0.734	0.000	30.397			8.310
Composite Condensate	1783.60		0	0	322	0.000	0.000	0.000	0.574			0.153
Total Out						0.000	0.734	0.000	30.971	0.000	108.960	38.20006
Delta												13.168

GF3 SRAT Carbon Balance

	Input					Calculation						
	Mass, g	TIC, mg/kg	Oxalate, mg/kg	Glycolic Acid, wt %	Formic Acid, wt %	TIC, g	Oxalate, g	Glycolate, g	Formate, g	CO, g	CO2, g	Total C, g
MW						12.0107	88.019	74.03548	45.01744	28.0101	44.0095	12.0107
Number of Carbons						1	2	2	1	1	1	1
SRAT Receipt	3,127.92	1000	815			3.128	2.549					3.824
Added Acid	278.10			68.25	10.32			184.768	28.072			67.439
Total In	3406.02					3.128	2.549	184.768	28.072			71.26264
	Mass, g	Carbonate, mg/kg	Oxalate, mg/kg	Glycolate, mg/kg	Formate, mg/kg	TIC, g	Oxalate, g	Glycolate, g	Formate, g	CO, g	CO2, g	Total C, g
Offgas											40.24	10.981
SRAT Product	2,422.83		2405	57250	0	0.000	5.827	138.707	0.000			46.595
Composite Condensate	1793.12			62.8	293	0.000	0.000	0.113	0.525			0.177
Total Out	4215.958					0.000	5.827	138.820	0.525	0.000	40.238	57.75306
Delta												13.510

GF1 SRAT Nitrogen Balance

	Mass, g	Nitrate, mg/kg	Nitrite, mg/kg	Nitric Acid, wt %	Nitrate, g	Nitrite, g	Ammonium, g	NO, g	N2O, g	Calculated NO2, g	Total N, g
MW					62.0049	46.0055	18.03846	30.0061	44.0128	46.0055	14.0067
Number of Nitrogens					1	1	1	1	2	1	1
SRAT Receipt	3,102.64	6135	16750		19.035	51.969					20.122
Added Acid	202.20			50.03	99.542						22.486
Total In					118.577	51.969	0.000	0.000	0.000	0.000	42.608
	Mass, g	Nitrate, mg/kg	Nitrite, mg/kg	Ammonium, mg/L	Nitrate, g	Nitrite, g	Ammonium, g	NO, g	N2O, g	Calculated NO2, g	Total N, g
Offgas								0.000	1.145	60.178	19.051
SRAT Product	2,481.38	20600			51.116	0.000	0.000				11.547
Composite Condensate	1,783.60	156			0.278	0.000					0.063
Scrubber Post SRAT	750.00			7110			5.333				4.141
FAVC Post SRAT	39.40			10600			0.418				0.324
Total Out					51.395	0.000	0.418	0.000	1.145	60.178	35.126
Delta											7.483

GF3 SRAT Nitrogen Balance

	Mass, g	Nitrate, mg/kg	Nitrite, mg/kg	Nitric Acid, wt %	Nitrate, g	Nitrite, g	Ammonium, g	NO, g	N2O, g	Calculated NO2, g	Total N, g
MW					62.0049	46.0055	18.03846	30.0061	44.0128	46.0055	14.0067
Number of Nitrogens					1	1	1	1	2	1	1
SRAT Receipt	3,127.92	6135	16750		19.190	52.393					20.286
Added Acid	224.80			50.03	110.668						24.999
Total In					129.858	52.393	0.000				45.286
	Mass, g	Nitrate, mg/kg	Nitrite, mg/kg	Ammonium, mg/L	Nitrate, g	Nitrite, g	Ammonium, g	NO, g	N2O, g	Calculated NO2, g	Total N, g
Offgas								1.932	0.000	35.431	11.689
SRAT Product	2,422.83	52650			127.562	0.000	0.000				28.816
Composite Condensate	1,793.12	132			0.237	0.000					0.053
Scrubber Post SRAT	750.00			461			0.346				0.268
FAVC Post SRAT	39.40			883			0.035				0.027
Total Out					127.799	0.000	0.035	1.932	0.000	35.431	40.827
Delta											4.459

Distribution:

A. B. Barnes, 999-W
D. A. Crowley, 773-43A
S. D. Fink, 773-A
B. J. Giddings, 786-5A
C. C. Herman, 999-W
S. L. Marra, 773-A
F. M. Pennebaker, 773-42A
W. R. Wilmarth, 773-A
C. J. Bannochie, 773-42A
J. M. Gillam, 766-H
B. A. Hamm, 766-H
J. F. Iaukea, 704-30S
J. E. Occhipinti, 704-S
W. O Pepper, 704-S
D. K. Peeler, 999-W
J. W. Ray, 704-S
H. B. Shah, 766-H
D. C. Sherburne, 704-S
M. E. Stone, 999-W
B. P. Pickenheim, 704-28S
J. R. Zamecnik, 999-W
M. A. Broome, 704-29S
R. N. Hinds, 704-S
J. P. Vaughan, 773-41A
J. M. Bricker, 704-27S
T. L. Fellingner, 704-26S
E. W. Holtzscheiter, 704-15S
A. V. Staub, 704-27S
K. R. Shah, 704-S
M. T. Keefer, 766-H
D. P. Lambert, 999-W
D. C. Koopman, 999-W
J. D. Newell, 999-W
D. R. Best, 999-W
R. E. Eibling, 999-W
W. T. Riley, 999-W
P. R. Jackson, 703-46A